UNIVERSITY „POLITEHNICA" OF BUCHAREST

DOCTORAL SCHOOL: APPLIED CHEMISTRY AND MATERIALS SCIENCE

No. Decision…….. from ……

DOCTORAL THESIS ABSTRACT

New solutions regarding catalytic transesterification integration with separation in biodiesel technology

Author: Eng. Cristian Eugen RĂDUCANU

Scientific coordinator: Prof.dr.eng. Tănase DOBRE

DOCTORAL COMMISSION

Chairman	**Prof. dr. ing. Văireanu Dănuţ-Ionel**	from	**University Politehnica of Bucharest**
Scientific coordinator	**Prof. dr. ing. Dobre Tănase**	from	**University Politehnica of Bucharest**
Referent	**Conf.dr.ing. Pârvulescu Oana Cristina**	from	**University Politehnica of Bucharest**
Referent	**Prof.dr.ing. Mămăligă Ioan**	from	**Universitatea Tehnică Gheorghe Asachi din Iaşi**
Referent	**Prof.dr.ing. Bomboş Dorin**	from	**University Petrol şi Gaze of Ploieşti**

BUCHAREST
2020

CONTENT OF THE DOCTORAL THESIS ABSTRACT

1. INTRODUCTION 3

2. CONTENT OF DOCTORAL THESIS 4

3. STRUCTURE OF DOCTORAL THESIS 6

4. DOCTORAL THESIS ABSTRACT 8

5. EXPERIMENTAL 9

6. CONCLUSIONS OF PHD THESIS 63

7. ORIGINAL CONTRIBUTIONS 64

8. FUTURE RESEARCH PERSPECTIVE 67

SELECTIVE REFERENCES 68

1. INTRODUCTION

There are already alternative solutions to fossil fuels at this time, with some applications already high on an industrial scale, if we consider bioethanol, biodiesel, hybrid fueled engines, hydrogen powered engines or electrically powered engines (batteries or supercapacitors). At this moment (2020) the only reason why biodiesel is produced in Romania is due to the *acquis communitaire*, imposed by the way, regarding the ~6% presence of biodiesel in total diesel #2 sold/produced, with possible increase from 2020.

In this context, there were several considerations that inspired us, and mobilized us, to start this research.

i) We wanted to bring back to attention the ease with which biodiesel can be produced and its relatively simple chemistry, as well as the multiple sectors where it could be used: agriculture, interurban transport, military field (simulations, military exercises), industrial field (heating, electric generators), residential (heating, electric generators), in Romania.

ii) We wanted, with this work, to bring to attention the properties of biodiesel, similar to those of diesel #2 and highlight its biodegradability and significant reduction, depending on the percentage used, of CO_2 emissions in use

iii) We wanted to add other methods of producing biodiesel, in addition to many of the existing ones (over 16 methods and techniques - see Chapter 2), precisely to inspire an increase in interest in biodiesel production;

iv) We wanted to highlight once again Romania's ability to provide raw materials for its production processes in the energy field and especially in the field of biofuels, as well as the relatively simple ability to adapt them to these processes;

v) We wanted to highlight the fact that biodiesel comes in addition to fossil fuels, anyway, in the case of Romania, Romania being an oil producer, but B20 (20% biodiesel-80% petrodiesel) approved by some car manufacturers, could be approved by the entire romanian car fleet from all industry fields or the entire fleet of machines with diesel engines;

vi) We wanted to show our respect, by continuing the work of many researchers in this field, adding the results and recommendations of our experimental research.;

vii) We also wanted to start preparing for a later stage of future research, and/or applications in the field, providing a part of the starting foundation, which is why we attached numerous images (pictures) from the various stages of research, to present them in as descriptive as possible;

viii) Last but not least, the entire doctoral thesis wants to be a manifesto for green chemistry, a manifesto for green energy, a manifesto for the intensive production of conventional but especially non-conventional bio-fuels, and especially a manifesto for our energy independence, which is easy to achieve if you aim for it, since Romania has all the advantages at hand: research, qualified staff, adequate climate and so many innovators who, historically, have left their mark on ambition, passion and on the Romanian DNA.

The thesis brings original contributions oriented on the three approached research directions: I.The study on homogeneous catalysis for vegetable oils conversion to biodiesel, followed by simulation and modeling processes of transesterification reaction of triglycerides with methanol; II. Study on heterogeneous catalysis, followed by heterogeneous catalyst preparation, for transesterification of triglycerides with methanol to biodiesel; III. Synthesis of biodiesel in heterogeneous catalysis, using the prepared catalyst, in a batch-type reactor with perfect mixing as well as in a fixed-layer catalytic reactor.

2. CONTENT OF DOCTORAL THESIS

CONTENT

CHAPTER 1 9

INTRODUCTION **9**

1.1. INTRODUCTION 9

1.2. MOTIVATIONAL CONTEXT 11

1.3. OBJECTIVES OF DOCTORAL THESIS 13

1.4. STRUCTURE OF DOCTORAL THESIS 14

CHAPTER 2 ..... **17**

LITERATURE REVIEW **17**

2.1. BIODIESEL – PROPERTIES, CHEMISTRY, CATALYSTS, REACTANTS AND PRODUCTS 17

2.1.1. Biodiesel chemistry 19

2.1.2. Catalysts and reaction mechanism in triglycerides transesterification to biodiesel 21

2.1.2.1. Homogeneous catalysts 21

2.1.2.1.a. Homogeneous acid catalysts 21

2.1.2.1.b. Homogeneous base catalysts 23

2.1.2.2. Heterogeneous catalysts 25

2.1.2.2.a. Heterogeneous base catalysts – mechanism and classification 25

2.1.2.2.b. Heterogeneous acid catalysts – mechanism and classification 29

2.1.2.2.c. Bifunctional heterogeneous catalysts 35

2.1.2.3. Enzymatic catalysts – mechanism and classification 38

Mechanism 38

2.1.2.4. Ionic liquids as catalysts 41

2.1.3.1. Triglycerides 45

2.1.3.1.a. Conventional sources 45

2.1.3.1.b. Non-conventional sources 47

2.1.3.2. Alcohols 48

2.1.4. Process products for triglycerides conversion to biodiesel 50

2.1.4.1. Biodiesel 50

2.1.4.1.a. Main physio-chemical properties of biodiesel 50

2.1.4.2. Glycerol – the main by-product in the process of biodiesel production 56

2.2. BIODIESEL FIELDS OF USE 59

2.3. CURRENT TECHNOLOGIES OF BIODIESEL PRODUCTION 64

2.3.1. Conventional technologies for biodiesel production 64

2.3.1.1. Homogeneous base-catalyzed transesterification (I) 65

2.3.1.2. Homogeneous acid-catalyzed transesterification (II) 67

2.3.1.3. Homogeneous two step acid-base catalyzed transesterification (III) 69

2.3.2.1. The process of biodiesel production in heterogeneous base catalysis (IV) 71

2.3.2.2. Heterogeneous acid-catalyzed transesterification (V) 73

2.3.2.3. Transesterification using bifunctional catalysts (VI) 74

2.3.2.4. Enzymatic catalyzed processes (VII) 75

2.3.2.5. Ionic liquids catalyzed processes (VIII) 77

2.3.2.6. Biox non-catalitic process (IX) 78

2.3.2.7. Ultrasound assisted processes (X) 79

2.3.2.8. Supercritical processes (XI) 81

2.3.2.9. Microwave assisted processes (XII) 83

2.3.2.10. Reactive distillation processes (XIII) 85

2.3.2.11. Biodiesel synthesis using membrane reactors (XIV) 87

2.3.2.12. Hydroprocesses to convert vegetable oils to biodiesel (XV) 89

2.3.2.13. Vegetable oils conversion to biodiesel using static mixer as reactor (XVI) 91

CHAPTER 3 ..... **94**

PREPARATION OF CATALYTIC SUPPORT FOR HETEROGENEOUS CATALYST SYNTHESIS USED FOR BIODIESEL PRODUCTION **94**

3.1. RESIDUAL LIGNOCELLULOSIC BIOMASS AND ALGAL BIOMASS FOR CATALYTIC SUPPORT PREPARATION 96

3.1.1. Residual lignocellulosic biomass 96

3.1.2. Residual algal biomass....100
3.2. PYROLYSIS AND ASSOCIATED PROCESSES FOR CATALYTIC SUPPORT PREPARATION....102
3.2.1. Pyrolysis....103
3.2.1.1. Materials in pyrolysis process....103
3.2.1.2. Experimental method....105
3.2.1.2.a. Pretreatment of raw material....105
3.2.1.2.b. Experimental set-up and procedures in pyrolysis process....108
3.2.1.3. Results and discussions....113
3.2.1.4. Conclusions....120
3.2.2. Activation – End process in carbon-type catalytic support preparation....122
3.2.2.1 Materials used in activation process....122
3.2.2.2 Experimental method....123
3.2.2.2.a. Pretreatment operations....124
3.2.2.2.b. Procedure and experimental set-up....125
3.2.2.3. Results and discussions....127
3.2.2.4. Conclusions and recommendations....130
3.2.3 Adsorption - process, testing and characterization....132
3.2.3.2. Materials....132
3.2.3.3. Experimental method....132
3.2.3.4. Results and discussions....136
3.2.3.5. Conclusions....138
3.3. RAW RESIDUAL LIGNOCELLULOSIC BIOMASS FOR CATALYTIC SUPPORT PREPARATION....139
3.3.1. Introduction and objectives....139
3.3.2. Materials....140
3.3.3. Experimental method....140
3.3.3.1. Physico-mechanical treatment....140
3.3.3.2. Chemical treatment....143
3.3.3.2. Drying process....144
3.4. BIOCELLULOSE – MATERIAL FOR CATALYTIC SUPPORT PREPARATION....146
3.4.1. Introduction and objectives....146
3.4.2. Materials....148
3.4.3. Experimental method....148
3.4.3.1. Biocellulose cultivation....148
3.4.3.1. Biocellulose post-cultivation treatment....149
3.4.4. Results and discussions....151
3.4.1. Conclusions....154

CHAPTER 4....155

GUANIDINE SYNTHESIS FOR USE AS BASE CATALYST FOR CATALYTIC SUPPORT IMPREGNATION....155
4.1. INTRODUCTION....155
4.2. MATERIALS....158
4.3. EXPERIMENTAL METHOD....159
4.3.2. Ammonolysis with alcohol-bonded guanidine formation....161
4.3.3. Distillation....162
4.3.4. Precipitation as final stage for alcohol-bonded guanidine formation....164
4.3. RESULTS AND DISCUSSIONS....165
4.5. CONCLUSIONS....169

CHAPTER 5....170

HETEROGENEOUS CATALYST SYNTHESIS FOR BIODIESEL PRODUCTION....170
5.1. INTRODUCTION....170
5.2. MATERIALS....171
5.3. EXPERIMENTAL METHOD....171
5.3.1. Heterogeneous catalyst from guanidine and carbon-based catalytic support (commercial carbon and pyrolyzed biomass-based carbon)....172
5.3.1.1. Functionalization with inorganic acids....172
5.3.1.1.a. Commercial activated carbon functionalization by sulfonation....173
5.3.1.1.b. Pyrolytic carbon functionalization by nitration....174

5.3.1.2. Functionalization with strong bases 175
5.3.1.2.a. Carbon functionalization with potassium hydroxide by impregnation and thermal activation 175
5.3.1.2.b. Heterogeneous catalyst from guanidine and both activated and functionalized carbon 176
5.3.2. Heterogeneous catalyst from guanidine and raw lignocellulosic biomass (fruit stones) 177
5.3.3. Heterogeneous catalyst from guanidine and BC 178
5.3.3.1. Catalyst from simple BC treated with potassium hydroxide 179
5.3.3.2. Catalyst from simple BC and guanidine 180
5.3.3.3. Catalyst from simple BC-methanol and guanidine 181
5.4. RESULTS AND DISCUSSIONS 181
5.5. CONCLUSIONS 186

CHAPTER 6 188

BIODIESEL IN HOMOGENEOUS CATALYSIS - SIMULATION AND MODELLING 188
6.1. SIMULATION AND MODELING OF BIODIESEL PRODUCTION PROCESS IN HOMOGENEOUS CATALYSIS 188
6.1.1. Introduction 188
6.1.2. Biodiesel synthesis modelling using a batch reactor with external recirculation simultaneous with separation 188
6.1.2.1. Considerations regarding the management of transesterification process and reactors type 188
6.1.2.1. Transesterification kinetics in homogeneous base catalysis 190
6.2. RESULTS AND DISCUSSIONS 195
6.3. CONCLUSIONS 205

CHAPTER 7 206

BIODIESEL IN HETEROGENEOUS CATALYSIS - CATALYSTS TESTING, BIODIESEL SYNTHESIS, STATISTICAL MODEL 206
7.1. INTRODUCTION 206
7.2. MATERIALS 206
7.3. EXPERIMENTAL METHOD 206
7.3.1. Biodiesel using heterogeneous catalyst from sulfonated activated carbon in perfect mixed reactor 206
7.3.2. Biodiesel using heterogeneous catalyst from KOH-functionalized activated carbon in fixed layer catalytic reactor 208
7.3.3. Biodiesel with heterogeneous catalyst from BC-Gu and SC_{SF}-Gu in batch reactor with perfect mixing 211
7.3.4. Biodiesel with heterogeneous catalyst from SC_{SF}cai-Gu in batch reactor with perfect mixing 213
7.3.5. Biodiesel with heterogeneous catalyst from guanidine and BC_{KOH} in batch reactor with perfect mixing 214
7.4. RESULTS AND DISCUSSIONS 217
CONCLUSIONS 220
GENERAL CONCLUSIONS 220
ORIGINAL CONTRIBUTIONS 221
FUTURE RESEARCH PERSPECTIVE 223
REFERENCES 224

3. STRUCTURE OF DOCTORAL THESIS

The present doctoral thesis was built similarly to the publishable scientific articles in the case of experimental results dissemination, with its structure generally consisting of an abstract, a short introduction (it was a must to attach bibliographic references specific to each chapter, which could not be treated in full in the introductory part of the thesis), a short materials description and the experimental method, followed by results and discusions and by conclusions and recommendations. The abstract was replaced, in some chapters, where a brief introduction was preferred to descriptively approach the chapter, with few details on operations and procedures, followed by a short introductory literature review to cite, with respect, used methods.

Chapter 1 presents a global political and economic situation synthesis and biodiesel can fit in this *equation* while insisting in **1.1. Introduction** part on the opportunity and on the need to develop the field of biodiesel production. Chapter 1.1. is supported by **Chapter 1.2.** through *motivational context*, which underline the reason behind this experimental research. **Chapter 1.3.**

describes the research objectives, in accordance with motivation, both anchored in the current reality, while **Chapter 1.4.** briefly presents the structure of doctoral thesis.
With **Chapter 2** we enter the literature review part, which describes the biodiesel, elaborating on its chemistry, on its relatively easy way to obtain, with the transesterification reaction on which the process is based and with the participating reactants, as well as with the description of the catalysts types and the process conditions. With the exception of non-catalytic unconventional processes, the reaction in the other processes between triglycerides and alcohol takes place in the presence of a catalyst. Without catalyst the process procede *painfully slow* [8]. Homogeneous catalysis involves specific separation techniques, not expensive necessarly, but which can be avoided while using heterogeneous catalysis, the latter being one of the *two pillars* of this research and the reason for insisting on them in Chapter 2. In Chapter 2 the multiple techniques and methods of producing biodiesel also mentioned, over 16 in number, the conventional ones being included, this large number being the proof of the existence of multiple solutions for obtaining bio-fuel from renewable resources. The biodiesel properties and characteristics are presented and described later in this chapter, for the obvious purpose of knowing biodiesel in detail and to know why it is so similar to petrodiesel. The elaboration, as a subject, of the study on heterogeneous catalysts, comes as a theoretical support for this research regarding the catalysts/products final separation strategies. We insisted also (pictures included -*1000 words*) on the biodiesel fields of use and on the possibility of using more than the minimum of the required 6% biodiesel mixed with petrodiesel, instituted by European Union. Chapter 2 ends with the presentation of the production, biodiesel and glycerine, as well as with several solutions for a purer glycerol already during the process.

With **Chapter 3** we enter our own experimental research and after *the abstract* or after a short introduction which could not be covered in Chapter 2, we present the *construction strategy of catalytic support* split in two directions: (I) use of an *entirely transformed* lignocellulosic biomass material by thermo-chemical processes, respectively (II) use the same type of material as such, in the raw form, but still undergo certain treatments in order to prepare it for the next stage of use. **Chapter 3.1.** develops the general topic regarding lignocellulosic biomass and its availability and describes the experiments through which it is possible to arrive at the construction of a catalytic support with the expected properties. **Chapter 3.2.** focuses on the total biomass transformation as the first direction of research being in turn subdivided into multiple stages with operations aimed at obtaining a material with properties different from those originally had and folded on the application targeted in this work. **Chapter 3.3.** develops the use of raw lignocellulosic biomass in the catalytic support construction as a second research direction, respectively the obtaining in another way of a different material for the same purpose. **Chapter 3.4.** approaches biocellulose as a possible catalytic support material and it is also the final sub-chapter of Chapter 3, and at the end of the latter we have both conclusions and recommendations, or experimental and data processing personal observations.

While Chapter 3 the construction of catalytic support was described, in Chapter 4 the synthesis of the base catalyst is presented, which, combined with the catalytic support will result in the final heterogeneous catalyst that can be used in the proposed chemical reactions, according to the experimental research operations protocol. The synthesis was governed by organic chemistry, from the recipe to the purification, and the obtained product was exactly the one pursued, respectively a superbase, following to take advantage of its particular properties. The synthesis was described in detail, because the didactic characteristic was pursued as well in this research.

With **Chapter 5** we remain, with the first part, also in the area of catalyst construction and present the strategies of combining the catalytic support with the base catalyst to create the final heterogeneous catalyst, with base properties, as a central point in the strategy of integrating the heterogeneous catalyst with separation to obtain biodiesel.

Chapter 6 develops simulation and modeling in the case of transesterification in homogeneous catalysis as the first contact with what chemistry, kinetics and synthesis strategies related to biodiesel mean.

With **Chapter 7** we enter the catalyst testing area by converting vegetable oils to biodiesel. The discussions are divided, on the one hand on the obtaining biodiesel in heterogeneous catalysis, while describing the second pillar of the experimental research about integration of separation, and on the other hand on the adding of a new equipment in the biodiesel production experimental set-up, while using two different types of reactor.

The Conclusions practically conclude this paper work with the part of General Conclusions, which highlight, starting from motivation and objectives, what was achieved in this research along with few recommendations that we considered necessary, as a results of the experiments, on the principle that the theory is extraordinary but the empirical experiment seems to be closer to reality. These are followed by Original Contributions and then by the Future Research Perspectives, which highlight the level reached with this research, and, concretely, the future research steps.

4. DOCTORAL THESIS ABSTRACT

CAPITOLUL 1

Chapter 1 is relevant in terms of motivational issues, as well as the objectives proposed in this doctoral research regarding the aspects related to motivation. Thus, after the brief presentation of the political-economic global context, necessary to anchor this work to current reality, the motivational context is then revealed, from which we note, in summary, bringing back to attention the biofuel characteristics of biodiesel, the ease with which it can be produced and the relatively simple chemistry of biodiesel, as well as the multiple sectors where it could be used: agriculture, interurban transport, the military (simulations, military exercises), the industry (heating, electri generators), residential (heating, electric generators). In the same motivational context part we also included the fact that the entire doctoral thesis wishes to be a manifesto for green chemistry, a manifesto for green energy, a manifesto for the intensive production of conventional but especially non-conventional biofuels and especially a manifesto for our energy independence. The proposed objectives are aimed at integrating heterogeneous catalysis in the transesterification of vegetable oils with methanol, while using batch operated reactor and the fixed layer catalytic reactor.

CAPITOLUL 2

Chapter 2 consider the chemistry of biodiesel, with transesterification as the main reaction and the types of practicable catalysis and, quite elaborately, the current techniques and technologies of biodiesel synthesis, over 16 in number, conventional (3) but especially non-conventional, some of them used at laboratory scale and others already at industrial scale level. Emphasis was also placed on the areas of biodiesel use, where is already used as B6 (6% biodiesel/94% petrodiesel), citing recommendations from car manufacturers, in support of our claims that the use of B20 is, if not recommended, at least possible without engine modofications, while pleading, with this paper, for the use of at least B20 for the entire car fleet in Romania.

5. EXPERIMENTAL

CHAPTER 3
PREPARATION OF CATALYTIC SUPPORT FOR HETEROGENEOUS CATALYST SYNTHESIS USED FOR BIODIESEL PRODUCTION

Chapter 3 enters the experimental part of this paper.

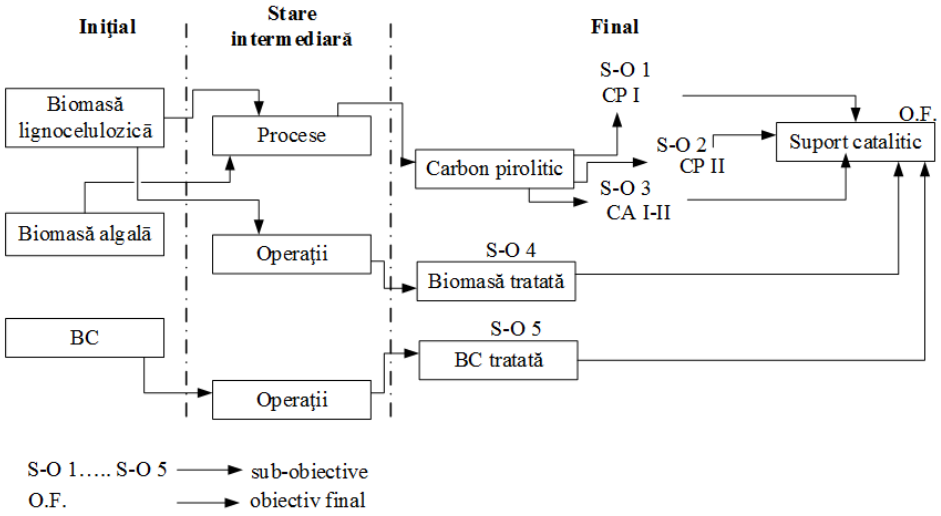


Fig. 3.1. The objectives for preparation of catalytic support stage

The main objective proposed for this stage of research was obviously catalytic support obtaining. However, several types of materials were used for is purpose so this objective was divided into sub-objectives (Fig. 3.1.).

The study of materials such as lignocellulosic biomass, algal biomass and biocellulose (BC) aimed at achieving a single target, respectively obtaining superior properties for the material and was carried out in two directions: I. Total transformation by thermal processes – pyrolysis followed by thermo-chemical activation, in the biomass case, and II. The use of of lignocellulosic biomass and BC as raw materials, by removing some chemical compounds using thermo-chemical tratments, but with preserving the main component polymers properties.

For the first direction (I) the use of pyrolytic carbon (PC) as a catalytic support was chosen. For the second direction (II) of experimental research on the type of catalytic support, lignocelluosic biomass from fruits (the stones) was used, over which different treatments were performed as well as algal biomass and biocellulose, subjected also to pretreatments before the final combination with the catalyst.

3.1. RESIDUAL LIGNOCELLULOSIC BIOMASS AND ALGAL BIOMASS FOR CATALYTIC SUPPORT PREPARATION

3.1.1. Residual lignocellulosic biomass

The quantity of available raw material (fruit stones) can be correlated with the annual production of the respective fruit, the figures or percentages regarding the stone/fruit mass ratio, although calculated empirically here (Fig. 3.7.), must nevertheless be considered indicative.

For a potential technological process that would use fruit stones as raw material the figures are reasonable, after a minimal study carried out in this paper, although they vary, even to the extreme, from one species to another and even within the same species (Tab. 3.1.).

Tab. 3.1. Stone/fruit mass ratio

Crt. no.	Fruit type	FPr [g]	FSp	Retained water	Retained water/F mass	FSp after 1 day		PuF with RRPF	S with RRPF	S without RRPF	S mass/F mass ratio	Totally dry mass S		S mass/F mass ratio
		Mass [g]	Mass [g]	Mass [g]	[%]	Mass [g]	Moisture loss [%]	Mass [g]	Mass [g]	Mass [g]	[%]	Mass ă [g]	Moisture loss [%]	[%]
1	Peaches/ nectarines	125.46	125.6	0.12	9.56E-04	110.51	-12.00	102.61	6.90	6.81	5.42	5.24	-23.05	4.18
		106.62	106.7	0.06	5.63E-04	102.72	-3.71	93.30	5.94	5.59	5.24	4.04	-27.73	3.79
		106.51	106.6	0.08	7.51E-04	100.49	-5.72	92.89	8.26	7.54	7.07	5.40	-28.38	5.07
2	Apricots	77.42	77.47	0.05	6.46E-04	74.04	-4.43	67.63	5.51	5.17	6.67	3.21	-37.91	4.15
		59.33	59.36	0.03	5.06E-04	57.35	-3.39	52.72	3.83	3.90	6.57	2.74	-29.74	4.62
		42.96	43.02	0.06	1.40E-03	41.65	-3.18	36.80	3.93	3.81	8.86	2.56	-32.81	5.96
3	Olives	9.16	9.18	0.02	2.18E-03	8.88	-3.27	6.99	1.59	1.37	14.92	1.03	-24.82	11.24
		9.12	9.14	0.02	2.19E-03	8.89	-2.74	7.25	1.42	1.14	12.47	0.87	-23.68	9.54
		7.70	7.73	0.03	3.90E-03	7.59	-1.81	6.20	1.38	1.09	14.10	0.80	-26.61	10.39
4	Cherry	5.42	5.43	0.01	1.85E-03	5.32	-2.03	4.52	0.56	0.42	7.73	0.27	-35.71	4.98
		13.29	13.32	0.03	2.26E-03	13.03	-2.18	11.34	0.84	0.60	4.50	0.43	-28.33	3.24
		10.20	10.22	0.02	1.96E-03	10.01	-2.05	8.53	0.54	0.45	4.40	0.31	-31.11	3.04
5	Mirabelles	17.66	17.68	0.02	1.13E-03	17.51	-0.96	16.40	0.95	0.77	4.36	0.64	-16.88	3.62
		16.62	16.63	0.01	6.02E-04	16.5	-0.78	15.24	0.88	0.81	4.87	0.63	-22.22	3.79
		19.50	19.53	0.03	1.54E-03	19.38	-0.77	18.22	1.01	0.87	4.45	0.69	-20.69	3.54
6	Plums	93.64	93.68	0.04	4.27E-04	92.75	-0.99	90.67	1.28	1.12	1.20	0.74	-33.93	0.79
		51.51	51.53	0.02	3.88E-04	50.77	-1.47	47.71	2.46	2.06	4.00	1.39	-32.52	2.70
		90.48	90.53	0.05	5.53E-04	88.72	-2.00	88.23	1.06	1.01	1.12	0.73	-27.72	0.81

FSp - washed fruit FPr - fresh fruit F - fruit
RRPF - residual fruit pulp residues PuF - fruit pulp S - stone



Fig. 3.7. Steps for stone mass/fruit mass ratio evaluation

3.1.2. Residual algal biomass

Species *Cystosteira barbata*[1] was selected for this work as a residual biomass, to be used



Fig. 3.8. Algal natural abundancy, viewed as a problem that need solving solutions [278-283]



Fig. 3.9. Solutions for the use of algae [284-286]

[1] *Cystosteira barbata* is a protected species, but extremely abundant on the beaches of the Romanian Black Sea coast, so we worked with quantities obtained from beaches and not from its habitat.

and transformed in catalytic support, in the pyrolysis process, but only after going through all the processing steps of its valorification.

Thus, the activated carbon from algal biomass, obtained experimentally by pyrolysis, was further functionalized and directed towards obtaining biodiesel, in this capacity as a catalytic support.

3.2. PYROLYSIS AND ASSOCIATED PROCESSES FOR CATALYTIC SUPPORT PREPARATION

The obvious goal, in the direction in which the total transformation of lignocellulosic biomass and algal biomass was chosen, was to building the base (starting material), the pyrolytic carbon I and II (PC_I, PC_{II}), from which to start the development of a first type of catalytic support from the proposed ones. This starting material was created using the pyrolysis of fruit stones and algae, with a minimum of raw material pretreatment, under the same similar process conditions, taking advantage of the experience of previous processes in terms of these process conditions [295-298]. The base once created later allowed the upgrading, as in diagram shown in Fig. 3.10., to AC_I and AC_{II}, materials with superior properties.

3.2.1. Pyrolysis

The solid material, the carbon as in the material of interest for this work, represents approximately 30-45%[2].

3.2.1.1. Materials in the pyrolysis process

[2] Obtained in the Mass Transfer Laboratory, at CBI Dep., – ACSM Faculty, UPB.

Tab. 3.2. Raw materials used in pyrolysis process

Crt.no	RM type
1	Nectarines/peaches stones (S.pi/n)
2	Apricots stones (S.cai)
3	Olive stones (S.m)
4	Cherry stones (S.ci)
5	Mirabelle stones (S.co)
6	Plum stones (S.p)
7	*Cystosteira barbata* algae (A.*Cyb*)

RM -Raw material



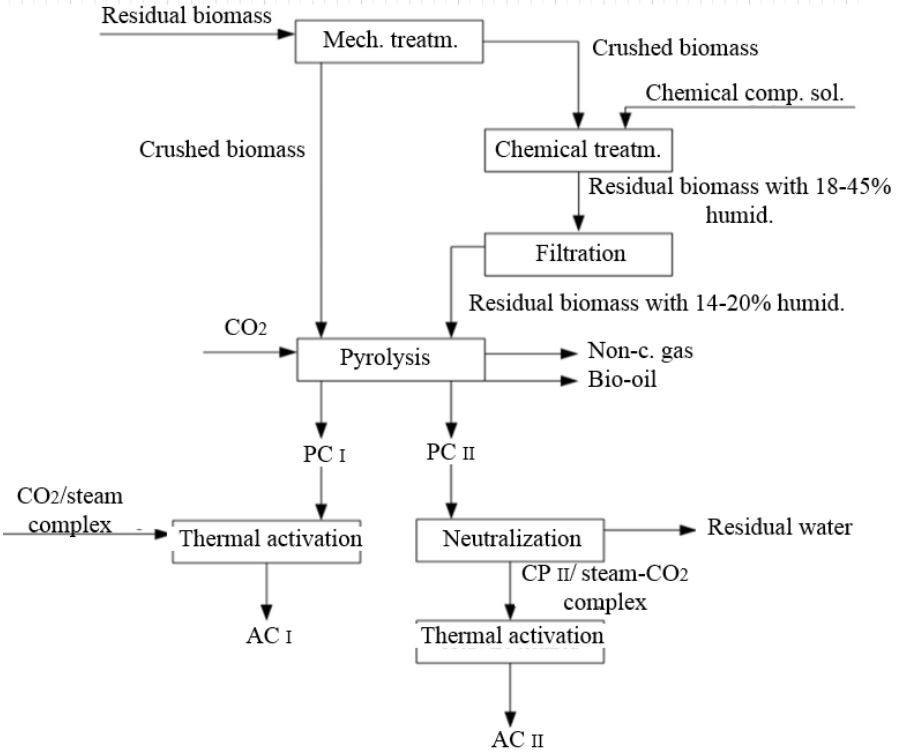


Fig. 3. 10 Flowchart of catalytic support PC $_{I-II}$ and AC $_{I-II}$ preparation

The selected *Cystosteira barbata* macroalgae species for catalytic support preparation is shown in Fig. 3.11.



Fig. 3.11. Algal biomass that can be processed, for feeding into the pyrolysis column

3.2.1.2. Experimental

3.2.1.2.a. Raw material pretreatment

Regarding the pyrolytic carbon obtaining, we opted also for two strategies: *i)* pyrolysis of the dry raw material, with a minimum mechanical treatment (only where it was needed, for example for large stones, of peaches/nectarines and apricot) and which was subsequently fed into the column as shown in Fig. 3.12.a) and *ii)* the use of a chemical treatment to force the creation of new channel in the material, as shown in the flowchart in Fig 3.12.b).

Tab. 3.3 Untreated raw materials fed into pyrolysis column

Crt.no	RM type	RM fed [g]
1	Nectarine/peaches stone (S.pi/n)	60.58
2	Apricots stone (S.cai)	120.00
3	Olive stone (S.m)	41.11
4	Cherry stone (S.ci)	100.00
5	Mirabelle stone (S.co)	55.63
6	Plum stone (S.p)	50.08
7	*Cystosteira barbata* algae (A.*Cyb*)	100.00

RM -Raw material

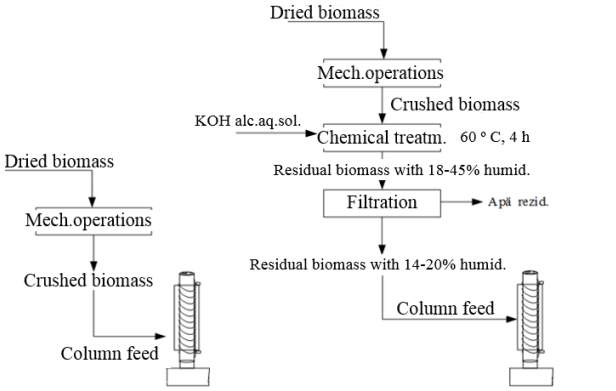


Fig. 3.2. Flowchart of RM treatment: a) without chemical treatment; b) with chemical treatment

In the chemical treatment used to influence the variation of specific surface area, we opted to treat the raw material with 1M KOH solution, before feeding into the pyrolysis column.

Tab. 3.2. Raw material (RM) and mass differences in column feedind in pyrolysyis of chemically treated mat.

Crt.no	RM type	RM fed [g]	Aq.sol. $KOH:H_2O:CH_3OH$ [g]	RM/alc.aq sol.		RM/ alc.aq.sol.after vac. filtr.		
				[g]	%	[g]	%	Rest [%]
1	S.pi/n	41.54		47.51	14.37	46.66	-1.79	12.58
2	S.cai	40.06		51.96	29.71	49.95	-3.87	25.84
3	S.m	20.31		25.69	26.49	24.66	-4.01	22.48
4	S.ci	40.11	8.4:94.6:50	54.06	34.78	51.21	-5.27	29.51
5	S.co	40.19		51.14	27.25	51.03	-0.22	27.03
6	S.p	40.16		47.25	17.65	45.39	-3.94	13.72
7	A.*Cyb*	40.50	10.85:196:60.69	192.14	374.37	70.00	-	72.84

3.2.1.2.b. Experimental set-up and procedures in pyrolysis process

The raw material was fed in the pyrolysis column piroliză (1) (of d_{COL}= 4 cm diameter, H_{COL}= 50 cm height and δ_{COL}= 0.4 cm thickness for the ceramic wall), on a layer of graphite rings of $\hbar_{1\ RINGS}$= 6 cm height. The column was fixed on a socle (2) made of high temperature resistant material and attached to a stand fixed on a support frame (3). A second layer of graphite of $\hbar_{2\ RINGS}$= 6 cm similar height was also placed over the raw material. The required energy for the pyrolysis process was provided by an electrical resistance (4) of Ni-Cr[3], of $\rho_{RES}= 1.10 \cdot 10^{-6}$ Ω·m high resistivity and $\sigma_{RES}= 9.09 \cdot 10^5$S/m conductivity, maintained by the modular glass jacket (5) of H_{jak}= 42 cm height, d_{jak} =10 cm diameter and g_{jak} =0.5 cm thickness, powered by a transformer (6), powered in turn at 220 V. The CO_2 flow, at Gv_{CO2}= 60-120 L/h values, measured and monitored by a rotameter (7), was provided by a pressurized CO_2 tank (8). The pyrolysis process temperature were measured using three chromel[4]-alumel thermocouples (9), the first one located at the base, inside the column (temperature t_s of the material layer), a second one located outside at the middle of the column, and the third thermocouple attached to the top of the column. Data on the temperatures of the integral pyrolysis process were collected with the data logger (10), which performed a signal conversion that could be taken over by the hardware system, analyzable using *Microsif* software (Fig. 3.19.)

The gases produced during pyrolysis and discharged from the column entered the condenser (11), from where one part of them condensed (bio-oil) and, using the vacuum system (12-13), could

[3]Nickel-chrom alloys, very often used, due to high resistivity and non-oxidation at very high temperatures;
[4]K-type, $\varepsilon_{AB} \sim 45$ μV/K, T_{max} = 1200 °C, where A and B are the component materials;

be collected in the graduated container (14), while the other part, in form of non-condensable gases, was vented (15), their use for other purposes[5] not being the subject of the present work.

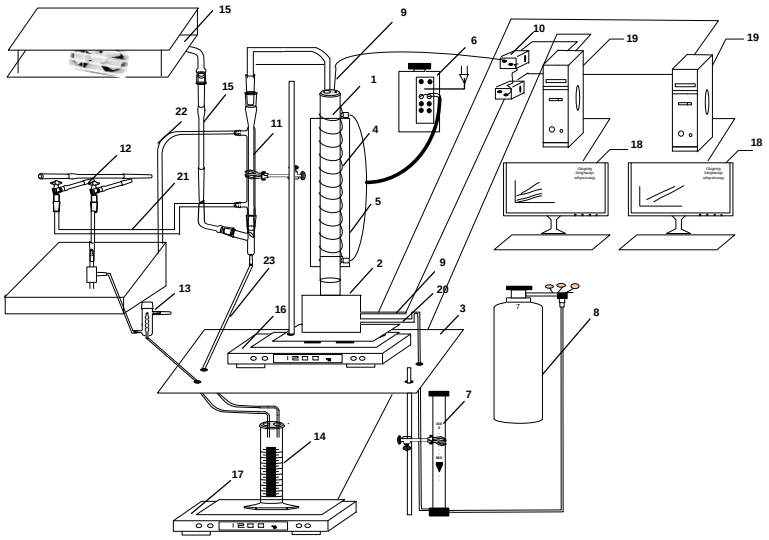


Fig. 3.17. Concrete scheme for pyrolysis experimental set-up: 1- pyrolysis column; 2- socle column; 3- installation support-frame; 4- electrical resistance; 5- column jacket; 6- transformer; 7- rotameter; 8- CO_2 tank ; 9- thermocouples; 10- data logger; 11- condenser (Liebig refrigerent); 12- water source; 13- vacuum system; 14- bio-oil collection container; 15- n.-c.gas vent; 16- carbon mass weighing balance; 17- bio-oil mass weighing balance; 18- real time monitoring; 19- hardware system; 20- column CO_2 feed; 21- cold water condenser feed; 22-condenser cold water out; 23- bio-oil control.



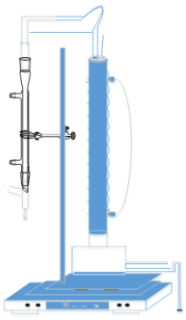
Fig. 3.18. Pyrolysis laboratory installation: pyrolysis column, vas bio-oil container, data logging and analyzing

The raw materials and the process conditions used to obtain the pyrolytic carbon (PC_I and PC_{II}) are presented Tab. 3.5. and in Tab. 3.6. The process went under similar conditions in terms of operation for all types of biomass.



Fig. 3.13. Process temperature monitored with *Microsif* app.: software interface (left- S.ci pyrolysis; right-cooling)

[5] Collection, study, reuse as energy source in the process etc



$V_{reactor}$	311.02 cm^3
$Area_{reactor}$	428.83 cm^2
Reaction temperature	520 °C
Operation duration	1.03 h
$H_{carbon\ layer}$	18 cm
Jacket ((module x (H x diam x gros.))	3 x (14 x 10 x 0.5 cm)

Fig. 3.21. Pyrolysis column technical data

Tab. 3.5. Materials and process conditions in Pyrolysis I

Crt.no.	RM type	RM fed [g]	*Gv* [L/h]	*U* [V]
1	S.pi/n	60.58	60	120
2	S.cai	120.00	60	165
3	S.m	41.11	35	140
4	S.ci	100.00	60	165
5	S.co	55.63	60	130
6	S.p	50.08	60	155
7	A.*Cyb*	100.00	120	165

RM – raw material

Tab. 3.6. Materials and process cond. in Pyrolysis II

Crt.no.	RM type	RM fed [g]	*Gv* [L/h]	*U* [V]
1	S.pi/n	46.66	60	120
2	S.cai	49.95	60	120
3	S.m	24.66	35	120
4	S.ci	51.21	60	120
5	S.co	51.03	60	120
6	S.p	45.39	60	120
7	A.*Cyb*	70	35	120

RM – raw material

3.2.1.3. Results and discussions

The characteristics of the obtained products were somewhat anticipated, given the experiments performed in previous work.

The two methods of thermo-chemical treatment, pyrolysis of *untreated* raw materials and pyrolysis of *treated* raw materials, led to the formation of products with significant differences in terms of pyrolytic carbon particle size (PC particle diameter), bio-oil mass and composition, PC texture (external surface) (Fig. 3.22.), disposing (arrangement) of PC particle. Pyrolytic carbon (solid material), as a product of the pyrolysis process, was the one we were particularly interested in, so the carbon yield was the one followed and compared between the two different methods of using the raw material for pyrolysis.



Fig. 3.22. Pyrolytic carbon from fruit stones:
Bottom row pyrolysis I (untreated stones); top row pyrolysis II (treated stones)

In the case of pyrolysis I (P I) higher percentages of solid were obtained in the algae case procente (39.80%), followed by olive stones (~28%), which would recommend them for achieving this thesis objectives (Tab 3.7.). But additional test of their behavior in the presence of chemical compounds was obviously necessary and performed later in this work. On the opposite side, the stones S.co and apricot resulted in 21.70% and 21.05% solid, respectively, in the transformation by pyrolysis, and in higher percentages than algae and olives in bio-oil, 44.22% and 48.58% respectively.

In the case of algae, the pyrolytic carbon particles evolved from dimensions of the diameter in the range 1-3 mm in P I, to agglomerations (*bulk*) with a diameter of 4-7 times larger in pyrolysis

P II, these differences being found in Tab. 3.9. PC $_{II}$ of the treated algae had a porous (macroporous) texture, dark black and crumbly, specific to all types of PC $_{II}$. On the other hand, PC $_{I}$ types had a more compact, bronze-colored external surface and kept the pre-pyrolysis geometry.

Tab. 3. 3. Pyrolysis I (untreated r.m.) and pyrolysis products

Crt.no.	RM type	RM fed [g]	CP $_{I}$ type	CP $_{I}$		Bio-oil		Non-c. gas	
				[g]	[%]	[g]	[%]	[g]	[%]
1	S.pi/n	60.58	CP $_{I}$ S.pi/n	13.37	22.07	22.90	37.80	24.31	40.13
2	S.cai	120.00	CP $_{I}$ S.cai	25.26	21.05	58.30	48.58	36.44	30.37
3	S.m	41.11	CP $_{I}$ S.m	11.60	28.22	14.70	35.76	14.81	36.03
4	S.ci	100.00	CP $_{I}$ S.ci	24.54	24.54	44.30	44.30	31.16	31.16
5	S.co	55.63	C P$_{I}$ S.co	12.07	21.70	24.60	44.22	18.96	34.08
6	S.p	50.08	C P$_{I}$ S.p	17.30	34.54	19.60	39.14	13.18	26.32
7	A.*Cyb*	100.00	C P$_{I}$ A.*Cyb*	39.80	39.80	31.30	31.30	28.90	28.90

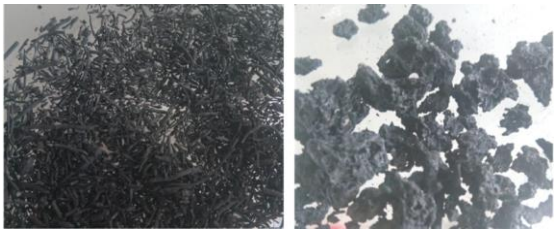


Fig. 3.23. PC $_{I}$ from untreated algae (left) and PC $_{II}$ from treated algae (right)

Regarding P II, the solid formation had a significantly changed variation and we can deduce that the impregnation influenced the raw material behavior in the pyrolysis process (Tab. 3.8.), the values for the bio-oil masses being higher but anticipated somewhat, given the percentage of aqueous alcoholic solutions present in stones and algae. More interesting was the dynamics of the solid mass, because the percentages were higher, but not for all fruit stones (Fig 3.24.).

Tab. 3. 4. Pyrolysis II (chemically treated r.m.) and pyrolysis products

Crt.no.	RM type	RM fed [g]	CP $_{II}$ type	CP $_{II}$		Bio-oil		Non-c. gas	
				[g]	[%]	[g]	[%]	[g]	[%]
1	S.pi/n	46.66	CP $_{II}$ S.pi/n	13.32	28.55	15.60	33.43	17.74	38.02
2	S.cai	49.95	CP$_{II}$ S.cai	14.55	29.13	28.50	57.06	6.90	13.81
3	S.m	24.66	CP $_{II}$ S.m	6.98	28.30	11.13	45.13	6.55	26.56
4	S.ci	51.21	CP $_{II}$ S.ci	14.94	29.17	22.60	44.13	13.67	26.69
5	S.co	51.03	CP $_{II}$ S.co	13.19	25.85	21.30	41.74	16.54	32.41
6	S.p	45.39	CP $_{II}$ S.p	13.83	30.47	17.20	37.89	14.36	31.64
7	A.*Cyb*	70.00	CP $_{II}$ A.*Cyb*	19.94	28.49	34.20	48.86	15.86	22.66

Tab. 3.5. Differences in physical characteristics of pyrolytic carbon: P I and P II comparison

Nr.crt	Tip sursă CP	Piroliza I		Tip sursă CP	Piroliza II	
		dp [cm]	Supraf. ext.		dp [cm]	Supraf. ext.
1	C $_{I}$ S.pi/n			C $_{II}$ S.pi/n		
2	C $_{I}$ S.cai			C $_{II}$ S.cai		Sfărâmicioasă
3	C $_{I}$ S.m	Geom.	Compactă	C $_{II}$ S.m	Geom.păstrată	Aspect
4	C $_{I}$ S.ci	păstrată		C $_{II}$ S.ci	parţial	cărbunos
5	C $_{I}$ S.co			C $_{II}$ S.co		Sâmburi sparţi
6	C $_{I}$ S.p			C $_{II}$ S.p		
7	C $_{I}$ A.*Cyb*	0.1-0.2		C $_{II}$ A.*Cyb*	0.4-1.4	

At CP $_{II}$ from S.pi/n, S.cai, S.ci and S.co the mass of solid had higher value then the one in P I, with percentages between 4 and 7%, while in the algae and plum stones case their mass in P I had values by 4-11% higher. The mass of solid of pyrolytic carbon from olive was similar in both types of pyrolysis.

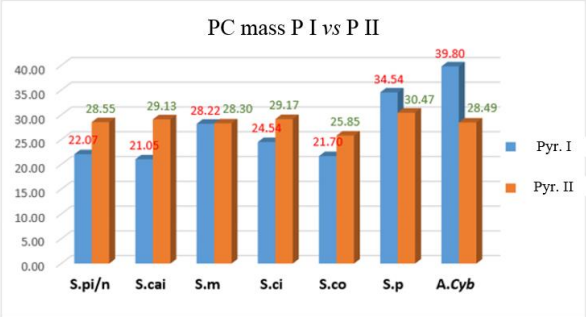


Fig. 3.4. Mass of solid (%) at the end of pyrolysis: P I and P II comparison

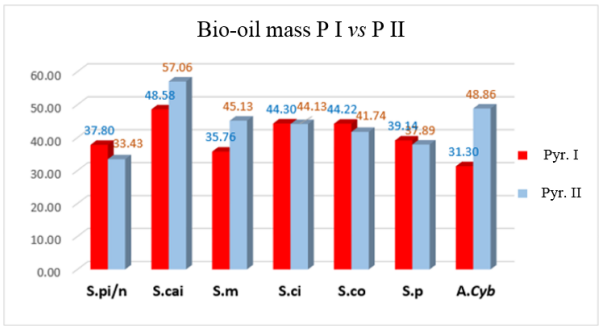
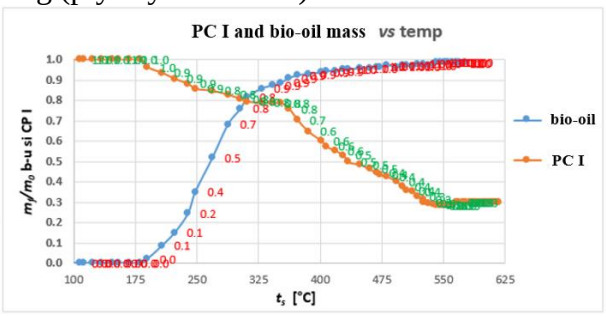


Fig. 3.5. Mass of bio-oil (%) at the end of pyrolysis: P I and P II comparison

In the case of the bio-oil mass, the same observations can be made at the end of the process (Fig. 3.25.), noting however that this is a particular case of pyrolysis technique, the proportion of *aqueous content* being more than significant at the start of the process and then again in the resulted bio-oil. In PC $_{II}$ from S.cai, S.m and A.*Cyb* the bio-oil were in percentages with 8.5-18% values, while in the rest they were lower (2.4-4.3%).

Using the same operating procedures, especially in terms of providing a minimum temperature in the column loaded biomass layer, the temperature variation over time and the mass of PC and bio-oil, respectively (Fig. 3.17) had similarities in the same technique of material processing (piyrolysis I and II).



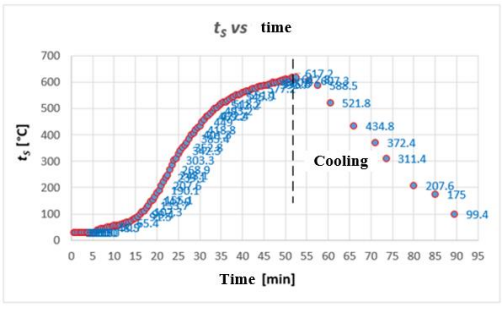


Fig. 3.6. PC $_{I}$ mass variation (left) and PC $_{II}$ mass variation (right), over t_s

Particular attention was paid to PC $_{I}$ and PC $_{II}$ having as source the algal biomass in order to achieve an extension of algal utility cycle, aiming that the total transformation by thermo-chemical treatment to represent a new start of their usefulness. An elemental analysis of PC $_{I}$ from algae was also performed, knowing that, in the case of organic material, PC contains atoms (elements) from precursors.

From the performed elemental analysis (*EDAX Apex*), shown in Fig. 3.27., we find heteroatoms, present, dispersed and (some) in significant proportions, also anticipated, because the pyrolysis proceded, in its integral, at a t_s layer temperature below 1000 °C. Or heteroatoms are present up to much higher temperatures.

In the particular case of algae we must also consider the marine environment in which they are found and, most importantly, are multicellular organisms, which implies the existence of metabolic processes, which explains the presence of peaks (or at least the existence), quite meaningful, of the elements.

PC $_{I}$ from pyrolyzed algae at t_s= 617.5 °C shows a morphology characterized by symmetry and a relatively small number of channels (pores), as shown Fig 3.28.-1.a. Similarities are also found in Fig 3.28.-2.a. and 3.a. (algae from the same batch), PC being obtained in the same operating conditions.

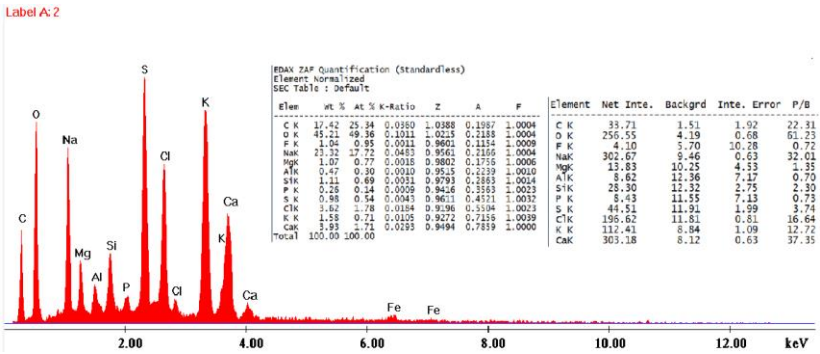


Fig. 3.7. PC $_{I}$ elemental analysis from pyrolyzed algae in P I

operation. By pyrolytic decompositionof the starting material the resulting elemental carbon is grouped by crosslinking into layers of polyaromatic compounds in a random manner. If we go in detail, in Fig.3.28.-1.b, 2.b. and 3.b this aspect is observed as well as agglomerations in the edges area, in conjunction with the interstices resulting from the bonding of these compounds.

BET analysis for PC $_{I}$ from pyrolyzed algae, carried out in order to characterize the S_{BET} specific surface area and PC porosity, was performed using *ASAP 2020 Micromeritics*, the value determined being S_{BET}= 55.49 $m^2 \cdot g^{-1}$. In the case of PC $_{I}$ from S.ci (Fig. 3.29.), the SEM analysis revealed a specific compact surface, with reletively reduced pore areas [294].

3.2.1.4. Conclusions

Residual biomass, algal or lignocellulosic type, comes with several advantages when it is considered to be used for the development of materials with new functions (functionalities), as a result of its processing. Thermo-chemical treatments on biomass managed to create these characteristics of materials, pyrolysis (usually followed by an activation at temperatures above the pyrolysis ones) overlapping applications in which these newly created materials can participate. The two strategies regarding the use of biomass, with or without treatment resulted in the creation of two new material types, with quite significant differences in their characteristics.

The assumption that the post-pyrolysis displacement of KOH molecules, from the treatment solution, will favour the creation of a more developed pores network, was validated by the subsequent activation process, to which the materials were subjected. A material was thus obtained (PC $_{I}$ and PC $_{II}$ type) for the catalytic support proposed, usable further in other functionalizations.

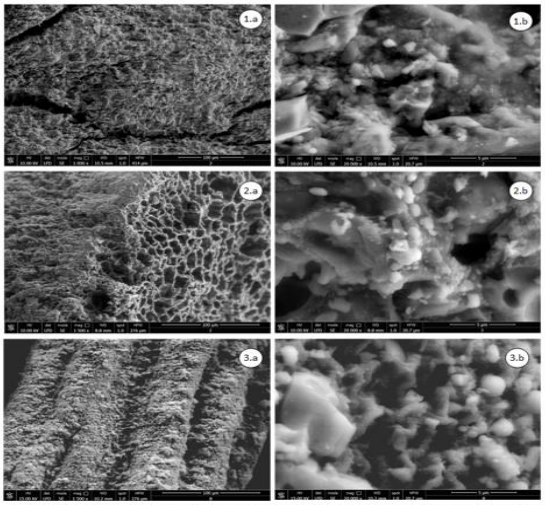


Fig. 3.19. SEM images of pyrolyzed algae: 1.a. and1.b algae studied in this work; 2.a. and b. and 3.a and 3.b –algae from same lot, pyrolyzed in the same operation conditions.

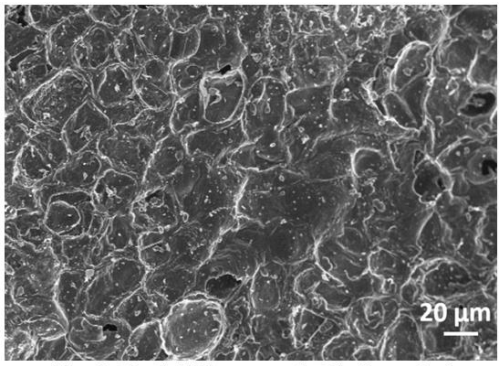


Fig. 3.29. SEM images of PC $_{I}$ from S.ci

3.2.2. Activation – End process in carbon-type catalytic support preparation

Thermal activation, as a strategy to improve the carbon properties, is positioned after the pyrolysis through which it is obtained, and before functionalization by various methods, with specificities modeled on applications.

3.2.2.1 Materials used in activation process

Tab. 3.10. Materii prime la activarea I (A_I)

Nr.crt.	Tip MP	MP alim. [g]	*Gv* [L/h]	*U* [V]
1	CP $_I$ S.pi/n	5.8	5	140
2	CP $_I$ S.cai	7.5	5	140
3	C $_I$ S.m	8.0	5	140
4	C $_I$ S.ci	10.01	5	190
5	C $_I$ S.co	10.03	10	165
6	C $_I$ S.p	8.2	5	150
7	C $_I$ A.*Cyb*	8.0	5	160

MP - materie primă

Tab. 3.11. Materii prime la activarea II (A_{II})

Nr.crt.	Tip MP	MP alim. [g]	*Gv* [L/h]	*U* [V]
1	CP $_{II}$ S.pi/n	6.20	20	165
2	CP $_{II}$ S.cai	7.13	20	160
3	CP $_{II}$ S.m	4.50	20	165
4	CP $_{II}$ S.ci	7.50	20	165
5	CP $_{II}$ S.co	6.07	20	130
6	CP $_{II}$ S.p	5.80	20	150
7	CP $_{II}$ A.*Cyb*	5.33	20	160

MP - materie primă

Tab. 3.10 Materials in Activation I (A_I)

Crt.no.	Tip MP	RM fed [g]	*Gv* [L/h]	*U* [V]
1	CP $_I$ S.pi/n	5.8	5	140
2	CP $_I$ S.cai	7.5	5	140
3	C $_I$ S.m	8.0	5	140
4	C $_I$ S.ci	10.01	5	190
5	C $_I$ S.co	10.03	10	165
6	C $_I$ S.p	8.2	5	150
7	C $_I$ A.*Cyb*	8.0	5	160

RM – raw material

Tab. 3.11. Materials in Activation II (A_{II})

Crt.no.	RM type	RM fed [g]	*Gv* [L/h]	*U* [V]
1	CP $_{II}$ S.pi/n	6.20	20	165
2	CP $_{II}$ S.cai	7.13	20	160
3	CP $_{II}$ S.m	4.50	20	165
4	CP $_{II}$ S.ci	7.50	20	165
5	CP $_{II}$ S.co	6.07	20	130
6	CP $_{II}$ S.p	5.80	20	150
7	CP $_{II}$ A.*Cyb*	5.33	20	160

RM – raw material

3.2.2.2 Experimental

The scheme of operations for this research part can be seen in Fig. 3.31. and describes the way in which the experiments are resumed after the pyrolysis process.

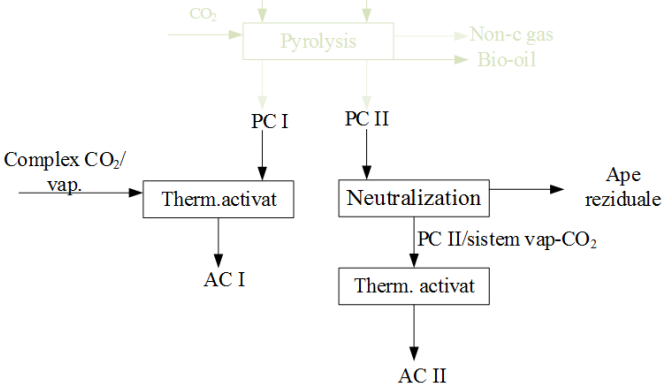


Fig. 3.8. Simplified diagram of operations for carbon *up-grade* using thermo-chemical activation

3.2.2.2.a. Pretreatment operations

Pyrolytic carbon activation

At the end of the pyrolytic process, the carbon was stored in optimal conditions, without acces to atmospheric humidity. Thus, for activation, it was used as such, without any other treatment.

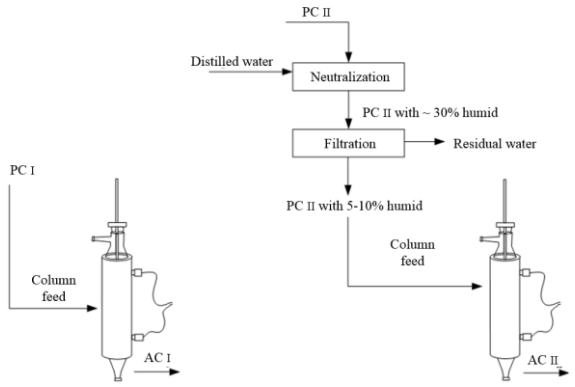


Fig. 3. 9. Operations for carbon activation PC $_{I}$ and PC $_{II}$

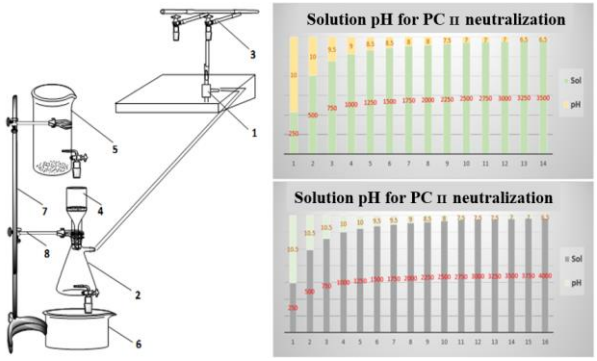


Fig. 3.10. Neutralization experimental set-up installation and pH dynamics (pH for CP $_{II}$ S.ci- above; CP $_{II}$ S. *A.Cyb* -below): 1) vacuum pump; 2) vacuum tube; 3) water source; 4) porosity funnel; 5) 2 L distilled water vessel;6) residual water collecting; 7) stand; 8) clamp

Chemically treated carbon activation

PC obtained after a chemical treatment was subjected to neutralization to displace KOH from the pyrolytic carbon pores, so that after the activation being possible to expand and rearrange the pores in a different network. The pH values of neutralization were pH=10 at the beginning of the PC immersion, reaching at the end, after successive washes, to the pH of distilled water (Fig 3.32.). The carbon thus treated was prepared for subsequent feeding into the thermal activation column.

3.2.2.2.b. Procedure and experimental set-up

The activation temperature in the layer, t_{Sa}, was measured using a thermocouple. The duration of the activation process was 1.5 h, consisting of the time required to reach the temperature of 837.5-1200 °C, to which was added the actual time to obtain the properties pursued by activation.

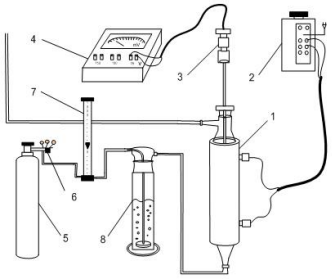
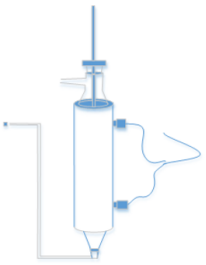




Fig. 3.11. Experimental installation for thermo-chemical activation of PC $_{I}$ and PC $_{II}$ 1) thermal activation column; (2) transformer; (3) thermocouple; (4) voltmeter; (5) CO_2 tank; (6) valve; (7) rotameter; (8) bubbler.



V $_{reactor}$	67.54 cm^3
Area $_{reactor}$	141.37 cm^2
Reaction temperature	937.5 °C
Operating duration	0.92 h
H $_{carbon\ layer}$	12 cm
Jacket (H x diam x thick.)	14 x 10 x 0.5 cm

Fig. 3.12. Technical data of thermal activation column

Tab. 3.12. PC $_{I}$ mass and process conditions in AC $_{I}$ activation

Crt.no.	RM type	RM fed [g]	CO_2 [L/h]	U transf. [V]	U Voltm. [mV]	Temp [C]
1	CP $_{I}$ S.pi/n	5.8	5	140	37	925.0
2	CP $_{I}$ S.cai	7.5	5	140	35	875.0
3	CP $_{I}$ S.m	8.0	5	140	35	875.0
4	CP $_{I}$ S.ci	10.01	5	190	48	1200.0
5	CP $_{I}$ S.co	10.03	10	165	38	950.0
6	CP $_{I}$ S.p	8.2	5	150	37	937.5
7	CP $_{I}$ A.*Cyb*	8.0	5	160	37	937.5

Tab. 3.13. PC $_{II}$ mass and process conditions in AC $_{II}$ activation

Crt.no.	RM type	RM fed [g]	CO_2 [L/h]	U transf. [V]	U Voltm. [mV]	Temp [C]
1	CP $_{II}$ S.pi/n	6.20	20	165	37.0	925.0
2	CP $_{II}$ S.cai	7.13	20	160	37.5	937.5
3	CP $_{II}$ S.m	4.50	20	165	38.5	962.5
4	CP $_{II}$ S.ci	7.50	20	165	38.0	950.0
5	CP $_{II}$ S.co	6.07	20	130	35.5	887.5
6	CP $_{II}$ S.p	5.80	20	150	35.5	887.5
7	CP $_{II}$ A.*Cyb*	5.33	20	160	37.2	930.0

3.2.2.3. Result and discussions

Initially, the activation of CP $_{I}$ was also attemted, directly, as a solid product from pyrolysis, in order to preserve the base centers resulted after the biomass treatment with aqueous potassium methoxide, but due to the KOH melting point of ~360 °C and boiling point of 1327 °C, it was

expected that, following the water condensation, the melted KOH would have been sequestered in the PC pores in formation (Fig. 3.36.).



Fig. 3.13. PC $_{I}$ at the end of P I, with traces of KOH on the external surface

The post-pyrolysis washes to remove the powders were practically transformed into neutralizations, the pH of the aqueous solution at the initiation of neutralization being 10-10.5, so that only at the end to reach values closed to the pH of distilled water (Fig. 3.33.). Thus, the displacement of KOH particles succeeded with these neutralizations of pyrolytic carbon PC $_{II}$, with significant differences in the mass of AC $_{II}$.

Tab. 3.14. PC $_{I}$ mass and process conditions in AC $_{I}$ activation

Crt.no.	RM type	RM fed	AC $_{I}$ type	AC $_{I}$ mass	
		[g]		[g]	%
1	CP $_{I}$ S.pi/n	5.80	CA $_{I}$ S.pi/n	5.40	-6.90
2	CP $_{I}$ S.cai	7.50	CA $_{I}$ S.cai	6.90	-8.00
3	CP $_{I}$ S.m	8.00	CA $_{I}$ S.m	7.28	-9.00
4	CP $_{I}$ S.ci	10.01	CA $_{I}$ S.ci	8.94	-10.69
5	CP $_{I}$ S.co	10.03	CA $_{I}$ S.co	9.64	-3.89
6	CP $_{I}$ S.p	8.20	CA $_{I}$ S.p	7.91	-3.54
7	CP $_{I}$ A.*Cyb*	8.00	CA $_{I}$ A.*Cyb*	7.62	-4.75

Tab. 3.15. PC $_{II}$ mass and process conditions in AC $_{II}$ activation

Crt.no.	RM type	RM fed	AC $_{II}$ type	AC $_{II}$ mass	
		[g]		[g]	%
1	CP $_{II}$ S.pi/n	6.20	CA $_{II}$ S.pi/n	5.40	-12.90
2	CP $_{II}$ S.cai	7.13	CA $_{II}$ S.cai	6.49	-8.98
3	CP $_{II}$ S.m	4.50	CA $_{II}$ S.m	3.95	-12.22
4	CP $_{II}$ S.ci	7.50	CA $_{II}$ S.ci	7.01	-6.53
5	CP $_{II}$ S.co	6.07	CA $_{II}$ S.co	5.69	-6.26
6	CP $_{II}$ S.p	5.80	CA $_{II}$ S.p	5.43	-6.38
7	CP $_{II}$ A.*Cyb*	5.33	CA $_{II}$ A.*Cyb*	4.76	-10.69

While PC $_{I}$ S.p and PC $_{I}$ S.co contracted with values of mass percentages of 3.54 and 3.89, respectively, it should be noted, at the opposite side, PC $_{I}$ S.ci, with a contraction of ~11%, which confirms the particular behavior of the source (cherry stones) throughout these treatments.

On the other hand, when activating PC $_{II}$, we find larger differences from PC $_{I}$, but explainable as mentioned, by the pores initially occupied and then emptied during the washing/neutralizations operations.

As with the pyrolysis carried out under similar operating conditions, a similar behavior was observed at activation also regarding the dynamic of the layer t_{Sa}, as can be seen in Fig.3.37.

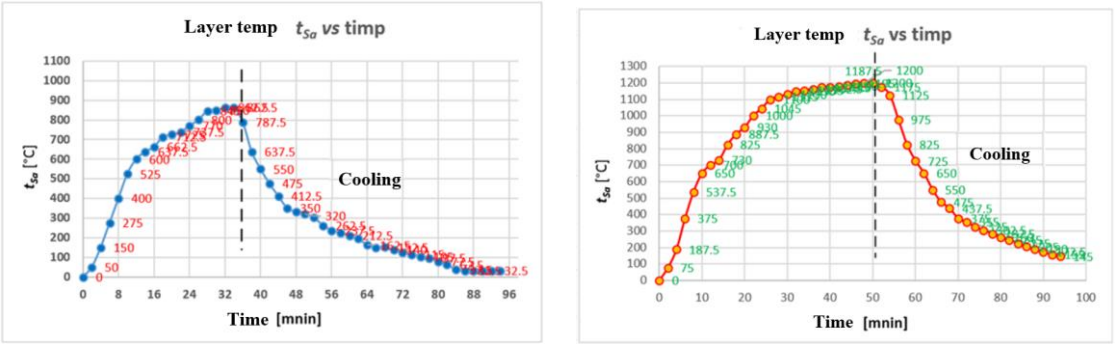


Fig. 3.14. Dynamics of pyrolytic carbon mass during activation: PC $_{I}$ S.m (left), PC $_{I}$ S.ci (right)

The activation conditions were identical for all types of carbon obtained by pyrolysis of residual biomass, from all sources.

The elemental analysis performed also in the case of algal AC $_{I}$ reveals minor changes regarding the presence of heteroatoms, because the activation also was carried out below 1000 °C of t_{Sa} layer temperature.

Regarding the algal AC $_{I}$ morphology, from the SEM images shown in Fig. 3.39. a difference is observed between the AC $_{I}$ A.*Cyb* surface (Fig.3.39.- CA.a) and that of PC A.*Cyb* (Fig.3.39.-1.a.), even if not significant, at the conformation of the walls and of the channels that appear to be newly created, a more pronounced difference probably being obtained in conditions of higher temperatures than t_{Sa} of 945 ºC.

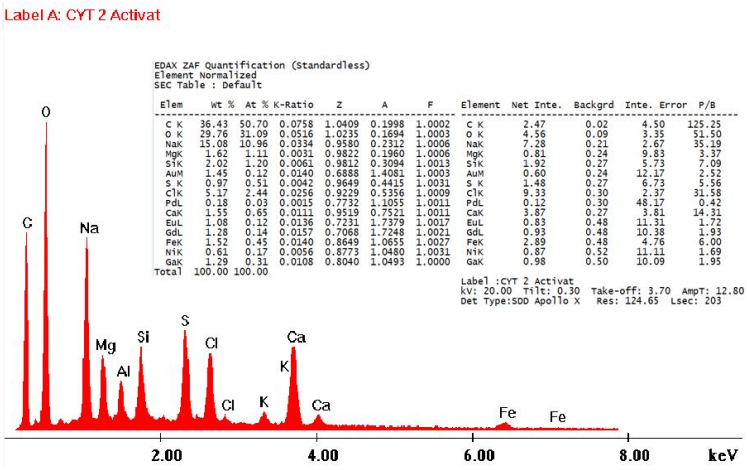


Fig. 3.15. Elemental analysis of C $_{I}$ A.*Cyb*

If we go more into detail we can draw the same conclusion regarding the presence of the same newly created channels, as show in Fig. 3.39.

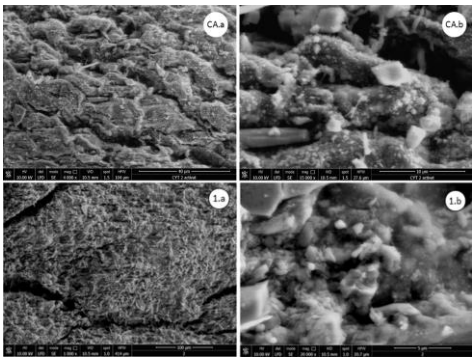


Fig. 3.39. SEM analysis for algal activated carbon AC $_{I}$ A.*Cyb*: CA.a (x4000) and detailed CA.b (x15000), in comparison with cu PC $_{I}$ A.*Cyb* algal pyrolytic carbon: 1.a and detailed1.b (x20.000)

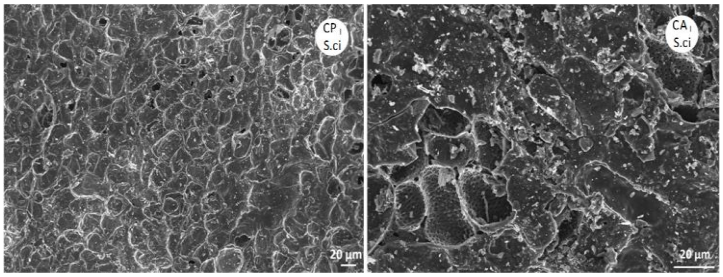


Fig. 3.16. SEM analysis for cherry stone activated din carbon AC $_{I}$ S.ci, in comparison with cherry stone pyrolytic carbon PC $_{I}$ S.ci

Same differences can be observed in the case of AC $_{I}$ S.ci, where SEM analysis of the surface morphology (Fig. 3.40.) reveals them in the pore structure, in terms of dimensions, larger in the case of AC $_{I}$ S.ci, compared with PC $_{I}$ S.ci, but also as form of the pores network, with a more numerous presence of them.

3.2.2.4. Conclusions and recommendations

The use of lignocellulosic biomass for the development of a catalytic support, through a process of total transformation followed by an upgrading, has led to obtaining materials with the expected properties, in terms of thermo-chemical stability or enhanced specific internal surface, represented by a network of different sizes, as future host centers for the molecules collision (and bonding) of different substances at further processing.

Following the pyrolysis process, the mass of the material obtained per batch, in the untreated raw biomass case, had values between 50-150 g/*batch* and reached yields in the expected ranges, due to the method used in previous work and applied here, highlighted in *Results and discussions*, chapter 3.2.1.3.

The novelty compared with our previous studies was the introduction of that percentage of moisture that would be present during pyrolysis, to the detriment of the composition of bio-oil, which should thus be further processed (separation and *upgrade*), but with obvious influence on

both on the external (visible) and the internal surface of the material, aspects that we will note as recommendations.

The discussion is also interesting from the perspective of the type of biomass material used. *S.cai* or *S.pi/n* had a different behavior from *S.m* for example, so that, regarding the material used, the recommendation is that in the pyrolysis process in which the raw material is of *S.cai* type, the process temperature of 600 °C is sufficient, obviously in correlation also with a lower energy consumption, thus with a lower end cost.

The differences also, in the case of biomass, between the properties of the materials obtained in the pyrolysis of the treated biomass, respectively of the untreated one, suggest a future approach to the treatment of the raw material, given that the characteristics regarding the specific surface and pore volume were significantly increased for the latter, which allows our recommendation to be in this regard.

The differences between the types of biomass could be made at this stage in terms of their characteristics and not their quality of catalytic support, the latter being able to be characterized only in the subsequent stages of research, during impregnation and testing.

By achieving the proposed for this stage, obtaining PC_{I-II} and AC_{I-II}, the catalytic carbon support was built but in the form of several materials type (Fig.3.41.)



Fig. 3.41. Lignocellulosic biomass catalytic material obtained by pyrolysis and thermal activation

3.2.3 Adsorption - process, testing and characterization

3.2.3.2. Materials

The materials used at this stage were silica gel, for drying the entraining agent (atmospheric air) Materialele folosite în acest stadiu au fost silicagelul, pentru uscarea agentului antrenant (aerul atmosferic), Trichloroethylene[6] (TCE) as volatile organic compound, while the adsorbent material was the one obtained in Chapter 3.2.2., respectively AC $_{I}$ and AC $_{II}$.

3.2.3.3. Experimental

In this context, the two types of activated carbon AC $_{I}$ and AC $_{II}$ were tested for their adsorption capacity at equilibrium [301], as an ability, on the one hand, for the subsequent activities of functionalization or combination of this type of catalytic support with a liquid catalyst as an ability to retain physically or even by chemosorption different chemical compounds and, on the other hand, as a method of obtaining, as verifying the appropriateness of the operations supported by the material in P I, P II, A I and A II.

AC $_{I}$ and AC $_{II}$ were in turn the adsorbents used (Tab. 3.16 and Tab. 3.17.). The time between measurements was set to 1 min, while 40 °C was selected as the process temperature, the process conditions being maintained when using each type of AC. The height H_{Sad} of the adsorbent layer in the column and *Gv* as the volumetric air flow measured by a rotameter, were considered.

[6] $ClCH=CCl_2$, M_{TCE}= 131.38 g/mol, ρ_{TCE}=1.46 g/cm, p.f.= 87.2 °C, p.vap.=7.8 kPa la 20 °C.

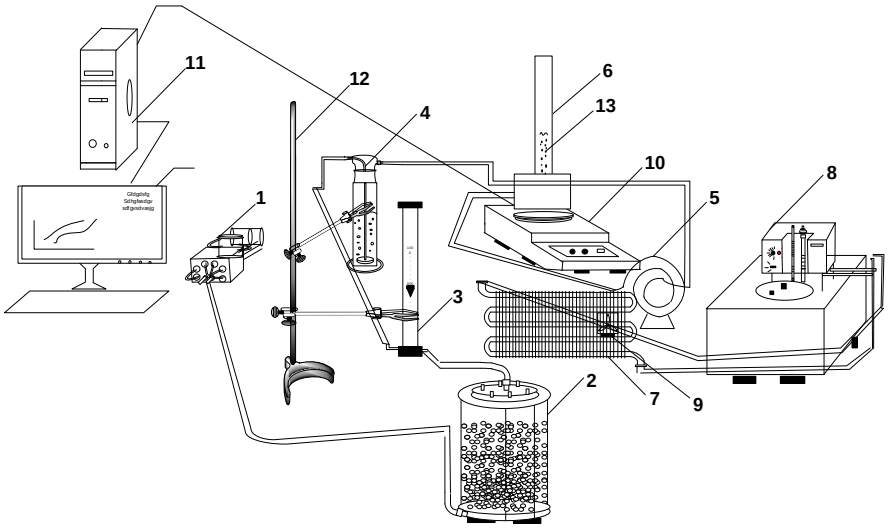
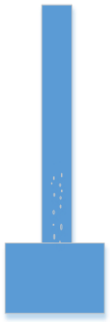


Fig. 3.17. Concrete scheme of laboratory adsorption installation: (1) – compressor; (2) – sealed silicagel chamber; (3) – rotameter; (4) – bubbler; (5) – circular heat exchanger; (6) – glass adsorption column; (7) finned tube heat exchanger; (8) – thermostatic water bath; (9) - fan (9); (10) – analytical balance; (11) – data acquisition system (computer) (11). (12) – stand; (13) – adsorbent activated carbon .



Fig. 3.18. Laboratory scale installation for adsorption process: full, adsorption column inside of chamber, compressor, bubbler, silica-gel chamber



$V_{reactie}$	41.55 cm^3
$Aria_{reactor}$	80.57 cm^2
Temp. reacție	40 °C
Durata de operare	1.30 h
$H_{strat\ carbon}$	10 cm
Grosime perete	0.5 cm

Fig. 3.19. Technical data for adsorption column

Tab. 3.6. Mass of AC $_I$ and adsorption process conditions

Crt.no.	AC Type	AC mass fed [g]
1	AC $_I$ S.pi/n	5.20
2	AC $_I$ S.cai	6.00
3	AC $_I$ S.m	5.90
4	AC $_I$ S.ci	8.00
5	AC $_I$ S.co	6.30
6	AC $_I$ S.p	5.60
7	AC $_I$ A.*Cyb*	10.00

Tab. 3. 7. Mass de CA $_{II}$ and adsorption process conditions

Crt.no.	AC Type	AC mass fed [g]
1	AC $_{II}$ S.pi/n	4.51
2	AC $_{II}$ S.cai	4.58
3	AC $_{II}$ S.m	5.60
4	AC $_{II}$ S.ci	6.02
5	AC $_{II}$ S.co	4.12
6	AC $_{II}$ S.p	6.11
7	AC $_{II}$ A.*Cyb*	3.29

In the case of using quantities of 20 g of adsorbent (commercially activated carbon), the operating time was in the range of 90-110 min, and 50-80 min in the case of using 10 g, under the

influence of process temperature (25-40 °C)[7]. Below these values of adsorbent quantities fed in the column, the operation duration was reduced to 30-45 min, and added to the time allocated to the pre- and post-process operation, it was in the range of 1.5-2.5 h per entire batch.

3.2.3.4. Results and discussions

The values obtained after the process can be found in Tab. 3.18 and Tab. 3.19

Tab. 3.8. VOC adsorption on AC $_{I}$ - results

Crt.no.	AC Type	AC				Bubbler		G_{vaer}	Temp.
		m_i [g]	d_mp cm	H_{Sad} [cm]	m_f [g]	m_{bi} [g]	m_{bf} [g]	[L/h]	[°C]
1	AC $_{I}$ S.pi/n	5.20	0.6	11	5.36	467.12	459.2	15	40
2	AC $_{I}$ S.cai	6.00	0.50	9.00	6.22	459.20	452.80	30	40
3	AC $_{I}$ S.m	5.90	0.35	9.00	6.07	422.30	416.40	15	40
4	AC $_{I}$ S.ci	8.00	0.25	10.00	8.31	416.40	406.10	15	40
5	AC $_{I}$ S.co	6.30	0.25	11.00	6.48	364.50	369.20	20	40
6	AC $_{I}$ S.p	5.60	0.45	11.00	5.73	387.12	382.24	20	40
7	AC $_{I}$ A.*Cyb*	10.00	0.15	10.00	10.26	382.24	373.20	15	40

Tab. 3.9. VOC adsorption on AC $_{II}$ - results

Crt.no.	AC Type	AC				Bubbler		G_{vaer}	Temp.
		m_i [g]	d_mp cm	H_{Sad} [cm]	m_f [g]	m_{bi} [g]	m_{bf} [g]	[L/h]	[°C]
1	AC $_{II}$ S.pi/n	4.51	0.8	11	4.81	398.04	389.30	30	40
2	AC $_{II}$ S.cai	4.58	0.50	9	4.94	365.20	353.55	30	40
3	AC $_{II}$ S.m	5.60	0.50	9	5.92	353.55	342.20	30	40
4	AC $_{II}$ S.ci	6.02	0.30	10	5.60	401.39	388.70	30	40
5	AC $_{II}$ S.co	4.12	0.30	11	4.40	417.82	410.42	30	40
6	AC $_{II}$ S.p	6.11	0.50	11	5.94	432.50	424.31	30	40
7	AC $_{II}$ A.*Cyb*	3.29	0.70	10.0	3.62	356.89	347.47	30	40

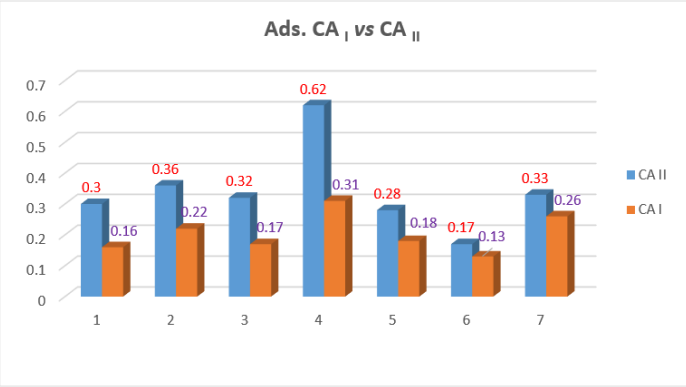


Fig. 3.20. Dynamic of adsorption capacity of *TCE* on AC I and AC II adsorbent types

What interested us after this test was the adsorption capacity of CA $_{II}$, by determining the distribution coefficient for TCE adsorption.

Determination of the distribution coefficient in TCE adsorption on AC $_{II}$ A.*Cyb*

Experimental trichlorethylene adsorption data on AC $_{II}$ A.*Cyb* (Fig. 3.46.) were performed using the experimental installation shown in Fig. 3.43. Recordings at 60 sec. of the mass dynamic of CA $_{II}$ A.*Cyb* fed into the adsorption column shows that here takes place a process of fixing the vaporized TCE from the air stream passing through the layer.

[7] VOC adsorption previously performed in the laboratory of TM, ICB, CASM, UPB

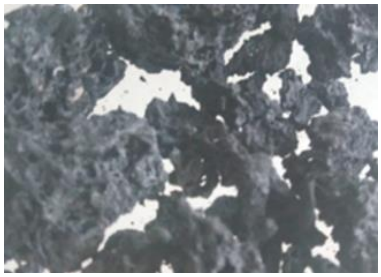


Fig. 3.46. AC $_{II}$ A.*Cyb* as adsorbent type at VOC (TCE) adsorption onto activated carbon

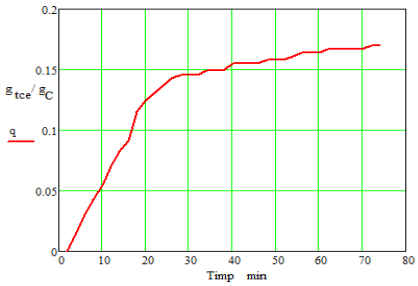


Fig. 3..47. Dynamic of AC $_{II}$ A.*Cyb* layer saturation with TCE

Considering $m_{iCA\ II\ A.Cyb}$ = 3.29 g as the mass of adsorbent layer, the saturation dynamics of the fixed blayer shown in Fig.3.47. was obtained.
It was found that the saturation was reached at q_∞ = 0.165 g_{tce}/g_C. Considering the experimental data, the TCE concentration in the air, in the experiment, expressible by the relation in Ec.3.1, was 0.76 $g_{tce}/l_{aer\ poluat}$.

$$c_\infty = \frac{m_{b0} - m_{bf}}{G_v \tau_f} \qquad \textbf{Equation 3.1.}$$

$$k_d = \frac{q_\infty}{c_\infty} \qquad \textbf{Equation 3.2.}$$

According to the relation in Ec.3.2., the distribution coefficient of TCE at adsorption on AC II A.*Cyb* has the value of 0.224 $l_{poluted\ air}/g_C$. It is a good value if this adsorbent material is used (aici CA $_{II}$ A.*Cyb* in this case) for the depollution of gases containing volatile organic components, a feature that benefits the selection of this type of adsorbent, or, in our case, of catalytic material that will later be used in combination with the base catalyst propesed for this research.

3.2.3.5. Conclusions

The adsorption capacity varied significantly between the two types of adsorbent used, which shows that the processing of materials, differently approached, gave results..
A particular case was that of AC_{II} S.ci, in which the adsorption capacity was high, but moreover, desorption was of 0.23 compared to 0.5 (values in grams for VOC residue in the adsorbent mass), which means that we can already discuss about the sequestration of the volatile organic compound rather than adsorption.

3.3. RAW RESIDUAL LIGNOCELLULOSIC BIOMASS FOR CATALYTIC SUPPORT PREPARATION



Fig. 3.48. Fruit types, with characteristic stones as residual lignocellulosic biomass

The selection of the lignocellulosic biomass was finalized, for study and experimental, by keeping six types of residual materials, respectively from six varieties of fruit stones, presented in Tab. 3.20.

3.3.2. Materials

The raw materials can be found in Tab. 3.20., and in order to bring them into an operable form they underwent operations. Thus, after the separation of the endocarp, it had to be further processed for the pulp residues removal, followed by the treatment with slightly base alcoholic solution, for decontamination and initiating to use the $–OCH_3$ functional group at this stage of the material, following successive external surface treatments.

Tab. 3.10. Materials used to develop the catalytic support

Crt.no	RM type
1	Nectarine/peaches stone (S.pi/n)
2	Apricots stone (S.cai)
3	Olive stone (S.m)
4	Cherry stone (S.ci)
5	Mirabelle stone (S.co)
6	Plum stone (S.p)

RM -Raw material





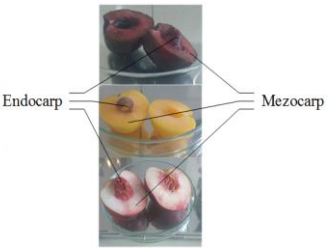


Fig. 3.49. Endocarp as residual lignocellulosic biomass of interest

3.3.3. Experimental

3.3.3.1. Physico-mechanical treatment

The treatments of physico-mechanical nature were applied in order to obtain the maximum finish in terms of the ability to model the material, in the sense of obtaining characteristics that allow the next stage of treatment, namely chemical treatment.

A series of operations were performed in an order imposed somewhat by the condition of the material immediately after the detachment of the endocarp from the mesocarp (Fig. 3.50), respectively the presence of mesocarp residues, or the existence of less hard or not well-attached textural pieces (which, under certain treatments or during the reaction, can detach easily, contaminating the reaction medium, as solid particles, with possible action of inhibitors or generators of additional centrifugation operations for their removal - Fig. 3.51.) etc.

Thus, after detachment, the mesocarp residues were manually removed (the fruit stones not being that large, otherwise mixing equipment being needed simultaneously with the washing of the residues) and then the stones were prepared them for drying process. Thermobalance drying, which



Fig. 3.50. Fruit and endocarp (stone) detached, with pulp residues that require additional removal operation

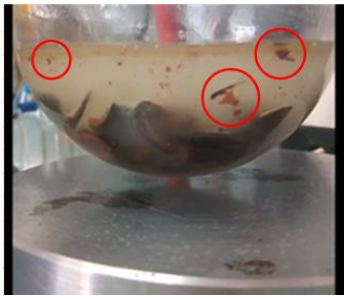


Fig. 3.51. Solid particles in the reaction medium with possible action of inhibitors or generators of additional centrifugation operations

is faster and easier to monitor, was preferred. We find in the operations diagram from Fig. 3.52. drying conditions of 5 h at 50 °C temperature, as well as the subsequent sanding and polishing operations, necessary for finishing the external surface. The differences in the material were visible after the sanding operation, the material obtained having a relatively smooth surface, characterized by the lack of initial residues. The peach/nectarine stones, however, kept their specific channels, as did the olive stones, the grinding not being taken to the extreme. Otherwise, the tips that would have come off easily or the edges in various extremities could have been removed in this way. Just washing them out would have not been enough, would have softened them without removing them as fragments. Polishing was also important, the removal of dust (very fine particles) left over from abrasive grinding being necessary, its action being completed by washing with chemical aqueous solutions. At the laboratory scale, these operations were not very complex, and the subsequent behavior of these materials proved to us that they were necessary.

At the end of the drying and of these operations and *intermediate* lignocellulosic material was obtained (Fig.3.52), ready for the next stage of chemical treatment.

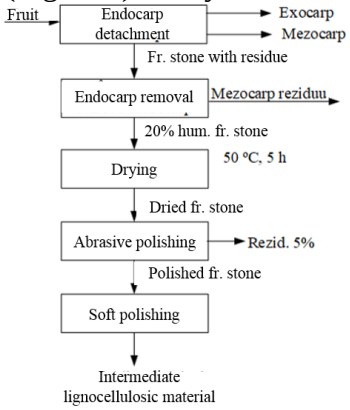


Fig. 3.52. Scheme of physio-mechanical operations with fruit stone processing



Fig. 3.53. Lignocellulosic biomass material before and after processing as a catalytic support

3.3.3.2. Chemical treatment

The chemical treatment applied was also not very complex; only a decontamination wash was targeted, so a concentration of 0.1 M KOH aqueous alcoholic solution was preferred. The procedure was similar for all the types of fruit stones. Thus, an amount of approximately 40 de g (in olives of approx.. 20 g) of each type of stone was placed separately in a round –bottomed flask (1), fixed to a stand (2), over which an alcoholic KOH solution was added.



Fig. 3. Treatment (*decontaminating washing*) of fruit stone

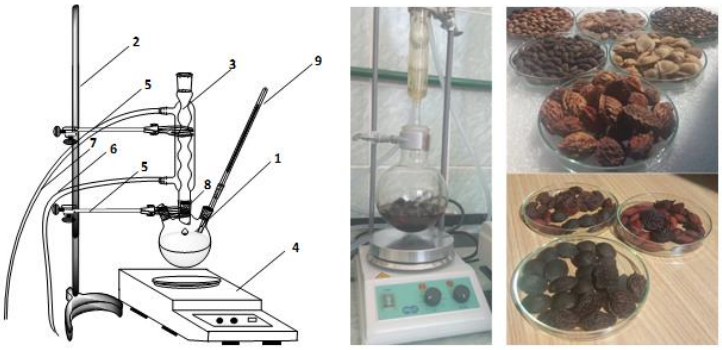


Fig. 3.21. Experimental installation for biomass treatment lignocellulosic: 1) 1 L reaction flask; 2) stand; 3) refrigerant; 4) magnetic stirrer with heating; 5) clamp; 6) water in; 7) water out 8) reduction; 9) reaction thermometer.

The end result was in the form of the SC_{SF} core catalytic support.

3.4. BIOCELLULOSE – MATERIAL FOR CATALYTIC SUPPORT PREPARATION

Bio-cellulose or bacterial cellulose (BC) is cellulose bio-produced by a number of bacteria, fungi, or even some types of algae[8] [303-306].

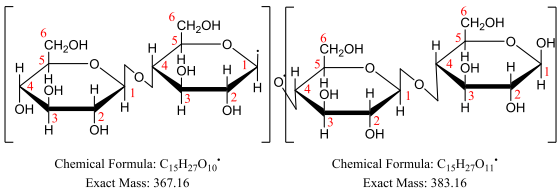


Fig. 3.56. Cellulose

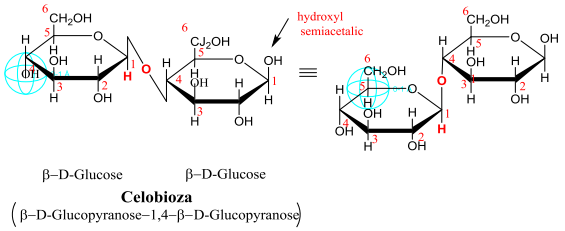


Fig. 3.57. Cellobiosis, as the basic structural unit of cellulose

The common bonds to reducing olygoglucides are C_1-C_4 bonds, because C_4 hydroxyl is in the *para* position relative to the semacetal hydroxyl of the same molecule and is more reactive [313]. All these features only facilitate the construction of multiple synthesis strategies in cases where cellulose-containing materials are used, such as the selected residual (ligno)cellulosic biomass for this research.

The use of biocellulose (BC) as a catalytic support is part of the same strategy to further make greener the process of obtaining biodiesel and was preferred for the *permissiveness* of *OH* groups of glycosidic residues to bind chemically to them, exactly what any chemist would want.

The objective was to obtain a fourth type of catalytic support. The starting point was the production of biocellulose, and the final stage was to enter the phase of sufficiently processed material, to facilitate the transition to the construction of the final catalyst with base properties.

3.4.2. Materials

The materials used in this stage were: methanol (~99.8% Honeywell, Germany), potassium hydroxide, pellets (Lachema Brno, Czech Republic), glucose, yeast extract, peptone, anhydrous disodium phosphate, citric acid monohydrate, acetic acid, water distillate (laboratory distiller Millipore Q-Gard A2 AFS 15E), BC produced in the Mass Transfer Laboratory of the Departament of Chemical and Biochemical Engineering, Faculty of Applied Chemistry and Materials Science, Polytechnic University of Bucharest.

3.4.3. Experimental

3.4.3.1. Biocellulose production

For this research it was chosen to produce biocellulose (BC) in static environment, using the conditions for BC obtaining from previous work [314-317], but the treatment after BC production was approached differently, based on the specific objectives of this thesis.

Bacterial cellulose was obtained in static culture, in a cylindrical container covered with a gauze coating, to allow aeration of the sample, using Hestrin-Shramm (HS)[9] as the culture medium. This medium contained 2% glucose, 0.5% yeast extract, 0.5% peptone, 0.27% anhydrous disodium phosphate and 0.15% citric acid monohydrate. The pH-ul was adjusted to ~5, using a 1 N acetic acid solution (Schramm and Hestrin, 1954).

In principle, by using this production technique, in a reactor in a static environment at an average temperature of 26 °C (or day 30-32 °C and night 18-24 °C), without thermostat temperature considered in the optimal range development of BC culture, the period of 7-10 days was sufficient to obtain BC membrane with a diameter of 110 mm, a thickness grosime (height) of 8 mm and

[8] *Valonia ventricosa, Chaetamorpha melagonicum,Glaucocystis*, freshwater algae species [311]
[9] Named in honor of the two researchers who developed it in 1954

final mass of 108 g, which, after post-production treatments and after the drying operation, to reach a diameter of 80 mm, thickness of 2.5 mm and for a humidity of 99,4% (experimentally determined), a mass of BC corresponding to 0.648 g of dry BC. In the present research, however, the period allocated to the process of obtaining BC was extended to 24-28 days, and at the end of it the membrane characteristics had obvious differences both in the mass of fresh material and obviously, for the dried BC.

3.4.3.1. Post-production BC treatment

A particularly important step was the chemical treatment applied immediately after the removing the membrane from the reactor at the end, to remove bacteria, a treatment which usually consists of a pre-wash (i), followed successively by a treatment with the use of alkaline chemical compounds, under high temperature conditions (ii), a wash with distilled water to neutral pH (iii) and storage by total immersion in acetic acid solution, pending further processing (iv) [314-317]. However, in the present research, the pre-washing operation followed by chemical treatment using 0.1 M aqueous KOH solution at high temperature was preferred, but it was chosen for storage in methanol, in an attempt to replace water molecules with the -OCH_3 group even now at this stage, as shown in operation scheme in Fig.3.59.

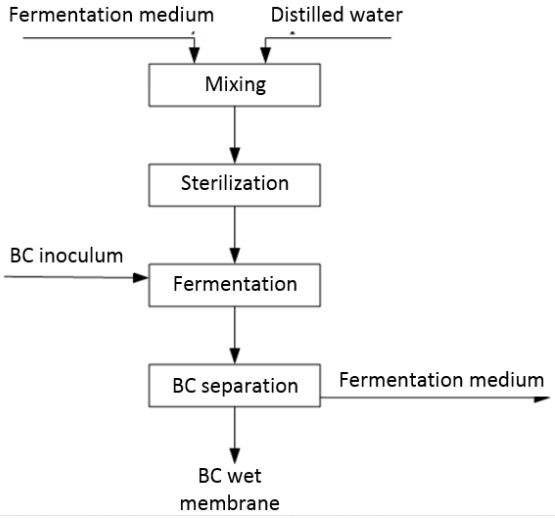


Fig. 3.58. Simplified scheme of operations of BC production

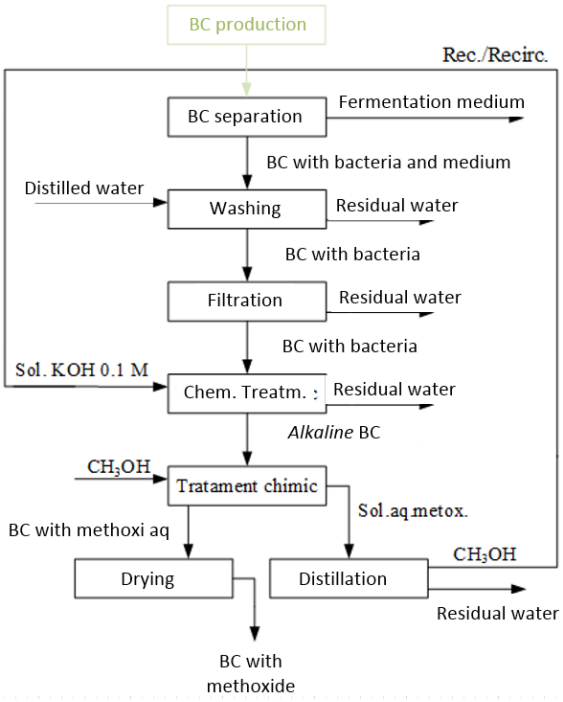


Fig. 3.59. Scheme of BC post-production operations

A 0.1 M alkaline solution was thus prepared by dissolving 11.2 g of KOH in 2 L of distilled water into which the BC membrane was introduced and kept at 100 °C for 2 h. However the washing step after the chemical treatment was omitted and vacuum filtration was chosen to remove as much of the aqueous alkaline solution as possible, after which the BC membrane was introduced directly into the methanol until drying operation.

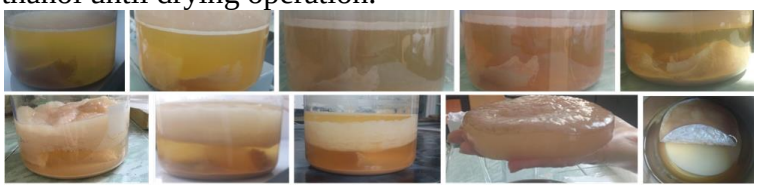


Fig. 3.60. BC in the culture medium: 3-28 days

In the next step, prior to the drying process, the solution of the mixture of the compounds in which the membrane was placed was distilled for methanol recovery. The amount of methanol recovered was reused for the same purpose, after obtaining the other biocellulosic membranes.

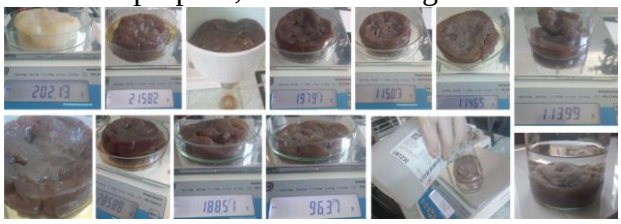


Fig. 3.61. Steps in BC processing, after antimicrobial treatment: dehydration by vacuum filtration and immersion in methanol

3.4.4. Results and discussions

A particular case (as in the impossibility to use the pyrolyzed biocellulose later in this research) was the pyrolysis of BC, in the same way as the pyrolysis of biomass: in a first process BC with a mass of 13.70 g was fed into the pyrolysis column and pyrolyzed at t_S = 650 °C, without using carbon dioxide (CO_2), for 80 min (combined heating/stationary/cooling durations), resulting in 4.01 g CP_{BC} pyrolytic carbon and m_{CPBC} = 3.7 g bio-oil; in a second process with BC fed with a mass of 16.53 g, a t_{Sa} = 647 °C temperature, with 3.60 g of CP_{BC} and 4 g of bio-oil mass resulted. It is interesting to note the masses of products, in the conditions in which the participation of CO_2 as inert was the only parameter that varied, otherwise all the others being identical.

After pyrolysis, the resulting BC having m_{CPBCin} = 1.71 g mass was fed to the thermal activation column and maintained at 650 °C (U_{Voltm} = 40 mV, U_{Transf} = 155 V) for 90 min (cumulative heating/stationary/cooling durations), at the end resulting in CA_{BC} activated carbon with mass $m_{CABCout}$ = 1.71 g (Fig.3.62.).

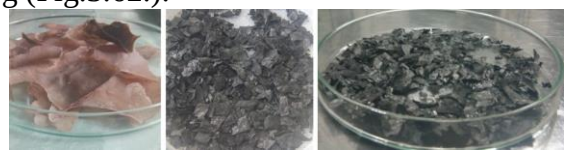


Fig. 3.62. BC before and after pyrolysis

However the physical characteristics of this pyrolytic carbon, especially those related to density and thickness, did not correspond to the requirements of the operations or subsequent syntheses in the research, the BV material being very light and thin, similar to fine carbon powders and would have created an addition process stage (centrifugation), instead of reducing (desired) the number of steps or operations in a process.

The morfology of the obtained membranes was studied with the help of scanning electron microscopy (SEM) for both dyr and lyophilized samples of BC, using a *FEI Quanta Inspect F* equipment. We find shown in Fig. 3.63. SEM image of a dry BC membrane before being purified. In addition to the fibrillar network of cellulose, the presence of acetic bacteria trapped between the BC fibrils is oberved.

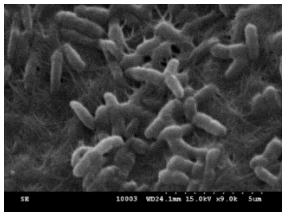


Fig. 3.63. SEM image with dry BC before antimicrobial treatment

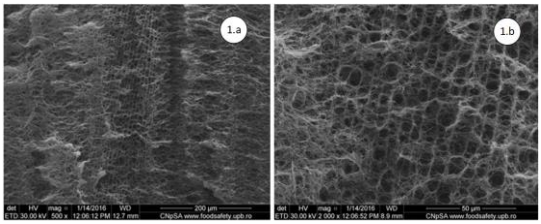


Fig. 3.64. SEM images of lyophilized BC after purification a) magnification x500 and b) magnification x2000**.**

Fourier transform infrared spectroscopy analysis was performed on membranes obtained in all experiment variants, using *JASCO FT/IR-6200* equipment. Scanning was performed from 4000 cm^{-1} to 500 cm^{-1} for each sample. Fig. 3.64 shows two SEM images at different magnifications for purified and the lyophilized BC. In this case the three-dimensional network of BC fibrils is visible, especially in Fig. 3.64 -1.b.

X-ray diffraction was performed with a Shimadzu XRD 6000 diffractometer. The X-ray spectrum for purified and dry BC is shown in Fig. 3.65. It is observed that BC presents Briggs peaks at 14.44º, 16.77º and 22.7º, which are also reported in the literature for BC (Park *et al.*, 2010).

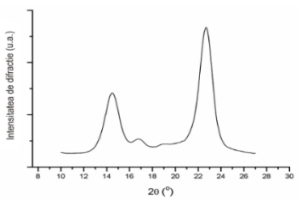


Fig. 3.65. X - ray spectra for BC purified and dried

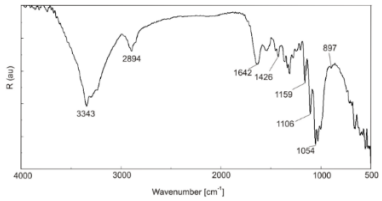


Fig. 3.66. FTIR spectra of CB membrane dried, obtained in static culture.

Fig. 3.66. shows the spectrum of a dry membrane after alkaline washing and washing with distilled water to neutral pH. The figure shows the streching vibrations of the OH groups at the wavelength este. The 2899 cm^{-1} band represents the tensile vibrations of the aliphatic C-H bonds.

The peak formed at 1642 cm^{-1} is due to the symmetrical deformation vibrations of the water molecules (cellulose moisture). The peaks at the wavelength 1054 cm^{-1}, 1365.35 cm^{-1} and 1432 cm^{-1} can be attributed to the extension of the C-O bonds, the C-H deformation and, respectively, the symmetrical bending of the C-H bond. The 1159 cm^{-1} band can be attributed to the asymmetric bending of the C-O-C bonds. Peaks at 1315 and 1426 cm^{-1} can be attributed to symmetrical streching and deformation of CH_2 groups. The obtained spectrum is similar to te literature data reported for biocellulose (Wu *et al.*, 2012).

3.4.1. Conclusions

The method of producing BC in 24-28 days resulted in a biocellulosic material with properties suitable for further processing, such as stability in the alkaline environment or adsorption capacity (chemosorption) in solutions with chemical compounds of interest.

The production of biocellulose in the static reactor was characterized by continuity, in a way of maintaining the same cultivating conditions from the beginning of the first cycle of obtaining the first membrane, for five (six - differences involved) cycles, but with the addition of certain amount of nutrients.

CAPITOLUL 4

GUANIDINE SYNTHESIS FOR USE AS BASE CATALYST FOR CATALYTIC SUPPORT IMPREGNATION

The transition from a conventional process for obtaining biodiesel to a process governed by green chemistry begins exactly with this selection of the catalyst: in the case of a raw material with an FFA below 1%, it is sufficient that the basicity of the catalyst be comparable with that of NaOH[10], but this catalyst must be characterized by green properties, the most important being biodegradability, reduced post-process toxicity, somehow the opposite of NaOH or KOH in terms of *environmentally friendly*.

Superbases are very often identified with organic bases, even if the latter are limited *ad litteram* to amines [318].

[10] $pK_{bKOH} = 13.6$

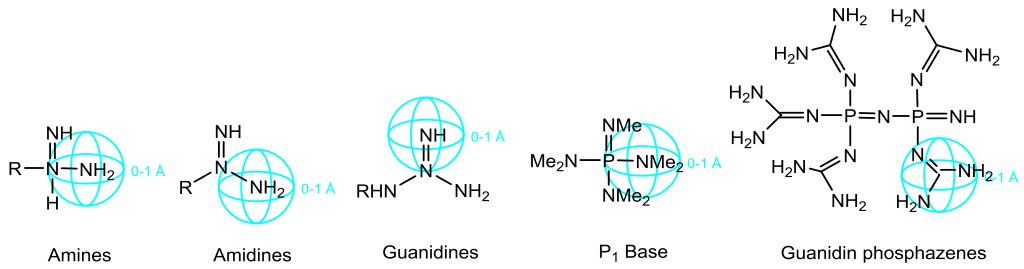


Fig. 4.1. Amines and organosuperbases with high basicity

Thus, in this research, the selection of *guanidine* as a base catalyst was reached due to the advantages that characterize this chemical compound, usable for this purpose: *i)* it is organic and biodegradable[11]; *ii)* it is both a product and mainly a precursor: the basicity of guanidine used *tale quale* is 13.6, but as guanidine derivatives, such as TMGF [4,5-bis(tetramethylguanidine) fluorine]) or TBD (1,5,7-Triazabicyclo[4.4.0]dec-5-ene), basicity (expressed in pK_{aH}) can reach values nup to 27-28 (Tab. 4.1.); *iii)* the pathway to the synthesis exclusively for this research, had two reaction products, both of final utility, as well as the possibility of recovery and reuse of the participating secondary reagents.

Guanidine is an amino derivative in a class of compounds in which, by introducing an imino- (=NH) functional group at amines C_1, the basicity can be increased [318], and guanidine, having two amino- (-NH_2) groups and one imino- (=NH) group, shows the highest basicity among these amino-derivatives [318, 323].

There are several pathways to guanidine synthesis, starting from various chemical compounds, and for this work is was preferred to adapt[12] the recipe of E.Roberts and J. Griffiths (1949) [325], due to factors related to the conditions of the synthesis, as well as to the subsequent use of the main product.

4.2. MATERIALS

Tab. 4. 1 Materials used in the synthesis of guanidine

Materials	Chemical formula	Notation	Molar mass [g/mol]	Boilling point [°C]	Use
Dimethyl sulfate	$(CH_3O)_2SO_2$	M_2SO_4	126.13	187.7	Reaction
Urea	$CO(NH_2)_2$	U	60.06	132.7	Reaction
Methanol	MeOH	MeOH	32.04	64.7	Solubilization
Ammonia, sol. 25%	$NH_5{\cdot}H_2O$	NH_3(aq)	35.05	38.0	Ammonolysis
Potassium hydroxide	KOH	KOH	56.11	-	Precipitation
Methyl red	$C_{15}H_{15}N_3O_2$	RM	269.30	182.0	pH indicator
Distilled water		AD			Adjustement/Washing

4.3. EXPERIMENTAL

Guanidine synthesis was performed in three steps, with successive methylation, ammonolysis (preceded by neutralization) and precipitation reactions.

4.3.1. Obtaining *O*-methyl-*iso*-urea hydrogen methyl sulfate

The first step in the methylation reaction (Fig 4.2.) involved the initiation of the reaction starting from urea **(1)** and dimethyl sulfate **(2)**. The assembly operations of the experimental

[11]Biodegradability of guanidine
[12] Initiation from dimethyl sulfate, methylation, stopping to alcoholic guanidine.

installation (Fig 4.3.) started with the filling of the thermal bath with ethylene glycol, in order to ensure and maintain the reaction temperature over 100 °C. One mole (126.16 g) of dimethyl sulfate (A) was then weighed and added to a 1 L 3-necked round bottom (1). In parallel, one mole (60 g) of urea (B) was weighed in a Berzelius beaker, and when the temperature of 100 °C of dimethyl sulfate was reached, urea was gradually added to the flask for 15 minutes, under vigorous continuous stirring. The reaction was exothermic and as such the reaction temperature increased, making necessary to maintain it in the temperature range of 110-120 °C. The temperature increased from 100 °C to 115 °C in 8 minutes (the variation of the temperature of the thermal bath and of the reaction mixture is shown in Fig. 4.4.). After the addition of the entire amount of urea, the reaction mixture was maintained at the same temperature of 115 °C for another 25 min to complete the reaction, after which the thermal bath temperature was lowered to 80 °C by feeding cold ethylene glycol into the bath. The reaction mixture was subsequently allowed to cool to room temperature and samples (Sample 1) were extracted for analysis. The resulting product was *O*-methyl-*iso*urea hydrogen methyl sulfate (C).

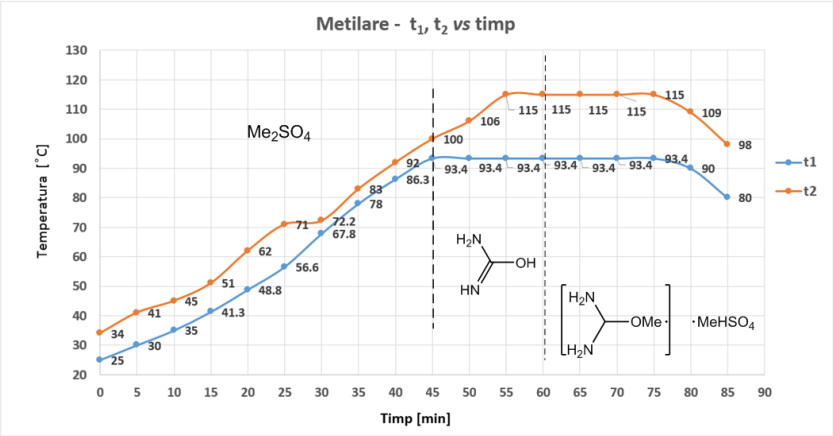


Fig. 4.2. Temperature variation over time at synthesis stage I of guanidine: t_1 - temperature of the thermal bath; t_2- reaction temperature.

4.3.2. Ammonolysis with alcohol-bonded guanidine formation

The solution of *O*-methyl-*iso*urea hydrogen methyl sulfate (C) contained base methyl urea, as the hydrogen methyl sulfate salt, being at the same time acidic (app. 25-26 g (m/v) hydrogen methyl sulfate [320]), so that ammonolysis reaction was preceded by neutralization with ammonia solution.

Using the same experimental installation, the temperature of the reaction was raised to 25 °C, using the thermal bath, after which the neutralization reaction was initiated by adding 25 mL (26 v/m faţă de metil sulfat) 25% NH_3 solution for 30 min.

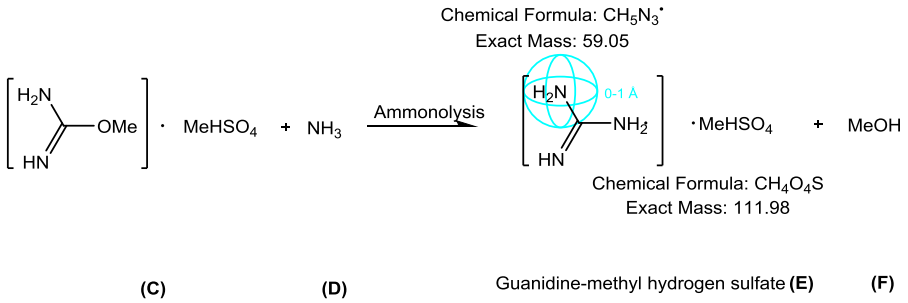


Fig. 4.3. Stage II of guanidine synthesis, with ammonolysis reaction

During neutralization the temperature of the reaction mixture was brought to 60 °C, at which point the ammonolysis reaction was initiated by adding 50 mL of 25% NH_3 solution, and then maintained at this temperature for 3 h.

The ammonolysis reaction led to the formation of amino- (-NH_2) group, and the resulting reaction product, guanidine-methyl hydrogen sulfate (E), had a clear, light brown, not very viscous appearance (Fig.4.7.).

4.3.3. Distillation

The production of guanidine-methyl hydrogen sulfate was carried out by concentration, at the end of the ammonolysis reaction, when distillation operation was performed, as a necessary step to remove the alcoholic aqueous solution resulting from the reaction.

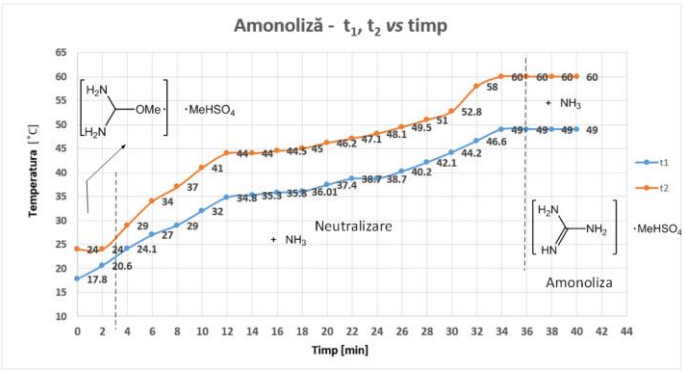


Fig. 4.4. Temperature variation over time at stage II of guanidine synthesis:
t_1 - temperature of the thermal bath; t_2- reaction temperature.



Fig. 4.5. Guanidine synthesis reaction mixture, left to right:
reaction initiation - formation of guanidine hydrogen methyl sulfate

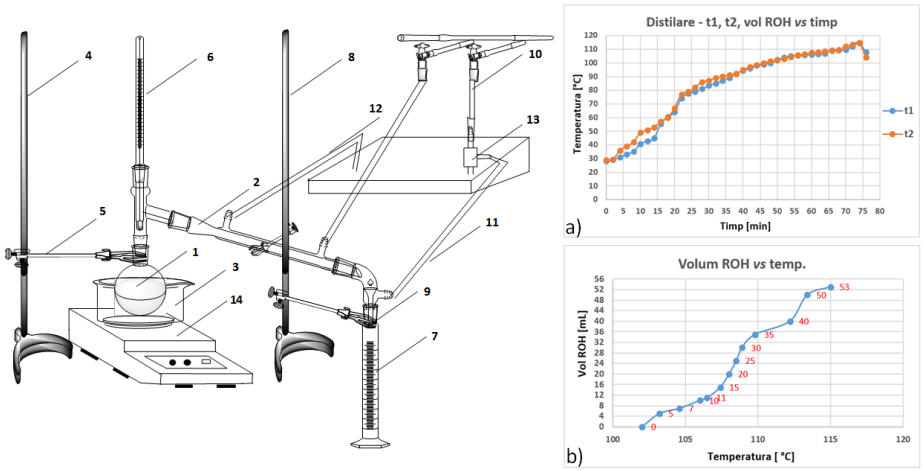


Fig. 4.6. Experimental guanidine-methyl hydrogen sulfate alcohol purification experimental installation

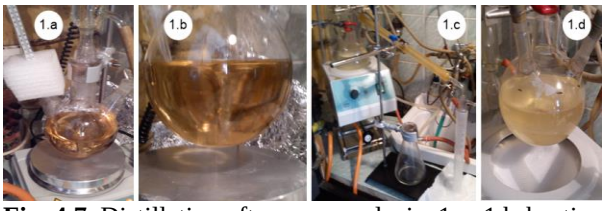


Fig. 4.7. Distillation after ammonolysis: 1.a, 1.b-heating;



Fig. 4.8. The reaction mixture at the end of distillation,

1.c-distillation; 1.d-intermediate distillation. - medium cooling, waxy appearance, light beige-brown

4.3.4. Precipitation as final stage for alcohol-bonded guanidine formation

Pure guanidine is relatively difficult to maintain in this state, so it is preferred that it be bound to a chemical compound, of which subsequently, depending on the application, it participates in chemical reactions.

For the present work it was chosen to obtain alcohol-bound guanidine (methyl), participating from this position much more easily in the reaction, due to the -CH_3 group. We then dissolved the distillation product, by heating, in 1000 mL of methanol (Fig. 4.11.), and after dissolution the reaction mixture was brought to 25 °C.



Fig. 4.9. Initiation of precipitation reaction: heating in the ethylene glycol bath and dissolution in methanol

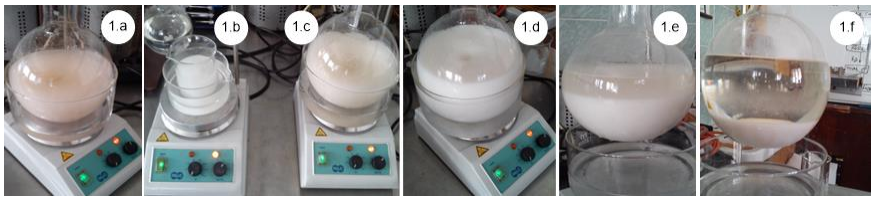


Fig. 4. 10. Precipitation with cu methoxide: 1.a.- dissolved mixture; 1.b – methoxide preparation; 1.c - methoxide feed; 1.d - reaction; 1.e, 1.f – precipitation.

We went to the water bath to make the temperature reduction easier and, in parallel, a 470 mL solution was prepared, which contained 11.34 g of KOH (m/v) per 100 mL of metanol (v/v). The solution thus prepared was gradually added with stirring and cooling between 10-20 °C, and following this treatment potassium methyl sulfate precipitated (Fig. 4.12.).

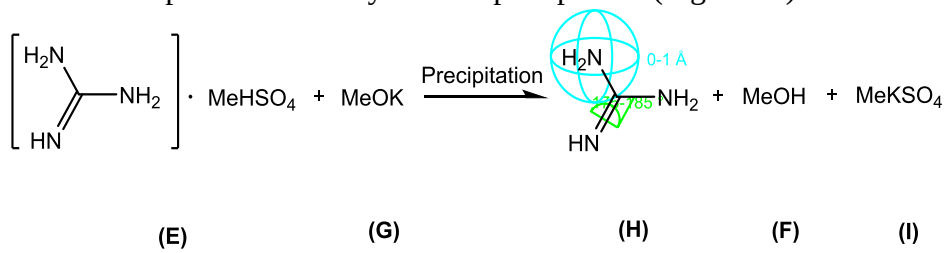


Fig. 4.11. Etapa finală de reacţie cu precipitarea sulfatului şi obţinerea guanidinei alcoolice

The precipitated thus obtained was subsequently filtered by successive washes with methanol (cold), until the release of guanidine; as for the guanidine, it was opted to keep it in the alcoholic solution.

4.3. RESULTS AND DISCUSSIONS

The multi-step guanidine synthesis therefore involved the formation of two intermediates and to ensure that were the right ones, samples were collected from each one as they formed.

FTIR analysis was performed using the ATR[13] technique on a *Nicolet 6700 -Thermo Scientific* FTIR spectrometer, on a wavelength range from 4000 cm^{-1} to 500 cm^{-1} and was performed to highlight the functional groups present at guanidine at the end of reaction (Fig. 4.14.). We find in the figure at the wavwlength 3357 cm^{-1} possible tensile vibrations of the NH groups (primary amines), of high intensity (strong intensity)[14], at the wavelength 1658 cm^{-1} possible bending vibrations outside the plane (asymmetric)[15] of the groups N-H (primary amines) and at the wavelength 761 cm^{-1} possible asymmetric bending vibrations of N-H groups (secondary amines).

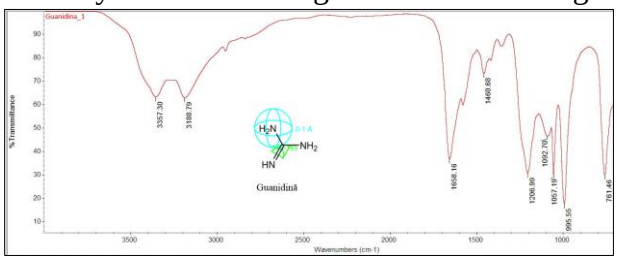


Fig. 4.12. FT-IR spectra of guanidine

The HR-MS (*high resolution mass spectrometry*) analysis performed for the quantification of chemical compounds was carried out using the HR mass spectrometer with 15T superconducting magnet (*SolariX-XR, QqqFT-ICR HR, Bruker Daltonics*), Fourier–Transform Ion-Cyclotron-Resonance (FT-ICR) type. Using the ionization technique of *ESI positive* type (*electrospray ionization*), the sample was introduced by direct infusion using a *Hamilton* 250ul pump, setting the sample flow rate at 120 µL/h and the parameters for the nebulization gas (nitrogen), respectively the pressure at 1.2 bar, temperature of 200 ºC and a flow rate of 4 L/min. The samples were dissolved in methanol, (Merck Millipore grade HPLC). For the spectra the small masses method was used, with the mass in the range *low m/z – 46.07, high m/z – 3000* uam, with accumulation in seconds *Accum* - 0.020 and at a source voltage of 4500 V.

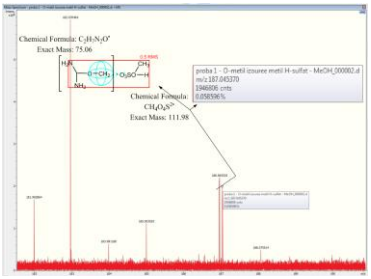


Fig. 4.13. ESI-MS spectra of *O*-methyl-isourea-H-methyl sulfate.

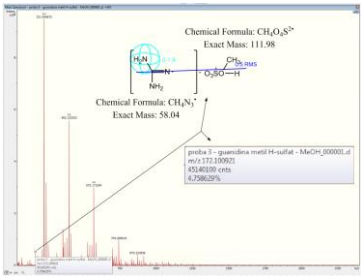


Fig. 4.14. ESI-MS spectra of guanidine-methyl-H sulfate.

The chemical compounds obtained one by one in the synthesis steps were thus identified and we find in Fig.4.15. first intermediate, *O*-methyl-isourea-*H*-methyl sulfate at m/z=187.05, on the intensity range $Ix10^6$ and the second intermediate in Fig. 4.16., on the intensity range $Ix10^8$, la m/z=172.10, guanidine-methyl-*H*-sulfate.

Regarding the reaction products, in Fig. 4.17. $MeKSO_4$ was identified at Intens $x10^6$, at m/z=151.57, considered in the reaction as the main by-product, the sulfate obtained in the precipitation reaction while in Fig. 4.18. guanidine (in alcohol) was identified in the 10^7 intensity range, at m/z=60.85.

[13] ATN - attenuation of total reflection.
[14] https://www.orgchemboulder.com/Spectroscopy/irtutor/aminesir.shtml
[15] https://www.orgchemboulder.com/Spectroscopy/irtutor/aminesir.shtml

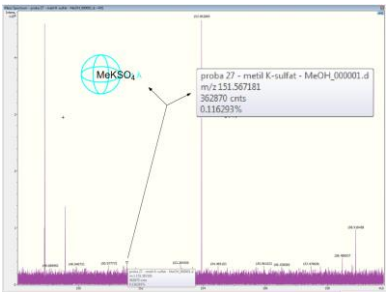


Fig. 4.15. ESI-MS spectra for secondary product

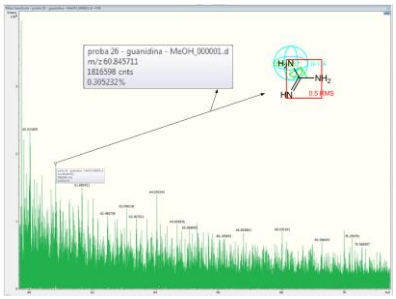


Fig. 4. 16. ESI-MS spectra of guanidine

4.5. CONCLUSIONS

The synthesis of guanidine, an organic chemical compound of high basicity, was successful, starting (and adapting) from the recipe of E. Roberts and J. Griffiths (1949), from Me_2SO_4 and urea. We considered the reaction conditions to be moderate(atmospheric pressures and reasonable temperatures for laboratory scale reactions, of 120-160 °C), with a yield of guanidine over urea higher than 60 %, and with a basicity comparable to that of potassium hydroxide.

For the by-product, $MeKSO_4$ (Fig. 4.19.), research was not deepened, but, as a future research, its acidity will also be studied, having the advantage of a liquid highly acidic chemical compound, although being solid.



Fig. 4.17.
Final products of guanidine synthesis: $MeKSO_4$ - left, guanidine - right.

As for guanidine (Fig. 4.19.), it was practically the liquid base catalyst that will be used in the construction of the heterogeneous base catalyst, by combining it with the types of catalytic support obtained in Chapter 3.

CHAPTER 5

HETEROGENEOUS CATALYST SYNTHESIS FOR BIODIESEL PRODUCTION

For the present work it was selected the method of combining a catalytic support, developed in Chapter 3, respectively the three different types of material, with a chemical compound with base properties synthesized in Chapter 4, guanidine. The objective of the experimental research at this stage was therefore their combination and construction of the final catalyst (Fig. 5.1).

5.2. MATERIALS

Three types of raw materials representing the catalytic support were obtained and intended for combination with guanidine: 1. Activated pyrolytic carbon (from thermo-chemically treated biomass); 2. Raw residual lignocellulosic biomass (fruit stones) and 3. Biocellulose (BC), after each has undergone a series of treatments, in order to increase performances in terms of thermal stability, specific surface area, the possibility of creating chemical bonds, various sites or centers (usually basic, but not only), etc. These raw materials are shown in Tab. 5.2.

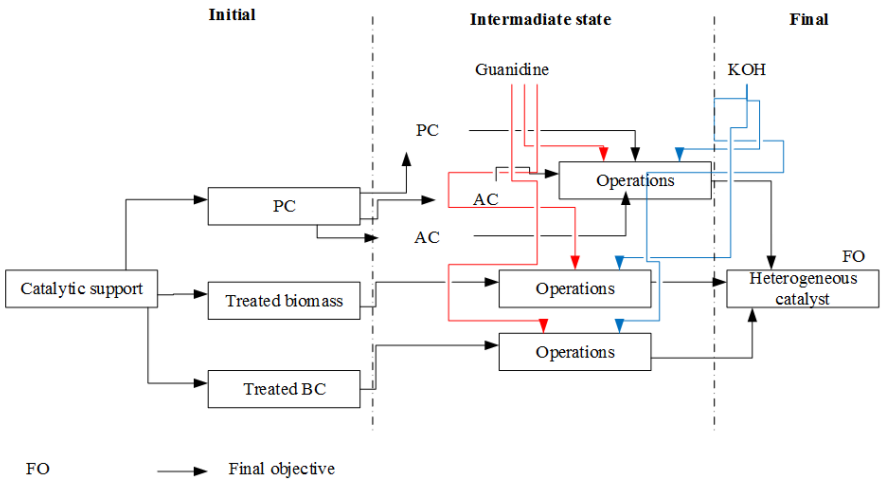


Fig. 5.1. Objectives for the development stage of the heterogeneous base catalyst

Tab. 5.1. Materials used in the construction step of the base heterogeneous catalyst

Materials	**Chemical formula**	**Density g/cm³**	**Molar mass [g/mol]**	**Boilling point [°C]**	**Use**
Sulfuric acid	H_2SO_4	1.83	98.79	337	Sulfonation / Functionalization
Nitric acid	HNO_3	1.51	63.01	83	Functionalization
Methanol	MeOH	MeOH	32.04	64.7	Solubilization
Potassium hydroxide	KOH	KOH	56.11	-	Impregnation
Distilled water		AD			Adjustment/Washing
Guanidine(in ROH)	$CNH(NH_2)_2ROH$				Impregnation

Tab. 5.2. Raw materials (RM) used as catalytic support in combination with guanidine

RM	RM type
CA_{I-II}	CA_{I-II} S.pi/n, S.cai, S.m, S.ci, S.co, S.p, A.Cyb
SC_{SF}	$S_{.pi}$/n, S.cai, S.m, S.ci, S.co, S.p,
BC	

5.3. EXPERIMENTAL METHOD

At this stage of the research, we also opted for the use of a commercially activated carbon CA_{COM}, with a specific surface area not very large, but with a value that exceeded the one of the specific surface area of pyrolytic carbon obtained by us in pyrolysis.

5.3.1. Heterogeneous catalyst from guanidine and carbon-based catalytic support (commercial carbon and pyrolyzed biomass-based carbon)

The objective of this stage of development of the heterogeneous catalyst was thus subdivided in its turn into 3 other major sub-objectives: *i)* chemical bonding of the catalytic solution to the functional groups, without altering its base properties, achievable through a functionalization of the catalytic support; *ii)* the actual impregnation of the catalytic solution, preserving the base catalytic properties required in the reaction to be subsequently heterogeneously catalyzed; *iii)* preservation of the newly created properties through a thermal treatment. However, the thermat treatment operations were also necessary during the stages from sub-objectives: *i)* and *ii)*.

5.3.1.1. Functionalization with inorganic acids

5.3.1.1.a. Commercial activated carbon functionalization by sulfonation [16]

The aim was to obtain high catalytic activity and stability for this catalytic support, possibly due to the high density of acidic sites, hydrophobicity that prevents hydration of species(-OH), hydrophilic functional groups (–SO_3H) that can improve methanol access to triglyceride and FFA, and large pores that can provide multiple acidic sites to reactants [331].

50 g CA_{COM} where washed with distilled water, to remove any fine powders, after which they were dried at 150 ºC for 4 h. The weighed mass was the fed into a 3-necked round-bottomed flask and then poured sulfuric acid (1:4 m/m carbon/H_2SO_4). It was then kept at reflux at 170 ºC, for 7 h, after which it was allowed to cool to room temperature, for 24 h. Subsequently, the carbon was washed, filtered and dried to give a final mass value of material of 54.2 g., which was stored in anhydrous conditions. Next, an amount of 3 g of $CA_{COM}S$, after a pre-drying in the oven, was treated with potassium hydroxide by impregnation, by introducing in 1M, 1.5M, 2M and 3M alcoholic alkaline solution. The process conditions were: temperature t^o_D= 50 ºC for dissolving KOH pellets and preparing the alcoholic solution, and reaction time t_D= 45 min, while for the impregnation after adding $CA_{COM}S$ in solution, t^o_I= 100 ºC and t_I = 90 min. Drying for 180 min, at 130 ºC was the last step, which resulted in the final $CA_{COM}S$/methoxide catalyst (noted bellow $CA_{COM}S/_K$, Fig. 5.3.1.d.)

5.3.1.1.b. Pyrolytic carbon functionalization by nitration

The treatment of the activated pyrolytic carbon, in a first phase, with concentrated nitric acid [333], aimed at the formation mainly of nitro- (-NO_2) group, to which the compounds of the second functionalization stage could be chemically bonded by chemisorption. The initially tested 2M and 4M nitric acid concentrations failed to provide the creation of such functional groups, , in a test performed in a transesterification reaction, so that the entire HNO_3 treatment was performed using 70% nitric acid. Functionalization was carried out performing same operations as those in the diagram shown in Fig. 5.2, in a similar installation, and the operations carried out were the initial washing of the material, followed by drying and feeding in the reaction flask.

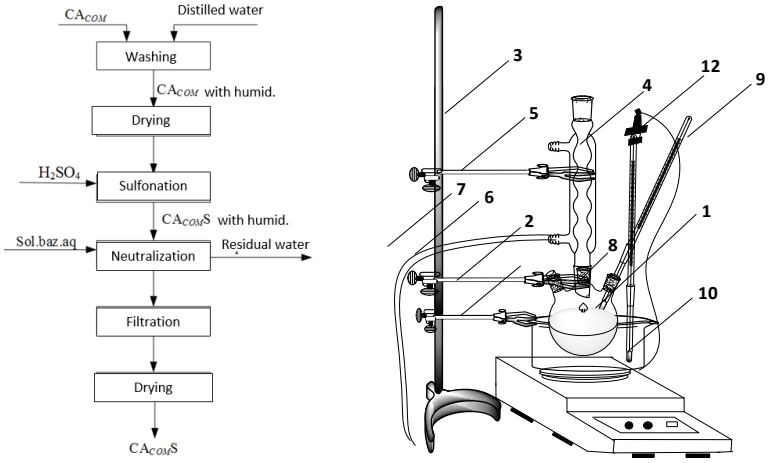


Fig. 5.2. Simplified diagram of CA_{COM} sulfonation operations and experimental laboratory installation for sulfonation: 1) 1 L reaction vessel; 2) flask clamp; 3) stand; 4) refrigerant; 5) refrigerant clamp; 6) water in.; 7) water out; 8) reduction; 9) reaction thermometer; 10) thermal bath $(CH_2OH)_2$; 11) heated magnetic stirrer; 12) thermostated thermometer

[16] Published in Bulletin of Romanian Chemical Engineering Society, Vol. 3, No. 1, 2016 ISSN 2360-4697 [332]

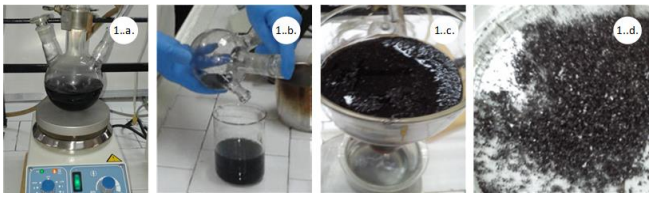


Fig. 5.3. Steps in sulfonation reaction: 1.a.- reaction; 1.b. and 1.c - separation; 1.d. - final



Fig. 5.4. Images from acid functionalization nitrogen: initiation of reaction and course of reaction

Subsequently, HNO_3 was added, based on the on the mass of carbon: CA_{II} S.ci/HNO_3 1:10.66 m/m ($m_{C\ AII\ S.ci}$ = 11.45g), C_{COM}/HNO_3 1:9.62 (m_{CCOM}= 2.6 g) C_{COM}/HNO_3 1:3.83 m/m (m_{CCOM}= 5.36 g), CA_{II} S.ci/HNO_3 m/m 1:5.82 ($m_{CA_{II}S.ci}$ = 4g), CA_{II}S.co/HNO_3 1:6.9 m/m ($m_{CA_{II}S.co}$ = 3.80 g), CA_{II}S.cai/HNO_3 1:7 m/m ($m_{CA_{II}S.cai}$ = 3.5g).

The temperature was maintained at t^o_N= 65 ºC, reaction to reflux, and reaction time t_N= 120 min, this mode of operation being repeated for each type of material subjected to nitration.

All types of materials doubled in mass upon removal from the reaction mixture, while filtration and drying were the final operations for nitric acid functionalized carbon (CA_N).

5.3.1.2. Functionalization with strong bases

5.3.1.2.a. Carbon functionalization with potassium hydroxide by impregnation and thermal activation [17]

This operation was carried out in two steps, the first being the impregnation of the support with the hydroxide, while the second being the thermal treatment (thermal activation) of the impregnated material.

The same experimental installations were used for impregnation, as in Fig 5.2, and the process began with an initial drying of the material and then the immersion in 2M alcoholic alkaline solution and kept at temperature $t_1{}^o_{Ic}$ = 80 ºC, $t_2{}^o_{Ic}$ = 100 ºC under mixing, for t_{1Ic} = 2 and t_{2Ic} = 3 h. At the end it was not completely dried, but a certain percentage of humidity being maintained.

In the second step, of thermal activation, the installation shown in Fig. 3.34. was used and the same operating procedure described in Chapter 3.2.2.2.b. was performed. The final CA_{KA} catalyst was thus obtained (Fig. 5.5).

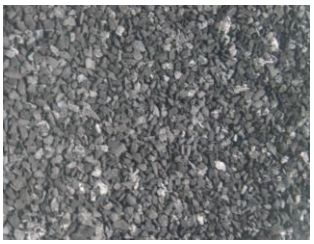


Fig. 5.5. Final catalyst of CA_{KA} type



Fig. 5.6. Combination of guanidine with *carbon* catalytic support type, by impregnation and distillation

5.3.1.2.b. Heterogeneous catalyst from guanidine and both activated and functionalized carbon

This step was the final one in catalyst construction, in which the catalytic support was in form of commercially (CA_{COM}) activated carbon, and in the form of pyrolytic activated carbon, (CA_{II}).

The operation were carried out mostly in a similar way to other impregnations performed above, with the difference that, for this stage, reflux followed by distillation were chosen as

[17] Published in Bulletin of Romanian Chemical Engineering Society, Vol. 4, No. 2, 2017 ISSN 2360-4697 [334]

impregnation methods (Fig. 5.6.). The experimental installation used for reflux was that of Fig 5.2. and for distillation the experimental installation of Fig. 4.8. was used.

Guanidine was used as Gu-ROH, from alcoholic solution in which was stored at the end of its synthesis, with 7.5 g (m/v) per 100 mL of Gu-ROH. For impregnations of the carbon material, as for the other materials, C_X (g), metanol (mL) and Gu-ROH (mL) were used as reactants. Thus, the amounts used were: for CA_N, a ratio 1:3:12; C_{COM}/Gu-ROH/Me had a mass value m_{CCOM} = 3 g, and for the rest of the materials the quantities had mass values between 3.5 - 5.5 g.

As an operating method, the carbon was kept in the reaction medium, at reflux, at temperature $t°_{ICX}$ = 68 °C and time t_{ICX} = 180 min, after which it was switched to the vacuum distillation process, in the same reactor, to which the condenser was attached, (Fig.5.7.), while a graduated cylinder with a grommet was a attached to it, for sealing and providing the vacuum pressure $p_{pv=}$ 25 mmHg. The distillation temperatures were $t_i°_{DCX}$ =78 and Δt = 23 °C, and the process duration was t_{DCX} = 90 min.

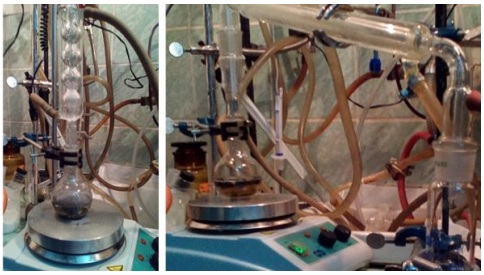


Fig. 5. 7. Carbon X when impregnated with Gu-ROH: impregnation followed by distillation



Fig. 5. 8. Lignocellulosic material of SC_{SF}, type used for combination with alcoholic guanidine

The final catalysts Cx-Gu and CA_{II}-Gu resulted.

5.3.2. Heterogeneous catalyst from guanidine and raw lignocellulosic biomass (fruit stones)

The catalytic support used was that obtained in Chapter 3.3., of the SC_{SF} type (fruit stone catalytic support), and as a method of combination with guanidine, impregnation was also used, in a reaction at reflux followed by distillation. For the large stones fragmentation was preferred, so that they could subsequently fit in the reactor for the following synthesis, while the small fruit stones were kept intact.

Catalytic supports with mass in the range of 5-9 g were added to the reaction flask, in a similar procedure, in admixture with Gu-ROH and pure methanol. The reaction conditions were $t°_{ISCSF}$ = 68 °C, t_{ISCSF} = 180 min.

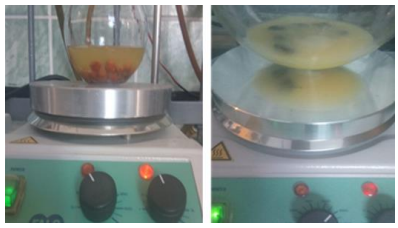


Fig. 5.9. Impregnation by reaction to reflux: SC_{SF}.ci (left), SC_{SF}.cai (right)

The types of base heterogeneous final catalysts resulted SC_{SF}-Gu.

5.3.3. Heterogeneous catalyst from guanidine and BC

In the case of using biocellulose (BC) as catalytic support, three types of catalyst were built, given the chemical composition of BC, which would allow chemical bonding strategies with different compounds, with the formation of different new functional groups. The operations scheme made at the beginning of the research implied a series of synthesis in which BC would have participated as material or catalytic support, so that, in addition to the method in Chapter 3.4., BC was obtained in parallel in cycles of 7-10 days, alternating with cycles of 24-28 days, to ensure

providing BC as raw material for multiple processes, the amount of BC evolving from 6-7 g initially predicted to over 70 g of dry BC.

5.3.3.1. Catalyst from simple BC[18] treated with potassium hydroxide

The first type of BC support used was that which was treated with 5% and 10% potassium hydroxide, without being dried before obtaining, but before the Chapter 3.4.3.2. immersion in methanol method. Thus, 5% and 10% KOH solutions were prepared, in several cycles, in which BC was immersed, at a ratio of 1:3 m/v BC undried/ KOH sol. (BC saturated of mass of 800 g, 600 g etc, as in Fig. 5.10.).



Fig. 5.10. 3 L crystallizer with wet BC (1400 g) when treated with potassium hydroxide solutions

The BC thus treated was maintained at ambient temperature for 3-5 days for each treatment cycle, after which it was dried and stored under anhydrous conditions. The resulting biocellulose was considered a final catalyst, of the type $BC_{KOH\ 5\%}$ and $BC_{KOH\ 10\%}$ (Fig.5.11 and Fig.5.12.)

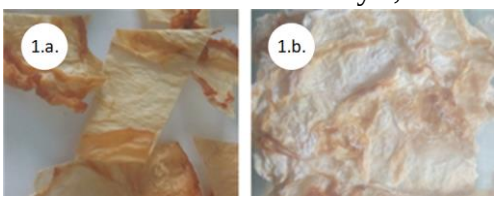


Fig. 5.11. BC treated with 5% and 10% solutions: 1.a.- BC with 5% KOH; 1.b.- BC with 10% KOH

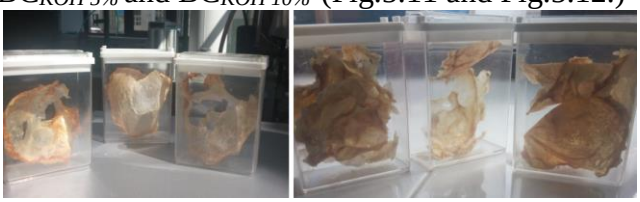


Fig. 5.12. $BC_{KOH\ 5\%}$ and $BC_{KOH\ 10\%}$ final catalysts

5.3.3.2. Catalyst from simple BC[19] and guanidine

This type of catalyst was prepared using biocellulose as a support, immediately after its production, BC undergoing only the antimicrobial treatment presented in Chapter 3.4. Obtaining this type of catalyst was derived from the method for obtaining the support, presented also in Chapter 3.4., while for the combination method the impregnation being performed with the same technique, in a reaction at reflux, associated with distillation. The reaction conditions were: temperature $t°_{IBC}$ = 65 °C and kept under stirring and time t_{IBC} =180 min. For analysis, drying was also performed, but for the synthesis for which it was built, it could have entered into reaction directly from the impregnation medium. The final catalyst BC-*Gu* was obtained.

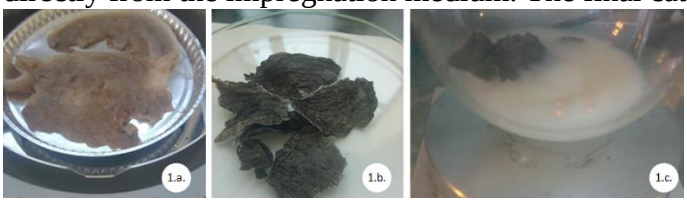


Fig. 5. 13 BC on Gu-ROH impregnation: 1.a.- final, after drying using thermobalance; 1.b.- BC dried, before impregnation; 1.c.- BC in reaction impregnation medium with Gu-ROH



Fig. 5. 14. BC immersed in methanol, driesd and treated with Gu

[18] Simple = removed from the culture medium, treated antibacterially with 0.1 M KOH at 100 ºC and not dried (used directly, wet).
[19] Simple = removed from the culture medium, antimicrobially treated with 0.1 M KOH at 100 ºC and dried.

5.3.3.3. Catalyst from simple BC[20]-methanol and guanidine

To create it, the procedure from Chapter 5.3.3.2. was repeated, and instead of simple BC, simple BC kept in methanol was used (Fig.5.14).

5.4. RESULTS AND DISCUSSIONS

The functionalized carbon behaved differently during the impregnation, being highlighted in this situation the influence of the source of origin.

In the case of commercial carbon, with an obviously larger specific surface area, the distillation time was similar, but the adsorption capacity of carbon was higher than in the case of other type of carbon.

The time for impregnation was the same in all cases, and the process temperatures were relatively close, so that a certain behavior of the catalyst in and post-reaction, or differences in characteristics, would not have been due to the influence ot these process parameters.

The success in term of impregnation process performances was confirmed by the SEM analyzes performed.

SEM analyzes were thus performed for the surface morphology for the SC_{SF}ci-Gu catalyst and we find in Fig. 5.15. a surface characterized by a special porosity, in terms of number and size, with a network of pores completely covered by the joint chemical compound (superbase formed by guanidine and potassium hydroxide), a coating that seems uniform, which could describe a homogeneous compound, i.e. the superbase which was hoped to be obtained and which appears to be spread over the entire surface of the catalytic support.

In Fig. 5.16. it is shown progressively, from an overall SEM image to a detail image, the presence of the compound deposited on the catalytic support with the presence of *crystals* of the base compound in Fig. 5.16.1.a. and 5.16.1.b., while in Fig. 5.16.1.c. we find the spread of sites with base compound next to sites that do not seems to have come into contact.

SEM analysis in the case of SC_{SF}cai-Gu in Fig. 5.17. reveals in the images a surface with a different geaommetry from that of the catalytic support from SC_{SF}ci-Gu. However, we also find the same *crystal* format characteristic of the base compound, also evenly distributed on the surface, with differces in the type of coating, visible in the detail image 5.17.1.c.

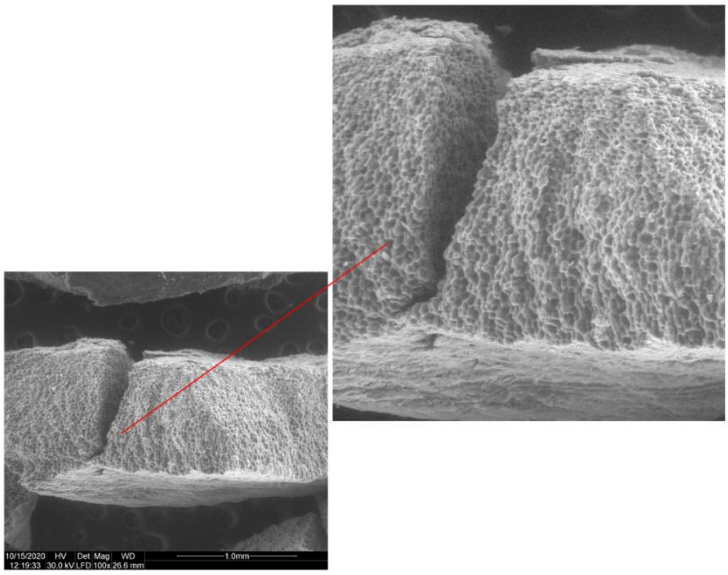


Fig. 5. 15. SEM images with SC_{SF}ci-Gu

[20] Simple = removed from the culture medium, treated antimicrobially with 0.1 M KOH at100 °C and kept for 7 days in methanol instead of acetic acid (vinegar).

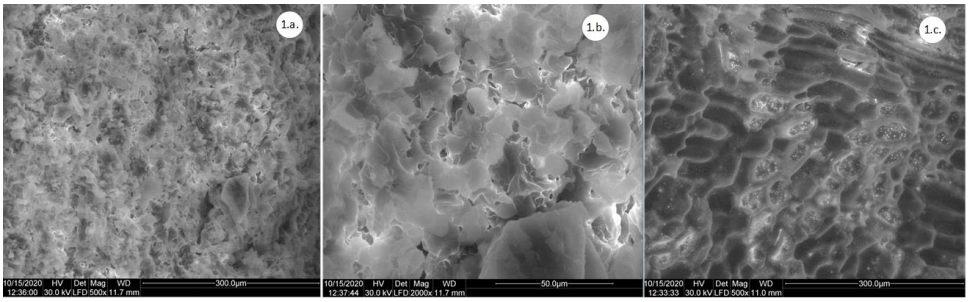


Fig. 5. 16. SEM for SC_{SF}ci-Gu: 1.a.- 1.b. nanoparticles-type deposit; 1.c.- sites occupied by the base compound

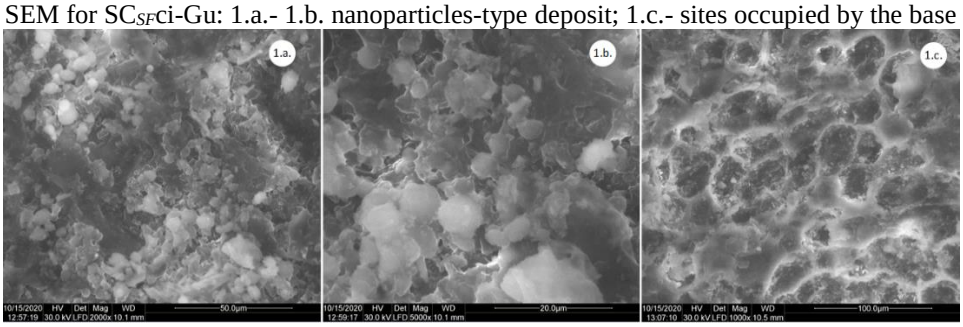


Fig. 5. 17. SEM images for SC_{SF}cai-Gu: 1.a and 1.b- alkaline compound nanoparticles;

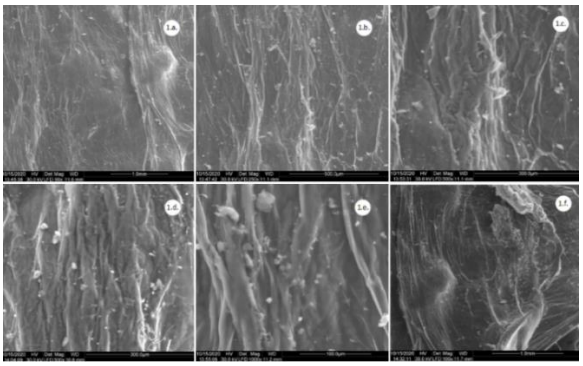
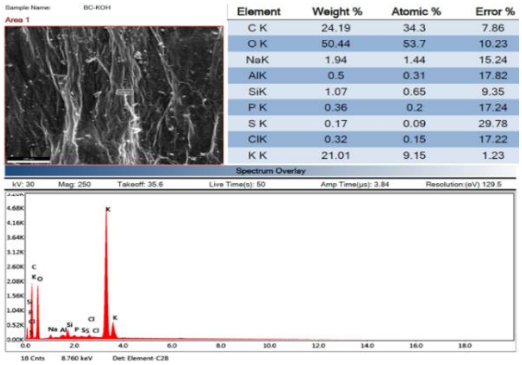


Fig. 5. 18. SEM cu BC_{KOH}: 1.a.-1.c. cellulose fibrils, with KOH nanoparticles; 1.d, 1.e- visible KOH nanoparticles in BC fibril netwoek



Element	Weight %	Atomic %	Error %
C K	24.19	34.3	7.86
O K	50.44	53.7	10.23
NaK	1.94	1.44	15.24
AlK	0.5	0.31	17.82
SiK	1.07	0.65	9.35
P K	0.36	0.2	17.24
S K	0.17	0.09	29.78
ClK	0.32	0.15	17.22
K K	21.01	9.15	1.23

Fig. 5. 19. Elemental analysis of BC_{KOH}

In case of BC_{KOH} catalyst (case of BC impregnation with potassium hydroxide) The SEM images from Fig. 5.18. shows, in image 1.a. and 1.b., hydroxide nanoparticles among the cellulose fibrils, and in the image of Fig. 5.18.1.d. we find in more detail the same particles, however, noting that no parallel can be made between their shape and that of nanoparticles on surfaces where potassium hydroxide was present togheter with guanidine (so the *superbase* theory would *stand*).

The elemental analysis performed for the BC_{KOH} catalyst confirms the presence of potassium in a convincing manner, the recorded peaks being correlated with the percentage mass that we find tabulated in Fig. 5.19.

In the case of SEM analysis for BC-Gu a progressively presentation of SEM images down to the detail, of the BC-Gu surface, was also preffered. We find thus in Fig. 5.20.1.a., 1b., and 1.c. cellulose fibrils, while in the images in Fig 5.20.1.d and 1.e. to observe the deposition of the base compound on the cellulose fibrils, and in the image from Fig. 5.20.1f. the base compound appears to be *wrapped* around the fibrils, simulating a perspective of homogeneity with them, and, at the same time, for even more detail on the SEM 1.h. and 1.i. images in Fig.5.20., to observe nanoparticles of the compound, somewhat similar to the nanoparticles observed in the SEM images from the other supports in Fig. 5.16. and Fig. 5.17.

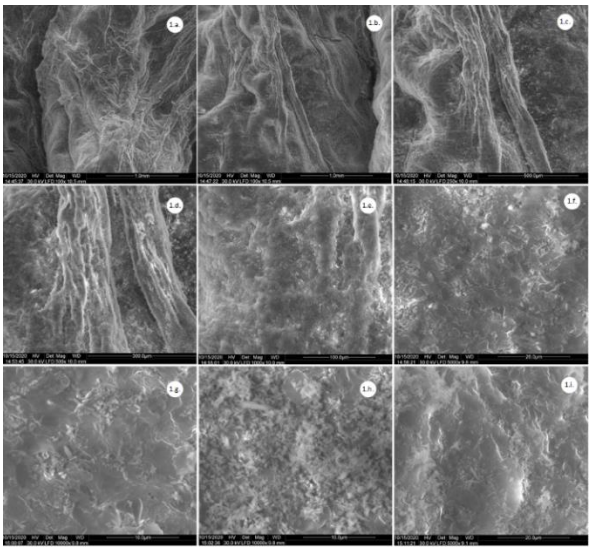
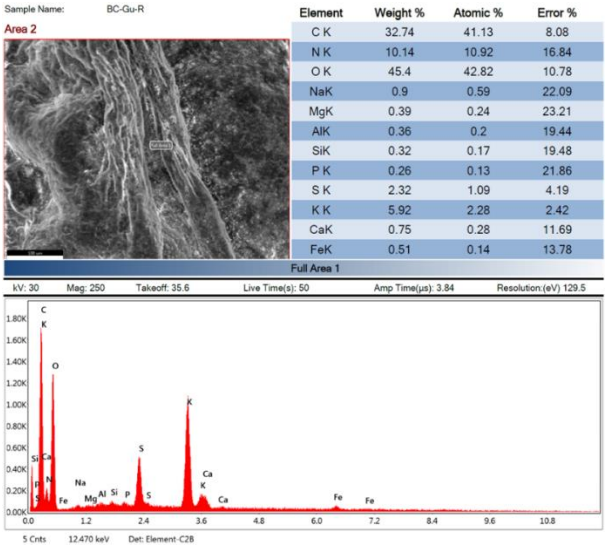


Fig. 5. 20. SEM imag.with BC-Gu:1.a, 1.b-BC fibrils network; 1.e-nanoparticles wrapped around the BC fibrils



Element	Weight %	Atomic %	Error %
C K	32.74	41.13	8.08
N K	10.14	10.92	16.84
O K	45.4	42.82	10.78
NaK	0.9	0.59	22.09
MgK	0.39	0.24	23.21
AlK	0.36	0.2	19.44
SiK	0.32	0.17	19.48
P K	0.26	0.13	21.86
S K	2.32	1.09	4.19
K K	5.92	2.28	2.42
CaK	0.75	0.28	11.69
FeK	0.51	0.14	13.78

Fig. 5. 21. Elemental analysis of BC-Gu

Elemental analysis, also performed for BC-Gu, confirms the obervations on the identification of the base compound from the interpretation of SEM images, by the presence of nitrogen in significant proportion, compared with BC-KOH[21].

5.5. CONCLUSIONS

The objectives achieved in this chapter brought us in the situation where we could develop, once again, certain properties of some materials, folded on our requirements. Thus, for the various types of activated carbon, the specific surfaces were functionalized, in order to introduce some functional groups necessary for the subsequent chemical bonding of guanidine. Application of strong acids was performed in order to change the chemical response to subsequent reactions with certain chemical compounds. The differences from the initial state to post-functionalization were highlighted in Chapter 5.4.

CHAPTER 6
BIODIESEL IN HOMOGENEOUS CATALYSIS - SIMULATION AND MODELLING

6.1. SIMULATION AND MODELLING OF BIODIESEL PRODUCTION PROCESS IN HOMOGENEOUS CATALYSIS

The conversion of oils to biodiesel by the transesterification reaction of triglycerides with methanol is an equilibrium reaction and one can try to influence the highest possible yield in at least two ways: 1) by shifting the equilibrium to the right (obtaining alkyl esters), by using an excess reactant and 2) by removing a product from reaction medium as it is formed. Industrial reactors that use this catalysis are reactors with perfect mixing (batch, semi-continuous and continuous), unlike those in the research or pilot stage (ultrasonic reactor, membrane reactor, steam phase methanol reactor etc.).

6.1.2. Biodiesel synthesis modelling using a batch reactor with external recirculation simultaneous with separation

[21] A *premeditated* comparison between the two, $\mathbf{BC}_{KOH}$ and BC-Gu

6.1.2.1. Considerations regarding the management of transesterification process and reactors type

Basic considerations regarding the transesterification process and its management in case of different types of reactors:

i) The transesterification process in alkaline catalysis is in fact a heterogeneous process, which take place at the methanol/catalyst interface, as droplets or films dispersed in the oil mass. Here begin the reaction process (reaction equation (1)), simultaneously with a complicated transport phenomenon (successive reactions (2) and (3) of the process), which occurs in the methanol phase, with the removal of glycerol due to the low solubility in this phase where the ester is accumulated [337].

ii) Vigorous mixing of the reaction mass causes the droplets of the methanol phase to break due to the *Eddy diffusion currents* formed, while a homogeneous phase similar to the emulsion develops here; process reactions take place without any significant associated transport phenomenon, excluding those of glycerol separation in the system.

iii) According to the mechanism below and due to the kinetics of the reaction rates, the *plug flow reacto*r is not recommended, because it cannot control the phase separation.

iv) All types of reactors operating with or without perfect mixing can be recommended for the control of transesterification for biodiesel synthesis.

v) The selection between batch and continuous operations, respectively, of a reactor with perfect mixing, is a complex phenomenon: the most relevant differences between batch and continuous processes is the size of the operation (it would also be related to the mode of operation, but does not influence a lot). Other issues such as seasonal demand, storage facilities, product *life*, labor operations, should also be considered, in order to make the right choice. Flexibility is an advantage of the batch process over the continuous one. For example, in the batch mode case, the same equipment can be used in multiple cycles of operations and also, depending on demand, the batch reactor can operate at any time of the year. On the other hand continuous processes, in order to be profitable, must have large plant capacities and operate as much as possible in a year, while storage capacities must exceed the availability of raw materials a seasonal demand, except all this would raise production costs [335, 336].

vi) A real competition manifests on the market of biodiesel installations, between those of low capacity and those of high capacity.

This work presents the performances obtained in the case of several transesterifications of vegetable oils with methanol, in reactors with perfect mixing. The reaction kinetics for the chemical reaction medium were considered accepted in homogeneous catalysis.

6.1.2.1. Transesterification kinetics in homogeneous base catalysis

Numerous studies address the kinetics of transesterification process in homogeneous catalysis. This type of process is associated with a certain type of vegetable oils, with a certain molar ratio between reactants or with a certain concentration of hydroxide (potassium or sodium) in the reaction mass and, of course, a certain reaction temperature. In some of these studies [337-344] the kinetic model adopted considers the reactions mechanism (1) - (3), through which the vegetable oil, considered as triglyceride (TG), results in fatty acid ester (E) and the corresponding diglyceride (DG), which continues esterification to (E) and the corresponding monoglyceride (MG), which, by esterification, releases glycerol (G) and fatty acid ester (E).

$$TG + \mathrm{CH_3}OH \underset{k2}{\overset{k1}{\Leftrightarrow}} DG + \mathrm{E} \qquad (1)$$

$$DG + \mathrm{CH_3}OH \underset{k4}{\overset{k3}{\Leftrightarrow}} MG + \mathrm{E} \quad (2)$$

$$MG + \mathrm{CH_3}OH \underset{k6}{\overset{k5}{\Leftrightarrow}} G + \mathrm{E} \quad (3)$$

It follows from (1) - (3) that all transesterification reactions are reversible. Considering the *subscript notations* for the reaction rate constants, 1 for methanol (ME), 2 for (TG), 3 for (DG), 4 for (MG), 5 for (G) and 6 for (E), we will have the reaction rates for the processes (1) - (3) described in equations (4) - (6).

$$v_{r1} = k_1 c_1 c_2 - k_2 c_3 c_6 \quad (4)$$

$$v_{r2} = k_3 c_1 c_3 - k_4 c_4 c_6 \quad (5)$$

$$v_{r3} = k_5 c_1 c_4 - k_6 c_5 c_6 \quad (6)$$

$$k_j = \mathrm{k}_{j0} \exp\left(\frac{-\mathrm{E}_j}{\mathrm{RT}}\right) \quad \mathrm{j} = 1,2 \ldots 6 \quad (7)$$

The rate constants of each of the six reactions have an *Arrhenius*-type temperature dependence. In a transesterification reaction it is shown that the vegetable oil is a mixture of triglycerides and each reacts in its own way. In this case the kinetic parameters cinetici E_j and k_j from the literature [337-344] were used, which correspond to *Jatropha* oil, palm oil, soybean oil, which were transesterified with methanol, under the conditions of using a molar ratio of methanol/oil of 6:1, at a reaction temperature of 30-60 °C and 1% m/m KOH catalyst.

In Tab. 6.1. we find the range of values for the 12 kinetic parameters (6 rate constants and 6 activation energies). The heat of the reaction enthalpies are calculated from heats formation [344] and are $\Delta H_R = -5.07 \cdot 10^3$ J/mol, for each reaction from equations (1)-(3). This reduced enthalpy of the exothermic reaction simplifies the mathematical model of the reactor by neglecting the heat balance, if the reactants are fed at a specially selected temperature and the reaction mass is kept at this temperature.

It should be noted that, although mathematical models in the class of heterogeneous ones are not mentioned in the literature on transesterification in alkaline catalysis of vegetable oils, we appreciate them as possible to create, especially that glycerol, which is a reaction product, is almost completely immiscible with homogeneous oil-methanol-ester system. Agglomeration of glycerol into microparticles and their coalescence is a process that can control the kinetics of the above-mentioned reaction (3). Thus from here can come the kinetic control of the whole process. Observing that this problem, almost completely new, of heterogeneous models in alkaline transesterification of vegetable oils, is not the subject of this chapter, we specify once again that, in the following development, the considered kinetics was mentioned above (three reversible reactions, characterized of 6 rate constants and 6 activation energies).

Tab. 6. 1. Values of kinetic parametrs for methanol transesterification bio-oils (catalyst: NaOH 1% w/w in methanol) [344].

j	1	2	3	4	5	6
k_{j0} l/(mol min)	13.04±4.16	27.21±5.63	104.87±9.89	90.88±7.69	0.078±0.0056	0.957±0.11
E_j KJ/mol	16,377±1567	19,202±2056	17,867±1536	19,283±2093	4,282±375	15,302±1447

Mathematical model of perfect mixing reactor operation

The mathematical model of the operation of the reactor with perfect mixing considers that the process takes place isothermally, and imposing the condition that in reactor there is a perfect mixing

is ensured. The procedures on how the reactors are operated are shown in Fig. 6.3. These allows the following 9 cases to operate the biodiesel synthesis reactor:

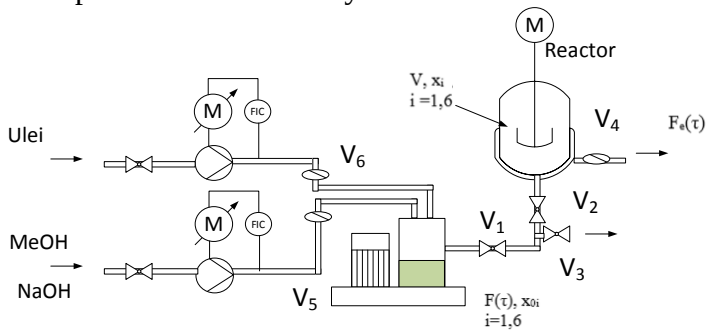


Fig. 6. 1. Simplified scheme of an installation with perfect mixing reactor for biodiesel synthesis

i) Once V_5, V_6, V_1 and V_2 valves are opened the reactor is readily fed at a pre-determined volume by the selected reactants molar ratio, then the batch mode start running (*batch reactor*); the glycerin stream flows post decantation through now opened V_3, as well as the biodiesel stream;

ii) Valves V_5, V_6, V_1 and V_2 open and the reactor is readily fed at a pre-determined volume by the selected reactants molar ratio, batch mode is running, with glycerine flow through V_3 sau V_4 (*batch reactor with glicerine flow*);

iii) Opened V_5, V_6, V_1 and V_2 feeds the reactor, while its volume increasing throughout the feed duration simultaneosly with transesterification reaction (*fed batch*); the glycerine after separation and then the biodiesel stream flow through opened V_3 after separation;

iv) Opened V_5, V_6, V_1 and V_2 feeds the reactor, while its volume increasing throughout the feed duration simultaneosly with transesterification reaction and with V_4 opening to remove glycerine, while it separates as main by-product in reaction mixture (fed batch with glycerine flow); glycerine after separation and then the biodiesel streams are removed by opening V_3;

v) Valves V_5, V_6, V_1 and V_2 open and the reactor is readily fed with calculated vegetal oil volume then with V_5, V_6, V_1 and V_2 opened valves the methanol/catalyst mixture is fed throughout the batch duration (*fed batch with methanol feed*); glycerine after separation and then the biodiesel stream are removed through opened V_3;

vi) Valves V_5, V_6, V_1 and V_2 open and the reactor is readily fed with calculated vegetal oil volume then with V_5, V_6, V_1 and V_2 opened valves the methanol/catalyst mixture is fed throughout the batch duration along with V_4 opening for glycerine stream to flow as it is formed and decanted (*fed batch with methanol feed and glycerine flow*)

vii) With V_5, V_6, V_1 and V_2 opened valves the reactor is readily fed with calculated methanol volume then with V_6, V_1 si V_2 opened valves methanol and oil are fed throughout the batch duration (fed batch with oil feed);

viii) With V_5, V_1 and V_2 opened valves the reactor is readily fed with calculated methanol volume then with V_6, V_1 si V_2 opened valves methanol and oil are fed throughout the batch duration while glycerine stream flows through V_4 (fed batch with oil feed with glycerine flow);

ix) With V_5, V_1 and V_2 opened valves it can be operated in steady state by bringing the reactor to this oparational mode by passing to fed batch mode (*fed batch*).

Using *i)-ix)* descriptions and the diagram shown in Fig. 1 a general mathematical model can be developed, associated with this synthesis in perfect mixing reactor, a model that can generate then the mentioned operation cases by simplification and by adequate choosing feed rates along with adequate evacuation flows. The goal is that, both by how the feed is selected (*e.g.* methanol over vegetable oil) and glycerol removing from reactor, to shift the reaction balance toward desired direction, yielding maximum in main product reaction. The mathematical model associated fed batch with methanol feed and glycerol flow reactor contains the total material balance equation

(Eq. 8.) and the conservation relation for five out of the six species involve in the process (Eq. 9.), as well as the equation for species partial material balance, if the total material balance equation is used as integral form (Eq. 10.).

$$\frac{\mathrm{dV}}{\mathrm{d}\tau} = \frac{F(\tau)}{\rho_m} - \frac{F_e(\tau)}{\rho_m} \tag{8}$$

$$\frac{\mathrm{dx_j}}{\mathrm{d}\tau} = \frac{F}{\rho_m V}(x_{oj} - x_j) + \frac{\phi_j}{\rho_m V},\ \mathrm{j} = 1,2..4,6 \tag{9}$$

$$\frac{\mathrm{dx_j}}{\mathrm{d}\tau} = \frac{F}{\rho_m V}(x_{oj} - x_j) + \frac{\phi_j}{\rho_m V} - \frac{F_e(\tau)}{\rho_m},\ \mathrm{j} = 5 \tag{10}$$

In equation (9) ϕ_j j= 1,2..6 expresses the *j* species participation in reactions, given by the equations (1)-(3): j = 1– ME, j = 2– TG, j = 3 – DG, j = 4 – MG, j = 5 – G, j = 6 – E, along with equations (11)-(16), where M_1, M_2, ..M_6 represents the molar mass of each of the six participating species in the kinetic transesterification process.

$$\phi_1 = -(v_{r1} + v_{r2} + v_{r3})VM_1 \tag{11}$$

$$\phi_2 = -(v_{r2})VM_2 \tag{12}$$

$$\phi_3 = (v_{r1} - v_{r2})VM_3 \tag{13}$$

$$\phi_4 = (v_{r2} - v_{r3})VM_4 \tag{14}$$

$$\phi_5 = (v_{r3})VM_5 \tag{15}$$

$$\phi_6 = (v_{r1} + v_{r2} + v_{r3})VM_6 \tag{16}$$

In equations (11)-(16) both average molar mass and the average density of the reaction mass can be obtained using weighted arithmetic mean, as is shown in equations (17) and equation (18):

$$\rho_{\mathrm{m}} = \sum_1^6 \left(\frac{x_j}{\rho_j}\right)^{-1} \tag{17}$$

$$M_{\mathrm{m}} = \sum_1^6 \left(\frac{x_j}{M_j}\right)^{-1} \tag{18}$$

It can easily be seen that the mathematical model mentioned above contains 7 differential equations that are associated with the related relations, for the epxression of some terms from the model. For a fixed situation regarding the dynamics of the reactor feed rate, as well as the composition of this feed, the initial conditions associated with the model must also specify the initial volume of reaction mass in the reactor, together with its composition.

6.2. RESULTS AND DISCUSSIONS

Simulation of operating cases and comparison of results

The following fixed variables were selected while building operating modes simulation: *i)* 60 °C reaction temperature (the most use in these type of processes) for which a table showing k_i reaction rate constant at 40 and 60 °C was associated; *ii)* in all cases 20 m^3 was selected as value for reaction volume; *iii)* in all cases, except for steady state regime ones, 80 min was the selected reaction time (generally used with commercial biodiesel); *iv)* 1% w/w catalyst to oil, as already showed while discussing pre-exponential factors and activation energies; *v)* in operating modes with glycerol removing, glycerol evacuation starting was 5 min after the beginning of reaction; *vi)* internal reactor flow, considered as perfect mixed, had influence on glycerol separation from mass reaction.

It is not the subject of this thesis to present the dynamics of the concentration field of the components of the transesterification process, but for comparison reason the concentration field

dynamic for reaction components for *batch with glycerol flow* (Fe(τ)= 19 kg/min for τ>5) respectively *fed batch with methanol feed and glycerol flow* (Fe(τ)= 21 kg/min for τ>5) operating modes (Fig. 6.4.), both cases using ME/TG= 6 methanol to oil ratio, showing significant differences between the reactant concentration profile as well as the final concentrations after 80 min, higher for DG and MG in *fed batch with methanol feed and glycerol flow*. At the same time both glycerol concentration decreasing to zero and evacuation rate higher (21 kg/min to 19 kg/min) were observed also in *fed batch with methanol feed and glycerol flow*.

At this stage, in each of the above-mentioned operating cases, their performances was highlighted in a graphical form and in a concentrated table. In the characteristics graphical representations, the dynamics of the concentrationsand the mass flow of glycerol generated (G_{mG}) were noted, as a variable that shows better the reaction rate in the reactor.

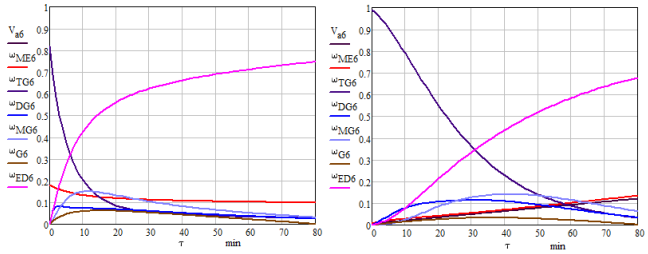


Fig. 6.2. Dynamics of mass fractions of reactions components and dimensionless reactor volume in batch with glycerol flow (left, Fe(τ)= 19kg/min for τ>5) respectively fed batch with methanol feed and glycerol flow (right, Fe(τ)= 21 kg/min for τ>5) at reactants molar ratio ME/TG =6

Classic batch operation (*batch reactor*), although hard to belive that it could be real (how would a reactor could be fill instantly if the reaction kinetics is that fast (80 minute), was strongly influenced by reactants molar ratio, as yield is shown in Tab. 6.2., while Fig. 6.3-6.5 show the dynamic of components concentration along with glycerol flow.

Tab. 6.2. Data input in pure batch operation and the resulted transesterification yield

	ME/TG	x_{01} kg /kg	x_{02} kg /kg	x_{03} kg /kg	x_{04} kg /kg	x_{05} kg /kg	x_{06} kg /kg	x_{10} kg /kg	x_{20} kg /kg	x_{30} kg /kg	x_{40} kg /kg	x_{50} kg /kg	x_{60} kg /kg	F(τ) kg/min	$F_e(\tau)$ kgG/min	Y
1	2	0	0	0	0	0	0	**0.068**	**0.932**	0	0	0	0	0	0	**0.716**
2	4	0	0	0	0	0	0	**0.138**	**0.872**	0	0	0	0	0	0	**0.914**
3	6	0	0	0	0	0	0	**0.181**	**0.819**	0	0	0	0	0	0	**0.96**
4	0	0	0	0	0	0	0	**0.226**	**0.774**	0	0	0	0	0	0	**0.986**

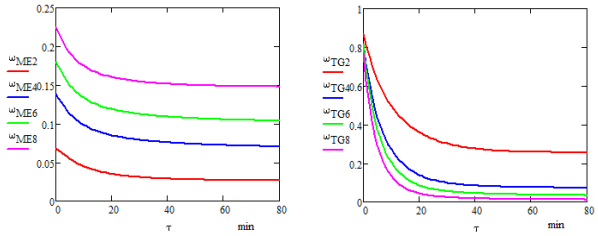
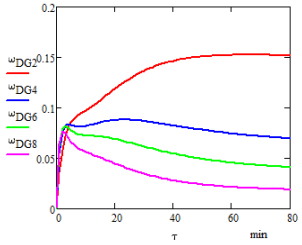


Fig. 6. 3. Dynamic of methanol and trygliceride concentration (mass fractions) at 60 ºC and ME/TG = 2 (red), 4 (blue), 6 (green) and 8 (magenta) in pure batch operation

Some observations can easily be made from the diagrams in Fig. 3-5: *i)* increasing yield in ME and E are not that significant over 4 as ratio ME/TG; *ii)* TG an G concentration dynamic is very tight for the same molar ratio of 4 for ME/TG; *iii)* there is a strong decreasing in glycerol concentration dynamic in the 20 m^3 reactor, after 20 min of transesterification; *iv)* this operating mode is difficult to run in practice.



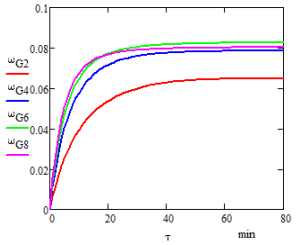
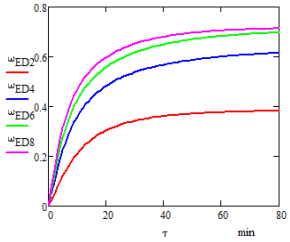


Fig. 6.4. Dynamics of diglyceride and respectively glycerol concentration (mass fractions) at 60 ºC and ME/TG =2 (red), 4 (blue), 6 (green) and 8 (magenta) in pure batch operation



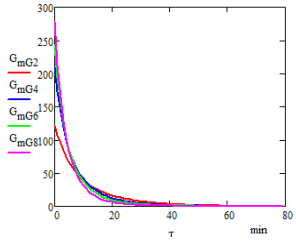


Fig. 6..5. Dynamics of ester concentration (mass fractions) and respectively glycerol flow rate (kg G/min) at 60 ºC and ME/TG =2 (red), 4 (blue), 6 (green) and 8 (magenta) in pure batch operation

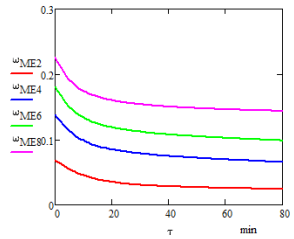
Batch reactor with glycerol flow operating mode is also difficult to run, while the glycerol evacuation is expected to shift the reaction balance. The glycerol evacuation from the reactor is expected to shift the balance somewhat. In addition, it considerably shortens the post-processing after the end of the reaction. The conditions and the yields obtained for this operating mode are shown in Tab. 6.3. and it can be seen a slight yield increasing. The function expressing glycerol evacuation is shown in Eq. (19), revealing that the glycerol evacuation begins after 5 min from reaction start.

$$F_e(\tau) = \frac{19 \; for \; \tau > 5}{0 \; for \; \tau < 5} \tag{19}$$

Tab. 6.3. Data input in batch operation with glycerol flow and the resulted transesterification yield

	ME/TG	x_{01} kg /kg	x_{02} kg /kg	x_{03} kg /kg	x_{04} kg /kg	x_{05} kg /kg	x_{06} kg /kg	x_{10} kg /kg	x_{20} kg /kg	x_{30} kg /kg	x_{40} kg /kg	x_{50} kg /kg	x_{60} kg /kg	$F(\tau)$ kg/min	$F_e(\tau)$ kgG/min	Y
1	2	0	0	0	0	0	0	**0.068**	**0.932**	0	0	0	0	15	**0.716**
2	4	0	0	0	0	0	0	**0.138**	**0.872**	0	0	0	0	18	**0.921**
3	6	0	0	0	0	0	0	**0.181**	**0.819**	0	0	0	0	19	**0.97**
4	0	0	0	0	0	0	0	**0.226**	**0.774**	0	0	0	0	18.5	**0.993**

The dynamics of the concentration of the participants in the process, along with flow of the glycerol produced has the results concentrated in Fig. 6.6 - Fig. 6.8.



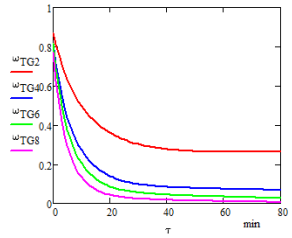
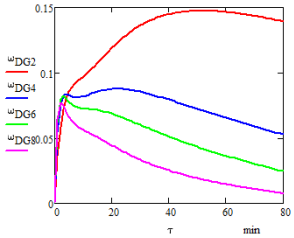


Fig. 6.6. Dynamics of methanol and respectively triglyceride concentration (mass fractions) at 60 ºC and ME/TG = 2 (red), 4 (blue), 6 (green) and 8 (magenta) batch operation with glycerol flow



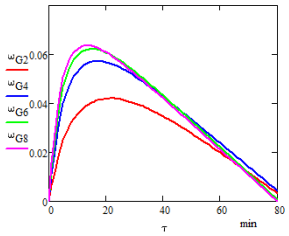
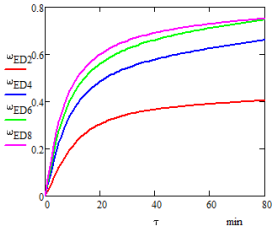


Fig. 6.7. Dynamics of diglyceride and respectively glycerol concentration (mass fractions) at 60 ºC and ME/TG =2 (red), 4 (blue), 6 (green) and 8 (magenta) in batch operation with glycerol flow



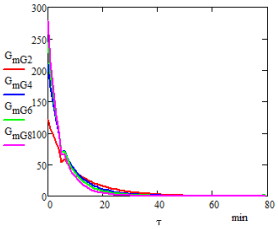


Fig. 6.8. Dynamics of ester concentration (mass fractions) and respectively glycerol flow rate (kg G/min) at 60 ºC and ME/TG =2 (red), 4 (blue), 6 (green) and 8 (magenta) in batch operation with glycerol flow

While comparing with the first operating mode we can observe: *i)* a slight increasing yield; *ii)* similar modification in components concentration and yield behavior while using higher than 4 molar ratio ME/TG; *iii)* absence of glycerol or very little glycerol in the product (Fig. 6.6.); *iv)* less

diglyceride in reaction product (Fig. 6.6.); *v*) good concentration for diglyceridic ester ED (over 0.7 kg ED/kg) for 6 and 8 molar ratio of ME/TG (Fig. 6.7.); *vi*) the clear revealing of the moment when glycerol evacuation begins (Fig. 6.8.)

Fed batch with pass to continuous perfect mixing operation has two components, *fed batch* first until the reactor is fed, passing then to continuous operation until steady state is reached. Process duration is 160 min in this case, with 80 min of continuous operation, started the min after filling the reactor. Input data and yields are presented in Tab 4.

Tab. 6.4. Data input in fed batch operation with pass to continuous process and the resulted transesterification yield

	ME/TG	x_{01} kg /kg	x_{02} kg /kg	x_{03} kg /kg	x_{04} kg /kg	x_{05} kg /kg	x_{06} kg /kg	x_{10} kg /kg	x_{20} kg /kg	x_{30} kg /kg	x_{40} kg /kg	x_{50} kg /kg	x_{60} kg /kg	$F(\tau)$ kg/min	$F_e(\tau)^*$ kgG/min	Y
1	2	**0.068**	**0.932**	0	0	0	0	**0.009**	**0.99**	0.000	0.000	0.000	0.000	250	250	**0.806**
2	4	**0.138**	**0.872**	0	0	0	0	**0.009**	**0.99**	0.000	0.000	0.000	0.000	250	250	**0.902**
3	6	**0.181**	**0.819**	0	0	0	0	**0.009**	**0.99**	0.000	0.000	0.000	0.000	250	250	**0.934**
4	0	**0.226**	**0.774**	0	0	0	0	**0.009**	**0.99**	0.000	0.000	0.000	0.000	250	250	**0.953**

* doar după umplerea reactorului de 20 m^3

To be noticed that the given yields are for the steady state reactor case. In this case for ME/TG= 2 we have a higher yield than in other cases which used similar ratio. For 4, 6 and 8 ME/TG ratio the yields are lower than the ones in the first two cases, as shown in Fig. 6.9.-6.11

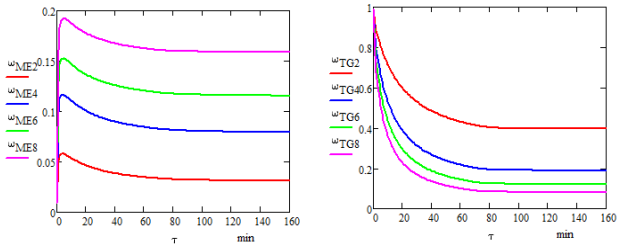


Fig. 6.9. Dynamics of methanol and respectively triglyceride concentration (mass fractions) at 60 ºC and ME/TG = 2 (red), 4 (blue), 6 (green) and 8 (magenta) in fed batch operation with passing to continuous

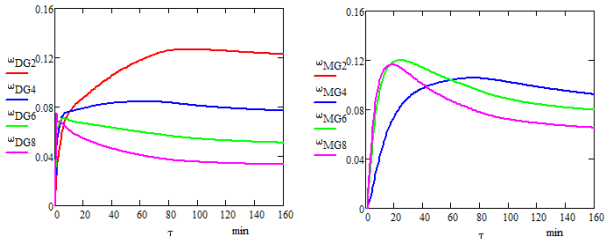


Fig. 6.10. Dynamics of diglyceride and respectively monogliceride concentration (mass fractions) at 60 ºC and ME/TG = 2 (red), 4 (blue), 6 (green) and 8 (magenta) in fed batch operation with passing to continuous

Fig. 6.9. shows that after 80 min, when the reactor is filled, ME and G concentration are slightly changed, showing an operation state close to the continuous steady state one. Same with DG and MG concentration dynamic, which shows also switching from batch to non-steady continuous and then to steady continuous state Fig. 6.10. We can also see significant concentration of DG and TG in reaction product (12 %), mixed with ME, E and G too.

In Fig. 6.11. the glycerol concentration dynamic shows the time interval in which the switch from fed batch operation to continuous non-steady operation take place, revealing at the same time how the continuous perfect stirred reactor for vegetable oil conversion to biodiesel works.

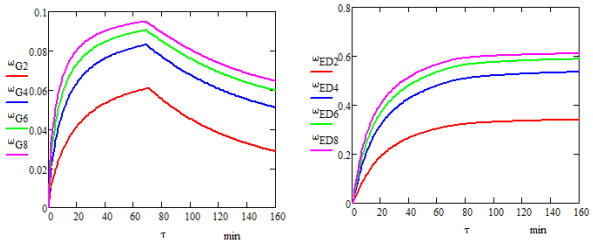


Fig. 6.11. Dynamics of glycerol and respectively ester concentration (mass fractions) at 60 ºC and ME/TG = 2 (red), 4 (blue), 6 (green) and 8 (magenta) in fed batch operation



Fig. 6.12. Experimental installation for synthesis fed-batch with oil feed (1- mixing reactants vessel, 2 - condenser, 3 – microdosing pump, 4 – liq. pump, 5, 6 – reactor (homog, heterog.)

with passing to continuous 7 – thermostated bath)

Fed batch with oil feed operation mode was experimented in previous work[22] (Fig.6.12.) and proved to be an interesting solution for transesterification process. Here the methanol is first fed into the reactor and then the heated oil is fed over methanol, using a selected flow that allow the reactor to be filled in the pre-selected duration.

Tab. 6.5. Data input in fed batch operation with oil feed and the resulted transesterification yield

	ME/TG	x_{01}	x_{02}	x_{03}	x_{04}	x_{05}	x_{06}	x_{10}	x_{20}	x_{30}	x_{40}	x_{50}	x_{60}	$F(\tau)$	$F_e(\tau)$	Y
		kg /kg	kg /kg	kg /kg	kg /kg	kg /kg	kg /kg	kg /kg	kg /kg	kg /kg	kg /kg	kg /kg	kg /kg	kg/min	kgG/min	
1	2	**0**	**0.99**	**0.005**	**0.005**	0	0	**0.99**	0.000	**0.002**	**0.003**	0.000	**0.005**	210	0	**0.658**
2	4	**0**	**0.99**	**0.005**	**0.005**	0	0	**0.99**	0.000	**0.002**	**0.003**	0.000	**0.005**	196	0	**0.789**
3	6	**0**	**0.99**	**0.005**	**0.005**	0	0	**0.99**	0.000	**0.002**	**0.003**	0.000	**0.005**	184	0	**0.869**
4	0	**0**	**0.99**	**0.005**	**0.005**	0	0	**0.99**	0.000	**0.002**	**0.003**	0.000	**0.005**	175	0	**0.909**

The results shown in Tab. 5. where the experimental results used for simulation, while Fig. 6.13-6.15 focus the data on the characterization of the dynamics for this operation mode. Lower yields and the way the reaction volume is used seems to make unattractive this operation mode. Under laboratory conditions, this operation coupled at the end with a period of pure batch operation could be interesting, not only from a didactic perspective, but especially for obtaining some esters from exotic oils.

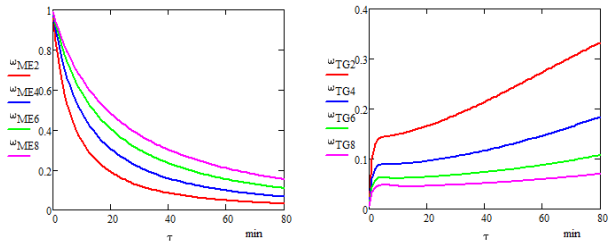


Fig. 6. 13. Dynamics of methanol and respectively triglyceride concentration (mass fractions) at 60 ºC and ME/TG = 2 (red), 4 (blue), 6 (green) and 8 (magenta) in fed batch operation with oil feed

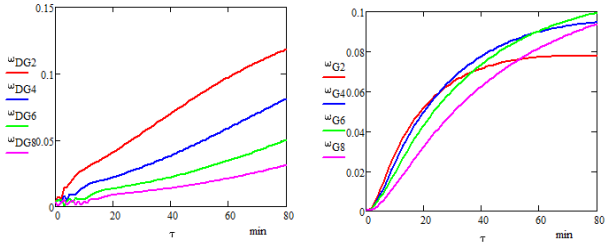


Fig. 6.14. Dynamics of diglyceride and respectively glycerol concentration (mass fractions) at 60 ºC and ME/TG = 2 (red), 4 (blue), 6 (green) and 8 (magenta) in fed batch operation with oil feed

This case is highlighting the important use only of 6 and 8 ME/TG molar ratio. If ME/TG=10 had been used it would probably have considerably increased the yield to 0.98. It can be seen that the reactions start slowly, then grow in speed, reaching a maximum rate in 10 to 15 min (Fig. 15. - G_{Mg} time dependency)

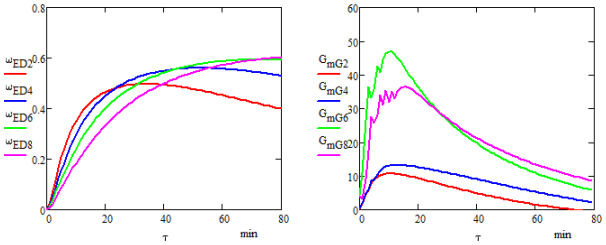


Fig. 6.15. Dynamics of ester concentration (mass fractions) and respectively glycerol flow rate (kg G/min) at 60 ºC and ME/TG =2 (red), 4 (blue), 6 (green) and 8 (magenta) in fed batch operation with oil feed

[22] *Cristian Eugen Răducanu, Oana Cristina Pârvulescu, Anghel Rodica, Tănase Dobre*, Considerations on biodiesel synthesis with fed batch reactor, PRIOCHEM-International Symposium, 27-28 October 2016;

Fed batch with methanol feed operation mode, also experimented in previous work, using an experimental installation shown in Fig. 6.12. in which the heated vegetable oil was fed first in reactor (1) and then from ME tank (2) the methanol was pumped (3) over at a pre-calculated flow in respect both with ME/TG ratio and filling the reactor in the selected duration. Tab. 6 shows simulation data input and the obtained yields

Tab. 6.6. Data input in fed batch operation with methanol feed and the resulted transesterification yield

	ME/TG	x_{01} kg /kg	x_{02} kg /kg	x_{03} kg /kg	x_{04} kg /kg	x_{05} kg /kg	x_{06} kg /kg	x_{10} kg /kg	x_{20} kg /kg	x_{30} kg /kg	x_{40} kg /kg	x_{50} kg /kg	x_{60} kg /kg	$F(\tau)$ kg/min	$F_e(\tau)$ kgG/min	Y
1	2	**0.99**	**0**	**0**	**0**	**0**	**0.005**	**0**	**0.99**	**0.002**	**0.003**	0.000	**0.005**	17	0	**0.725**
2	4	**0.99**	**0**	**0**	**0**	**0**	**0.005**	**0**	**0.99**	**0.002**	**0.003**	0.000	**0.005**	34	0	**0.912**
3	6	**0.99**	**0**	**0**	**0**	**0**	**0.005**	**0**	**0.99**	**0.002**	**0.003**	0.000	**0.005**	45	0	**0.962**
4	0	**0.99**	**0**	**0**	**0**	**0**	**0.005**	**0**	**0.99**	**0.002**	**0.003**	0.000	**0.005**	56	0	**0.985**

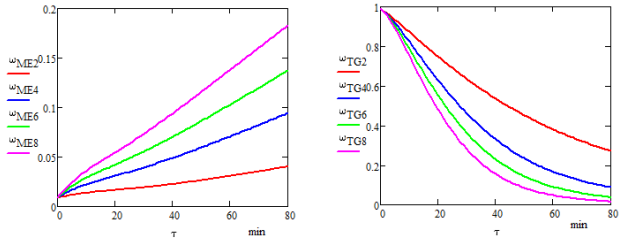


Fig. 6.16. Dynamics of methanol and respectively triglyceride concentration (mass fractions) at 60 ºC and ME/TG = 2 (red), 4 (blue), 6 (green) and 8 (magenta) in fed batch operation with methanol feed

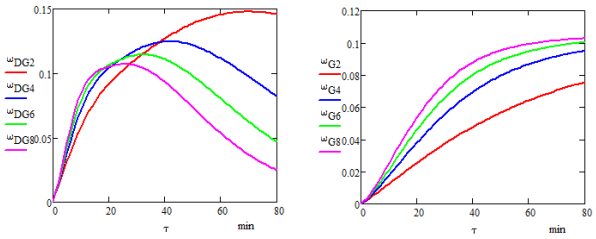


Fig. 6.17. Dynamics of diglyceride and respectively glycerol concentration (mass fractions) at 60 ºC and ME/TG = 2 (red), 4 (blue), 6 (green) and 8 (magenta) in fed batch operation with methanol feed

Fig. 6.17. shows the diglyceride concentration dynamic while Fig. 6.18. shows the glycerol production dynamic both highlighting and increased rate reaction followed slower ones. The yields obtained here recommend this type of operation mode, feasable by its characteristics, especially the uniform distribution of the fed methanol all over the mass reaction, as shown in Fig. 6.16-6.18.

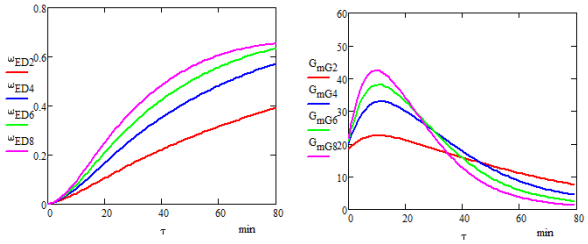


Fig. 6.18. Dynamics of ester concentration (mass fractions) and respectively glycerol flow rate (kg G/min) at 60 ºC and ME/TG =2 (red), 4 (blue), 6 (green) and 8 (magenta) in fed batch operation with methanol feed

6.3. CONCLUSIONS

A mathematical model was developed, applicable, with appropriate particularizations, to all cases of conducting the methanol transesterification reaction of vegetable oils using a perfect mixing reactor as the key element of the installation, while the kinetic data necessary for the concrete implementation of the model were chosen.

Using the proposed scheme for a biodiesel plant with a mixing reactor, it was shown how no less than seven operating modes can be implemented.

For a reactor with industrial volume mixing from the seven operating modes, five were used in simulation models, and the results obtained were graphically and tabulated presented.

All simulated cases shown as feasable the use of the ME/TG reaction ratio above the value 4.

It has been shown that the operation with glycerol removal from the process, as it is formed and separated, is a solution to increase the separation efficiency.

CAPITOLUL 7

BIODIESEL IN HETEROGENEOUS CATALYSIS - CATALYSTS TESTING, BIODIESEL SYNTHESIS, STATISTICAL MODEL At this stage the catalysts prepared in Chapter 5 were used for the synthesis of biodiesel from fresh and used vegetable oils. The reactor types were batch with perfect mixing and catalytic fixed-bed reactor.

7.2. MATERIALS

The raw materials used were waste oils collected from fast food-type restaurants or house holds and fresh sunflower oil from supermarket, as feedstock for conversion to biodiesel, as well as the catalysts obtained in Chapter 5.

7.3. EXPERIMENTAL METHOD

7.3.1. Biodiesel using heterogeneous catalyst from sulfonated activated carbon in perfect mixed reactor

For this research step a batch mode was selected, in a perfect mixing reactor, while the first catalyst used was $CA_{COM}S$, functionalized in Chapter 5. The first step was to activate the catalyst, by adding it to the reactor, with methanol and kept at a temperature of 50 °C, to form methoxide (activation). Heated oil was then added to the methoxide to allow the reaxction mixture to rapidly reach the process temperature. Process conditions were: catalyst/oil molar ratio 12:1, reaction time 75-240 min and catalyst/oil 5-7% m/m, while yields in biodiesel (η_{ME}) and glycerol (η_G) can be found in Tab. 7.1.

Tab. 7. 1. Biodiesel using $CA_{COM}S$: process conditions and products yield

Exp.no	Oil type	Cat.preparation mode KOH	MeOH/oil molar ratio	Reaction temp. [°C]	Reaction time [h]	X	Y_{ME} [%]	Y_G [%]
1		2M-1h	12:1	65	2	0.90	88.64	85.27
2		2M-1h	12:1	65	4	0.95	84.92	69.77
3		2M-0.5h	12:1	65	4	0.84	88.98	85.27
4		1.5M-0.5h	12:1	65	4	0.75	67.80	77.52
5		2M-1h	12:1	65	2	0.67	55.08	42.64
6		2M-1h	12:1	65	4	0.50	46.61	15.50
7		2M-1h	12:1	65	0.75	0.76	81.36	73.64
8	sun	3M-1h	12:1	65	0.75	0.83	84.32	69.77
9	flower,	2M-1h	12:1	65	0.75	0.94	92.37	85.27
10	used	3M-1h	12:1	65	1	0.94	89.83	73.64
11		3M-1h	12:1	65	1	0.79	74.58	62.02
12		3M-1h	12:1	65	1	0.80	76.68	54.26
13		3M-1h	12:1	65	1	0.85	81.78	69.77
14		3M-1h	12:1	65	1	0.86	79.66	85.27
15		3M-1h	12:1	65	3	0.68	78.81	21.71
16		3M-1h	12:1	65	2	0.61	62.71	17.44
17		3M-1h	12:1	65	2	0.62	59.32	19.77

Notations: X = *conversion,* η_{ME} = methyl ester yield, η_G = glycerol yield

7.3.2. Biodiesel using heterogeneous catalyst from KOH-functionalized activated carbon in fixed-bed catalytic reactor

At this stage of the research, the experimental installation from Fig. 7.2.

The raw material used for the conversion to biodiesel was sunflower oil (200g/per batch), in a 1:6 molar ratio with methanol. Thus the oil was fed in a four-necked flask (reactor feed vessel) (1) together with the methanol, where two layers were formed, due to the difference in the density of the reactants, the top layer being the one with methanol, of which, with the help of a microdosing pump (2), a flow was directed, for 2 min, in the column-type catalytic reactor (3) with fixed-bed catalyst (4) to activate it. The process temperature was provided by means of a thermostated bath (5). Addition of new equipment to the installation, respectively a dosing pump and a separating funnel (6), modified with an adapter that allowed recirculation in the mixing vessel of the reactants

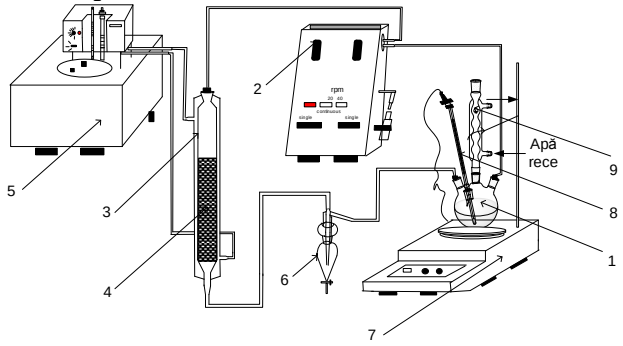


Fig. 7.1. Experimental installation with fixed-bed catalytic reactor for oil conversion to biodiesel:
1) - feed vessel; (1) - microdosing pump; 3) - fixed-bed catalytic reactor;
4) - activated carbon catalyst layer; 5) - thermostated bath; 6) - separating funnel;
7) - heated magnetic stirrer

it optimized the phase separation, intervening at the end of the reaction, by keeping the glycerin to settle in the separation funnel, simultaneously with its formation after the beginning of the transesterification reaction. The feed vessel was also heated by means of a heated magnetic stirrer (7).

In this case, the characteristic factors for the transesterification process were selected (Tab. 7.2.) and an experimental design based on a factorial plan 2^3 (with 3 factors and two levels for each factor) was performed with 8 experiments

Tab. 7. 2. Characteristic factors for the transesterification process

	Characteristic factors	Symbol	Selected values	
1	Fixed-bed catalyst height	*h*	20 40	cm
2	Superficial velocity	*W*	0.14 0.28	cm/s
3	Operating temperature	*T*	55 65	°C

The influence of process factors on the responses in terms of biodiesel yield (Y_{FAME}), glycerol (Y_G) and glycerol formation time (τ_G), were determined as a percentage of the theoretical values of the product masses. The statistical model for the process performance based on the factorial plan 2^3 has the process factors and the answers described in Tab. 7.3., and the dimensionless values for the process factors are given by the equations (Ec. 7.1.- Ec. 7.3.), where *hcp*=30 cm, *tcp*=60 °C, *wcp*=0.21 cm/s are the values at the center.

$$x_1 = \frac{h - 30}{10} \tag{7.1}$$

$$x_2 = \frac{t - 60}{5} \tag{7.2}$$

$$x_3 = \frac{w - 0.21}{0.07} \tag{7.3}$$

The regression coefficients described by Ec.7.4., *i.e.*, βi, (i=1..N=8, j=1..3), (Tab 7.3.) Were determined according to the procedure characteristic of the factorial plan in Tab. 7.1. (1-8)

$$y_j = \beta_{1j} + \beta_{2j}x_1 + \beta_{3j}x_2 + \beta_{4j}x_3 + \beta_{5j}x_1x_2 + \beta_{6j}x_1x_3 + \beta_{7j}x_2x_3 + \beta_{8j}x_1x_2x_3 \tag{7.4}$$

Tab. 7.3. Regression coefficients significance for Ec. 7.4.

	i	1	2	3	4	5	6	7	8
j=1	β_{i1} (%)	**93.65**	**0.5**	-0.03	**-0.088**	**0.533**	**-0.25**	**0.14**	**1.287**
	$y_{1,mn,cp}$ (%)	93.66							
	$\sigma_{rp,1}$ (%)	0.052							
	$\sigma_{\beta,1}$ (%)	0.018							
	t_{i1}	**5089**	**27.17**	1.630	**4.755**	**28.94**	**13.59**	**7.608**	**69.97**
	t_{i1}-3.176	**>0**	**>0**	<0	**>0**	**>0**	**>0**	**>0**	**>0**
j=2	β_{i2} (%)	**81.91**	**2.151**	**-3.481**	**-2.129**	-1.269	-0.036	-1.464	**-2.371**
	$y_{2,mn,cp}$ (%)	82.18							
	$\sigma_{rp,2}$ (%)	1.31							
	$\sigma_{\beta,2}$ (%)	0.463							
	t_{i2}	**176.8**	**4.643**	**7.514**	**4.595**	2.739	0.078	3.159	**5.118**
	t_{i2}-3.176	**>0**	**>0**	**>0**	**>0**	<0	<0	<0	**>0**
j=3	β_{i3}	**14.25**	**-6.25**	-0.50	-0.25	**1.00**	**-1.25**	0	0
	$y_{3,mn,cp}$ (min)	14.5							
	$\sigma_{rp,3}$ (min)	0.577							
	$\sigma_{\beta,3}$ (min)	0.204							
	t_{i3}	**69.81**	**30.62**	2.45	1.225	**4.899**	**6.124**	0	0
	t_{i3}-3.176	**>0**	**>0**	<0	<0	**>0**	**>0**	=0	=0

To determine the significance of the regression coefficients using the Student's test, 4 more experiments were performed at the center (Ncp=4) 9-12 în Tab. 7.1, while the characteristic parameters for these experiments, *mean response value* (yj,mn,cp), *reproducibility standard deviation* ($\sigma rp,j$) and *the number of degrees of freedom* (υ_1), as well as the *standard deviation* ($\sigma rp,j$) associated with the coefficients of regression and random variables *Studen*t (*tij*), given by Ec. 7.5.-7.9. are found in Tab. 7.2.

$$y_{j,mn,cp} = \frac{\sum_{k=1}^{N_{cp}} y_{jk,cp}}{N_{cp}} \tag{7.5}$$

$$\sigma_{rp,j} = \sqrt{\frac{\sum_{k=1}^{N_{cp}} \left(y_{jk,cp} - y_{j,mn,cp}\right)^2}{\upsilon_1}} \tag{7.6}$$

$$\upsilon_1 = N_{cp} - 1 = 3 \tag{7.7}$$

$$\sigma_{\beta,j} = \frac{\sigma_{rp,j}}{\sqrt{N}} \tag{7.8}$$

$$t_{ij} = \frac{\left|\beta_{ij}\right|}{\sigma_{\beta,j}} \tag{7.9}$$

$$y_1 = Y_{FAME} = 93.65 + 0.5x_1 - 0.088x_3 + 0.533x_1x_2 - 0.25x_1x_3 + 0.14x_2x_3 + 1.287x_1x_2x_3$$ (7.10)

$$y_2 = Y_G = 81.91 + 2.151x_1 - 3.481x_2 - 2.129x_3 - 2.371x_1x_2x_3$$ (7.11)

$$y_3 = \tau_G = 14.25 - 6.25x_1 + x_1x_2 - 1.25x_1x_3$$ (7.12)

Regarding the influence of the process factors on the height of the catalytic fixed-bed (x_1), of the operating temperature (x_2) and of the superficial velocity of the reactant (x_3), Ec. 7.10 - 7.12. highlights the following: (1) the Y_{FAME} yield increases by x_1, x_1x_2, x_2x_3 and $x_1x_2x_3$, but at the same time decreases with the increase in x_3 and x_1x_3; (2) Y_G increases with x_1 and decreases with increase in x_2, x_3 and $x_1x_2x_3$; (3) he interaction between $x_1x_1x_3$ negatively influences the formation time τ_G, while the interaction x_1x_2 has a positive influence.

The statistical model described by Ec. 7.10-7.12. could help to estimate the performances of the transesterification process for the level factors, in the interval considered in the statistical analysis, respectively *h*=20-40 cm, *t*=55-65 °C and *w*=0.14-0.28 cm/s.

Regarding the efficiency of this process, Y_{FAME} (91.60 - 95.74%) varied with *h*, *ht*, *tw*, *htw* and decreased with an increase of the interaction between *w* and *hw*. The yield of glycerol (73.31 - 90.48%) increased with *h* and decreased with increasing interaction between *t*, *w* and *htw*. Glycerol formation time (6-23 min) was negatively influenced by the *h* and *hw* interaction, in parallel with a positive effect from the *ht* interaction.

7.3.3. Biodiesel with heterogeneous catalyst from BC-Gu and SCSF.-Gu in batch reactor with perfect mixing

The biodiesel synthesis using the catalyst consisting of the support and guanidine was carried out in a batch reactor, with perfect mixing. The vegetable oil used was that of used sunflower, and the amounts used were similar in all reactions, respectively of m_{TG}= 50 g. The reaction conditions are found in Tab. 7.3.

The uses of BC-Gu and $SC_{SF.}$-Gu were studied due to the similarities in operation and to succeed the cycles (syntheses), following the application of the same pattern.

The experimental installation used was that of Fig. 7.1.

Tab. 7. 2. Reactants and reaction conditions for biodiesel synthesis using BC-Gu and $SC_{SF.}$-Gu catalysts

Exp.no.	Oil type	Catalyst type	Oil [g]	MeOH/oil molar ratio	Reaction temp [°C]	React time [h]	*X*	Y_{ME}	Y_{ME} *[g/]*
1	Uzat floarea soarelui	BC-*Gu*	50	6:1	65	1.5	0.94	0.96	48.2
2		$SC_{SF.}$**ci**-Gu	50	6:1	65	1.5	0.86	0.90	45.0
3		$SC_{SF.}$cai-Gu	50	6:1	65	1.5	0.93	0.94	47.0
4		$SC_{SF.}$m-Gu	50	6:1	65	1.5	0.88	0.84	41.8
5		$SC_{SF.}$p-Gu	50	6:1	65	1.5	0.74	0.77	38.4
6		$SC_{SF.}$pi/n-Gu	50	6:1	65	1.5	0.81	0.83	41.3
7		$SC_{SF.}$co-Gu	50	6:1	65	1.5	0.79	0.76	38.2

Fig. 7.4. presents the experimental results following the performance of biodiesel syntheses, in heterogeneous catalysis, in which the catalyst used was that of BC on which guanidine was impregnated BC-Gu and the types of $SC_{SF.}$-Gu. The aim of these syntheses was strictly the conversion to biodiesel. When it is close to 100% it is assumed (often confirmed) that the yield of methyl esters is also proportional. Glycerol formation times have not been studied, as in the case

of the syntheses from Chap. 7.3.2, because they will be part of a protocol of future studies and operations, which will analyze, separately from the process conditions, the reduction of the total catalyst mass (support plus catalyst), together with its influence on the efficiency in methyl esters.

The values for the obtained conversions are reasonable, given that this study was in its *debut*, quite far from when it comes to optimizing process parameters, which is still an achievable goal.

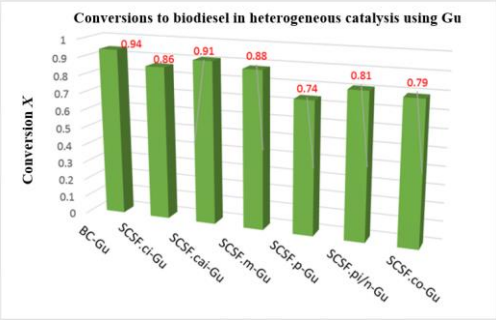


Fig. 7. 3. Conversions for biodiesel synthesis using BC-Gu and $SC_{SF.}$-Gu catalysts

7.3.4. Biodiesel with heterogeneous catalyst from SC_{SF}.cai-Gu in batch reactor with perfect mixing

These experiments were performed in order to study the catalytic activity in the sense of reusing the catalyst in several production cycles. The experimental installation for this step was the one shown in 7.1.

All R-type reactions (catalyst reuses) had a common pattern and similar behavior throughout the reaction. The mode of operation was as follows: after the first reaction, classical, with heterogeneous catalyst, the reaction mixture was discharged, but the catalyst remained in the reactor, being fed only methanol for the next synthesis (this was the meaning of reusing the catalyst). Unlike the first reaction, however, all the others benefited from residues, at the end of the study concluding that they seemed to have a positive influence: residual biodiesel and residual glycerin (and probably methanol, etc.). All R-type experiments had the same reaction onset and the same course, in the moments of interruption of the stirring, but maintaining the reaction temperatures, being able to observe how the conversion at the methanol interface with the catalyst takes place.



Fig. 7. 4. Steps in biodiesel synthesis using $SC_{SF.}$cai-Gu catalyst

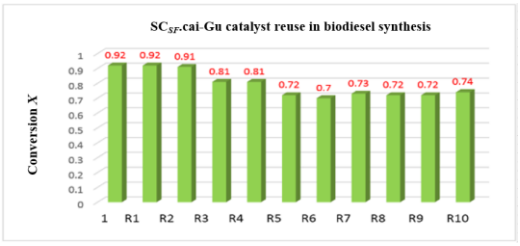


Fig. 7. 5. Dynamics of methyl ester conversion *vs.* re-uses from synthesis with same catalyst

After conversions above 0.9, even if they have (in)evolved to 0.7, the number of catalytic cycles for this type of catalyst is still noteworthy.

This study of SC_{SF}.cai-Gu catalyst reuse showed excellent results in terms of catalyst reuse, announcing an interesting future perspective to address in terms of catalysis cycles with these types of materials.

7.3.5. Biodiesel with heterogeneous catalyst from guanidine and BC_{KOH} in batch reactor with perfect mixing

At this stage of the research, the synthesis of biodiesel was performed by transesterification of sunflower oil with methanol in heterogeneous base catalysis, in a batch reactor with perfect mixing, using as catalyst BC_{KOH}. The reaction conditions can be found in Tab. 7.4., and the experimental installation is that of Fig. 7.1.

Data analysis for obtaining biodiesel with catalyst on BC support

The experimental investigation of the influence of process factors on the yield of biodiesel, expressed as yield in methyl ester, respectively yield in glycerol, followed a factorial program with 4 factors, each at two levels. The process factors referred to the *solution for obtaining* the catalyst, respectively to the *control of the transesterification reaction*. Thus the first factor expressed by the *concentration of KOH* in the biocellulose saturation solution (BC) and the fourth factor specifying the *temperature at which the saturated BC was dried in KOH*, refers to obtaining the catalyst. The second factor showing the *dose of catalyst in transesterification* and the third factor specifying the *molar ratio of methanol/oil*, refers to the development of the reaction.



Fig. 7. 6. Steps of using BC as heterogeneous catalyst for vegetable oil conversion to biodiesel: 1.a-c – heat treatment; 2.a-c – activation before transesterification reaction; 3.a-c. – transesterification reaction

Tab. 7.4. contains data from the experimental program. We observe here 4 experiments in the center of the factorial plan (exp. 17-20), their purpose being to establish the dispersibility of reproducibility of the working method.

Tab. 7. 4. Factorial plan 2^4 for biodiesel production using catalyst on BC_{KOH} support

Nr. Crt	KOH in BC-KOH %	Catalyst dose g/100 g	Methanol/oil molar ratio	Drying temperature of BC-KOH	Biodiesel yield (ester)	Glycerol yield
1	5	2	6	75	94.8	71.1
2	5	2	4	75	95.1	69.4
3	5	4	6	75	91.7	80.1
4	5	4	4	75	93.6	74.6
5	10	2	6	75	94.1	83.3
6	10	2	4	75	93.6	89.1
7	10	4	6	75	93.5	86.2
8	10	4	4	75	93.3	85.3
9	5	2	6	105	95.2	91.1
10	5	2	4	105	95.7	88.2
11	5	4	6	105	94.0	93.0
12	5	4	4	105	93.3	89.6
13	5	2	6	105	94.2	98.4
14	5	2	4	105	94.5	83.8
15	5	4	6	105	94.5	97.4

16	5	4	4	105	94.4	94.0
17	7.5	3	5	90	92.9	89.1
18	7.5	3	5	90	92.2	87.7
19	7.5	3	5	90	93.8	86.7
20	7.5	3	5	90	93.4	87.2

7.4. RESULTS AND DISCUSSIONS

For a factorial plan 2^4 a response *y* dependent on the 4 factors is expressed according to the relation in Ec.7.13. Here x_i expresses the dimensionless values of the process factors and these, according to the relation in Ec.7.14., have values of *+1* and *-1*

$$y(x_1, x_2, x_3, x_4) = +\sum_{i=1}^{4} \beta_i x_i + \sum_{i=1}^{4}\sum_{j=i+1}^{4} \beta_{ij} x_i x_j + \sum_{i=1}^{4}\sum_{j=i+1}^{4}\sum_{k=j+1}^{4} \beta_{ijk} x_i x_j x_k + \beta_{1234} x_1 x_2 x_3 x_4 \quad (7.13)$$

$$x_i = \frac{z_i - z_{iC}}{\Delta z_i} = \frac{z_i - \frac{z_{i,max} + z_{i,min}}{2}}{\frac{z_{i,max} - z_{i,min}}{2}}, i = 1 \dots 4 \quad (7.14)$$

In identifying β the coefficients from the relation from Ec.7.13 a calculation algorithm specific to the experimental programs of type 2^n is performed,where *n* represents the number of factors in the process. This procedure includes [Dobre T, Sanchez J.M, Chemical engineering modeling simulation and similitude): 1) the transition of the matrix of experimental data from the form with factors in natural values (z_i in the relation from Ec.7.14. to the form with dimensionless expressed factors, 2) the calculation of all β according to the each specific relations, 3) the calculation of the reproducibility dispersion associated with the experimental method, 4) the use of the reproducibility dispersion in the calculation of the Student variable associated with each coefficient β, 5) the elimination between β coefficients of those for which the associated Student variable is inferior to the Student variable with n_c*-1* degrees of freedom (n_c experiments number in the center of the experimental plan) at significance level α=0.05, 6) use of the Fischer test to verify the adequacy of the model that remains after the elimination of insignificant β coefficients.

The particularization of this procedure in relation to the data from Tab. 7.4. led to the relationships in Ec.7.15. şi Ec.7.16. They express the dependence of the process factors for the methyl ester yield, respectively the glycerol yield, on the use of the alkaline catalyst on BC_{KOH} support in the transesterification of sunflower oil..

$$\eta_E = 0.941 - 0.0057x_2 + 0.0043x_1x_2 + 0.00093x_3x_4 - 0.00575x_1x_2x_3x_4 \quad (7.15)$$

$$\eta_G = 0.859 + 0.038x_1 + 0.016x_2 + 0.017x_3 + 0.06x_4 - 0.0058x_1x_2 - 0.023x_1x_4 + 0.014x_3x_4 - 0.0095x_1x_2x_4 - 0.0076x_1x_3x_4 - 0.0066x_2x_3x_4 - 0.015x_1x_2x_2x_4 \quad (7.16)$$

Analysis of the dependence of the ester yield on process factors shows that all factors have influence. However, the small values of the coefficients that multiply the factors in the relation in Ec. 7.15 may suggest that this influence is not extremely strong. It appears that for x_3 and x_4 in the center of the plane (molar ratio 5 and catalyst drying at 90 °C) the technique with low catalyst mass and low KOH concentration in catalyst preparation leads to methyl ester yields of up to 99%. Fig7.9. supports this statement.

In the case of the dependence of the yield of transesterification over glycerol on process factors, their influence is much more complex. We have in the relation from Ec. 7.16. 11 terms, *i.e.* all linear influences, almost all binary and ternary interaction influences of process factors and even the interaction of all 4 process factors. This complex form of the relationship probably says that over the chemical reaction on the surface of the catalyst is added the physio-chemical process of glycerol release and then coalescence and separation. Some coefficients with values above 0.01 indicate a strong influence. We thus find that the factor x_2 (catalyst dose), factor x_3 (molar reaction

ratio) and the interaction of all factors are in this position to strongly influence the process yield, expressed by the ability to separate glycerol.

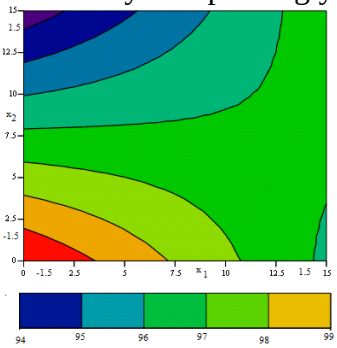


Fig. 7.7. Ester yield dependence on x_1 and x_2 factors for $x_3 = x_4 = 0$

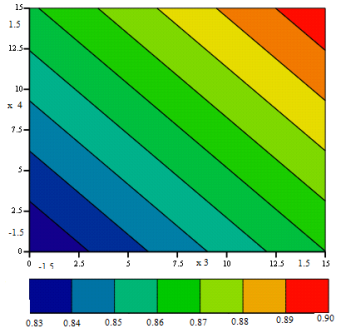


Fig. 7.8. Glycerol yield dependence on x_3 and x_4 factors for $x_1 = x_2 = 0$

The important influence of the factors x_3 and x_4 on the glycerin yield on the transesterification is shown graphically in Fig.7.10. When x_1 and x_2 are in the center of the plane, it should be noted that we reach a yield of 0.9, if we work with a well-dried catalyst (drying at 105 °C of the catalyst) and if we have a high molar ratio of methanol/oil.

$$\frac{\partial \eta_G}{\partial x_1} = \frac{\partial \eta_G}{\partial x_2} = \frac{\partial \eta_G}{\partial x_3} = \frac{\partial \eta_G}{\partial x_4} = 0 \qquad (7.17)$$

The interest is always to maximize the yield of transesterification. With reference to the relation in Ec.7.16 maximizing the yield means solving the system of equations (Ec.7.17). The solution of this system finds $x_1 = 1.51$, $x_2 = 3.129$, $x_3 = 1.51$, $x_4 = 0.362$, when $\eta_{Gmax} = 0.965$. Even if the value x_2 is not close to the range of associated factors from Tab. 7.4 and even if x_1 and x_3 are at the outer limit of this range, the result obtained requires: to obtain a high yield, the catalyst must be *concentrated* in KOH, it is necessary to use a *large mass* of catalyst, with the *molar ratio at 6* and the catalyst drying at *~90 degrees Celsius*.

6. CONCLUSIONS OF PHD THESIS

GENERAL CONCLUSIONS

At the beginning of the research and later in almost all the chapters of this paper, some objectives were proposed and as we advanced from one stage to another, the objectives varied in fulfillment depending on this advance.

We set out and managed, with the literature analysis part, to clarify many aspects in the *field of biodiesel*, chemistry, raw materials, reagents or synthesis techniques, so we are convinced that biodiesel has really been brought back to the general attention and even become *easy to decipher*.

To be clear: we wouldn't mind having biodiesel in homogeneous catalysis (commercial biodiesel) produced and used by as many users as possible, but we focused on this area of heterogeneous catalysis in biodiesel synthesis, with attempts to find efficient methods (in terms of catalytic activity) and, why not, cheap at the same time. Abundance is generally synonymous with low price, so materials such as lignocellulosic or algal biomass, BC produced on a laboratory scale, seem to be solutions that fold on this type of catalysis. If we add a base catalyst to be deposited on these types of support, the recipe seems almost complete.

In this context, we managed, over 3 chapters (Chapters 3, 4 and 5), to build from scratch (actually from fruit stone) materials with certain characteristics or properties, and we were able to take advantage of some, while on others we had to work to increase their performance. Thus, the materials created in Chapter 3, (cheap, abundant, of different types) *managed to catalyze the transesterification reaction* of vegetable oils to methyl esters and some even in multiple reaction cycles ($SC_{SF.}$cai-Gu). The construction steps of $SC_{SF.}$cai-Gu, for example, were relatively easy to perform: in Chapter 3, multiple treatments, in Chapter 4 the synthesis of the base catalyst that was to be deposited on them, and Chapter 5 with the methods of combining them.

The results were more than satisfactory, taking into account what it started from (fruit stones). Deepening the methods of combining catalytic support with the catalyst will probably lead, or will probably bring, greater satisfaction, but they will be based on exactly what has been achieved in this work.

Chapter 6 also succeeds in deciphering the mechanisms by which transesterification occurs and has also provided solutions or increasing strategies, for example of one of the yields, or recommendations regarding the feeding or evacuation of one of the reactants.

And Chapter 7 somehow closes this cycle of catalyst development for transesterification in heterogeneous catalysis (but not only), by testing, practically, of this type of catalyst, in reactions of conversion of vegetable oils to biodiesel, with results, after as we mentioned, more than satisfying.

7. ORIGINAL CONTRIBUTIONS

The use of heat-treated biomass has allowed the development of new materials, for example as a solid material, intended for catalytic support, as in the case of this work.

It was obvious the possibility to obtain a much larger area of the specific surface, both in the case of pyrolytic carbon, and especially in the case of activated pyrolytic carbon. Additional crushing operations (or laboratory grinding) and subsequent treatment would have increased the performance of the material derived from this characteristic of the material. But for this work these operations would not have facilitated the integration of the material in the architecture of the process, but on the contrary, would have caused operations with additional costs, both economic, by introducing the stages of filtration or separation by decantation or centrifugation, especially in terms of low yields due to inhibition.

The heat treatment was thus associated with a series of chemical treatments applied to the material subjected to pyrolysis and activation, starting with the treatment with alkaline or acidic solutions and up to the use of a relatively high percentage of moisture, provided to the material before initiating pyrolysis. The differences were significant compared to the untreated material and subjected to pyrolysis under similar process conditions, in terms of pore volume and size, differences confirmed by the adsorption processes used as tests for the products obtained from the pyrolysis process.

Approaching lignocellulosic biomass (fruit stone) in terms of materials with potential in various applications and adapted here by developing strategies for their functionalization, in order to overcome the level of residual biomass material, by increasing performance in terms of intrinsic characteristics, in terms of porosity and a chemical composition, that allows the bonding of those to chemical compounds that increase their ability to participate in chemical synthesis.

The approach of biocellulose, similarly, in terms of viable and reliable materials, capable of participating in reactions, is not a novelty, but in order to do so for a long time, it was necessary to use techniques with low costs of treatment or functionalization, which they allowed us, they rather opened us, the way to the integration of BC in the architecture of the process of obtaining biodiesel through the transesterification reaction and, why not, in any other process or reaction that requires a permissive matrix in accessing it.

On the synthesis strategies of the chemical compounds, it can be highlighted the obtaining of a special organic compound, with special base (alkaline) properties, respectively by the synthesis of guanidine, by a not very complex reaction and with reasonable process conditions, moderate, and considered successful here, by the value of the main reaction product obtained for this research, but not only, as well as the value of the reaction by-product, considered a solid variant of sulfuric acid, which can just as easily find reactions to participate in.

Also here we can include the idea and practice of bringing to the *table of raw materials* this type of lignocellulosic materials (fruit stones), it is true, subjected to multiple treatments, but which, once helped to increase or double their strengths (for example from the present porosity to the functional porosity, from *available* to *very available*), by participating in their raw state as well as later, at the *end of the career*, by pyrolysis, with a new *way* of uses).

Going further with the evaluation regarding the original contributions, we managed here, through simulation and modeling, to ensure access to understanding the aspects related to the kinetics of the transesterification process, the method of quantification or evaluation of the mechanisms of this type of process and the choices that you can do in terms of the technique or the direction to go on the road from precursors to product.

While discussing the pieces of the *biodiesel puzzle* (catalysis, catalysts, transesterification, waste oil), it seems obvious that we succeeded in what we set out to do at the beginning of the research, namely to bring back to the general attention: *it is the easiest to synthesize biofuel*, with the most types of raw materials from which the conversion can be made and with the most moderate reaction conditions, from production to separation.

And we note finally, but just as important, the solutions offered by us regarding the technique of recirculation of one of the reactants, simultaneously with the separation already during the process, with the help of additional equipment at the experimental installation, both in the case of homogeneous catalysis and in the case of heterogeneous catalysis to obtain biodiesel.

Participation with oral presentations and posters at international conferences:

Tănase Dobre, Cristina Ionela Gogoasă, **Cristian Eugen Răducanu**, *Biodiesel Production Using a Sulphonated Activated Carbon-Based Catalyst*, **SICHEM** - Symposium of the Young Chemical Engineers, University POLITEHNICA of Bucharest, POLITEHNICA Central Library, **8 – 9 September, 2016**; - Comunicare orală

Cristian Eugen Răducanu, Oana Cristina Pârvulescu, Anghel Rodica, Tănase Dobre, *Considerations on Biodiesel Synthesis with Fed Batch Reactor*, **PRIOCHEM** - International Symposium, **27-28 October 2016**; - Comunicare orală

Cristian Eugen Răducanu, Adina Gavrilă, Oana Pârvulescu, Petre Chipurici, Tănase Dobre, *Alternative catalyst in transesterification of waste vegetable oils to biodiesel*, **RICCCE 20**- Romanian International Conference on Chemistry and Chemical Engineering, Poiana Brasov, **6-9 September 2017**; - Comunicare orală

Cristian Răducanu, Doinița Roxana Cioroiu, Bogdan Trică, Oana Pârvulescu, *Effects of Process Factors on Pyrolysis of Some Algaes from Black Sea*, **Scientific Communications at Danube/Danube Delta-Black Sea (3D-BS) Cluster Blue Growth** strategy-workshop: The Use of

Algae from the Black Sea Coast, Ovidius Constanta University, **27 September 2017**; - Comunicare orală
Ali A. Abbas Al Janabi, **Cristian Eugen Răducanu**, Oana Cristina Pârvulescu, Tănase Dobre, *Organic superbases as heterogeneous catalysts for biodiesel production*, **SICHEM** - International Symposium of Chemical Engineering and Materials, **6-7 September 2018**; - Poster
Cristian Eugen Răducanu, Adina Gavrilă, Oana Pârvulescu, Petre Chipurici, Tănase Dobre, *Modelling of batch biodiesel synthesis with external recirculation and simultaneous separation*, **RICCCE 21**-Romanian International Conference on Chemistry and Chemical Engineering, Constana Mamaia, **4-7 September 2019**; - Comunicare orală

B. List of articles published in the UPB Scientific Bulletin:
1. **Cristian Eugen Răducanu**, Oana Cristina Pârvulescu, Tănase Dobre, *Modelling of Biodiesel Synthesis: Batch Mode With ExternaL Recirculation and Simultaneous Separation*, U.P.B. Sci. Bull., Series B, **2021**, ISSN 1454-2331.
2. Alina Georgiana Ciufu, Ali A. Abbas Al Janabi, **Cristian Eugen Răducanu**, Doinița Roxana Tîrpan, Tănase Dobre, *Natural Wool Fibers: A Viable Substitute to Commercially Available Oil Synthetic Sorbents*, U.P.B. Sci. Bull., Series B, 81 (4), **2019** ISSN 1454-2331
3. Bogdan Trică, Oana Cristina Pârvulescu, **Cristian Eugen Răducanu**, Tănase Dobre, *Thin Layer Convective Drying of Cystoseira Barbata Brown Macroalga*, U.P.B. Sci. Bull., Series B, 82 (2), **2020** ISSN 1454-2331

C. Published articles, indexed in international databases
1. **Cristian Eugen Răducanu**, Tănase Dobre, Cristina Gogoașă, *Biodiesel production using a sulphonated activated carbon-based catalyst*, Bulletin of Romanian Chemical Engineering Society, 3 (1), 2016 ISSN 2360-4697
2. **Cristian Eugen Răducanu**, Oana Cristina Pârvulescu, Tănase Dobre, *Transesterification of Vegetable Oils to Biodiesel in a Fixed Bed Catalyst Reactor*: *Experimental and Modelling*, Bulletin of Romanian Chemical Engineering Society, 4 (2), 43-51, 2017, ISSN:2360-4697.
3. **Cristian Eugen Răducanu**, Oana Cristina Pârvulescu, Tănase Dobre, T., Iuliana Dumitru, Florentina Drăgușin, *Air Drying of Aromatic Plants Coupled with Recovery of Volatile Compounds*, Bulletin of Romanian Chemical Engineering Society, 5 (1), 58-67, 2018, ISSN:2360-4697.
4. Tănase Dobre, Oana Cristina Pârvulescu, **Cristian Eugen Răducanu**, Roxana Mihaela Lazăr, *Mathematical Model for Fixed Bed Sorbent Chromatography: Chromatographic Separator*, Bulletin of Romanian Chemical Engineering Society, Vol. 6, No. 1, 2019 ISSN 2360-4697
5. Alexandru Boscornea, Tănase Dobre, Oana Cristina Pârvulescu, **Cristian Eugen Răducanu**, *Kinetics of Copper Etching with Ammonium Persulfate*, Bulletin of Romanian Chemical Engineering Society, 5 (1), 83-91, 2018, ISSN:2360-4697.
6. Tănase Dobre, Oana Cristina Pârvulescu, **Cristian Eugen Răducanu**, Bogdan Trică, Gheorghița Jinescu, *Stochastic modelling of polysaccharide hydrolysis*, Journal of Engineering Sciences and Innovation, 3 (1), 25-38, 2018, ISSN:2601-6699.

D. Articles published in ISI Thomson Reuters indexed journals
1. **Cristian Eugen Răducanu**, Adina Ionuţa Gavrilă, Tănase Dobre, Petre Chipurici, *Study on Alumina Supported Heterogeneous Catalysts for Biodiesel Production*, REV.CHIM., 69 (8), **2018**; F.I. – **1.755**

2. Doiniţa Roxana Cioroiu, Oana Cristina Pârvulescu, Claudia Irina Koncsag, Tănase Dobre, **Cristian Răducanu**, Rheological Characterization of Algal Suspensions for Bioethanol Processing, Rev. Chim. (Bucharest), 68 (10), 2311-2316, **2017**, ISSN:0034-7752; F.I. – **1.755**.
3. Bogdan Trică, Oana Cristina Pârvulescu, Tănase Dobre, Ali A.A. Al Janabi, **Cristian Răducanu**,Claudia Patrichi, *Modelling of Ethanol Fermentation Coupled with Product Recovery by Pervaporation*, Rev. Chim. (Bucharest), 68 (11), 2708-2715, **2017**, ISSN:0034-7752; F.I. – **1.755**.
4. Doiniţa Roxana Cioroiu, Oana Cristina Pârvulescu, Tănase Dobre, **Cristian Răducanu**, Claudia Irina Koncsag, Alexandra Mocanu, Narcis Duţeanu, *Slow Pyrolysis of Cystoseira Barbata Brown Macroalgae*, Rev. Chim. (Bucharest), 69 (3), 553-556, **2018**, ISSN:0034-7752, F.I. – **1.755**
5. Petre Chipurici, Alexandru Vlaicu, **Cristian Eugen Răducanu**, Ştefania Daniela Bran, Adina Ionuţa Gavrilă, *Biodiesel Production from Waste Oil and Its Blends with Glycerol Ketals*, REV.CHIM., 69 (7), **2018**; F.I. – **1.755**
6. Aurel Diacon, Alexandra Mocanu, **Cristian Eugen Răducanu**, Cristina Busuioc, Raluca Şomoghi, Bogdan Trică, Adrian Dinescu, Edina Rusen, *New carbon/ZnO/Li2O nanocomposites with enhanced photocatalytic activity*, Scientific Reports, 2019 (9), 16840; F.I. – **3.998**
7. Alina Georgiana Ciufu, **Cristian Eugen Răducanu**, Oana Cristina Pârvulescu, Doiniţa Roxana Cioroiu,Tănase Dobre, *Natural Wool for Removal of Oil Spills from Water Surface*, Rev. Chim. (Bucharest), 70 (11), 3977-3980, **2019**, ISSN:0034-7752; F.I. – **1.755**
8. Alina Georgiana Ciufu, Ali A. Abbas Al Janabi, Oana Cristina Pârvulescu, Tănase Dobre, **Cristian Răducanu**, *Romanian Merino Wool Sorbent for Oil Spill Cleanup*, REV.CHIM., 69 (9) 2018; F.I. – **1.755**

Total F.I. – **16.283**

8. FUTURE RESEARCH PERSPECTIVE

In this research, only the *first bricks* were built, because a part of what we proposed as experimentation and testing was successful and must be deepened: the recirculation of one of the reactants, both in homogeneous catalysis and in heterogeneous catalysis at the conversion of triglycerides to methyl esters, simultaneously with the separation of glycerol (seen only as a mode of operation, but not the only one), indicates the direction to follow, respectively the heterogeneous catalysis area, where we must insist on establishing an appropriate catalytic support/base catalyst ratio, in the sense increasing the bonding capacity on the support in higher concentrations of the base catalyst at lower masses of material.

The extension of the cycles number in which a catalyst can participate (an increase in catalytic activity) must also be deepened in both reactor types, batch with perfect mixing and fixed-bed catalytic reactor.

Further development or keeping of these types of materials, cheap, abundant but at the same time viable, for this type of process, whether it is BC, with several advantages in the chemical bonding area, whether it is algae or lignocellulosic biomass is also *a must* for a future project.

Deepening in the area of heterogeneous catalysis, in terms of modeling and simulation, is as well a *desideratum* for future research.

SELECTIVE REFERENCES

[8] *B. Freedman, R.O. Butterfield, E.H. Pryde*,Transesterification Kinetics of Soybean Oil, JAOCS, Vol.
[116] *M. Bala*t, Potential alternatives to edible oils for biodiesel production – A review of current work, Energy Conversion and Management 52 (2011), 1479–1492;
[275] https://www.britannica.com/science/algae/Reproduction-and-life-histories
[276] *H.W. Yen, I.C. Hu, C.Y. Chen, S.H. Ho, D.J. Lee, J.S. Chang*, Microalgae-based biorefinery – From biofuels to natural products, Bioresource Technology, 2013 (135), 166-174;
[277] *S.H. Ho, C.Y. Chen, D.J. Lee, J.S. Chang*, Perspectives on microalgal CO_2-emission mitigation systems — A review, Biotechnology Advances, 2011 (29), 189-198;
[278]https://www.google.ro/search?q=algae&source=lnms&tbm=isch&sa=X&ved=0ahUKEwiIgqyuyr7WAhXoCpoKHdLlD7sQ_AUICigB&biw=1280&bih=670#imgrc=axWHxZvYJHdSfM:
[279]https://www.google.ro/search?q=algae&source=lnms&tbm=isch&sa=X&ved=0ahUKEwiIgqyuyr7WAhXoCpoKHdLlD7sQ_AUICigB&biw=1280&bih=670#imgrc=TWWG-HfAwEd9GM:
[280]https://www.google.ro/search?q=algae&source=lnms&tbm=isch&sa=X&ved=0ahUKEwiIgqyuyr7WAhXoCpoKHdLlD7sQ_AUICigB&biw=1280&bih=670#imgdii=zp4eNCBHlfxkEM:&imgrc=TM-1IRvWgTFiCM:
[281]https://www.google.ro/search?q=algae&source=lnms&tbm=isch&sa=X&ved=0ahUKEwiIgqyuyr7WAhXoCpoKHdLlD7sQ_AUICigB&biw=1280&bih=670#imgrc=empizxYo8tf9WM:
[282]https://www.google.ro/search?q=alge+pe+plaja&source=lnms&tbm=isch&sa=X&ved=0ahUKEwivv3Fwr_WAhXIK8AKHQXFBykQ_AUICigB&biw=1280&bih=670#imgrc=NXwnga2lkwYtXM:
[283]https://www.google.ro/search?q=alge+pe+plaja&source=lnms&tbm=isch&sa=X&ved=0ahUKEwi-vv3Fwr_WAhXIK8AKHQXFBykQ_AUICigB&biw=1280&bih=670#imgdii=PTi30H-Q52UTHM:&imgrc=tSZvFR02HG_aaM:
[284] https://www.nrel.gov/bioenergy/algal-biofuels.html
[285] https://www.earthmagazine.org/article/green-it-gets-algae-biofuels
[286] https://www.algenol.com/
[294] *A. Diacon, A. Mocanu, C. E. Răducanu, C. Busuioc, R. Şomoghi, B. Trică, A. Dinescu, E. Rusen*, New carbon/ZnO/Li_2O nanocomposites with enhanced photocatalytic activity, Sci Rep 2019 (9), 16840;
[295] *T. Dobre, O.C. Pârvulescu, I. Rodriguez Ramos, L. Ceatră, M. Stroescu, A. Stoica, R. Mirea*, Global Reaction Kinetics and Enthalpy in Slow Pyrolysis of Vegetal Materials, Rev. Chim. (Bucharest), 2012, 63 (1), 54-59;
[296] *O.C. Pârvulescu, T. Dobre, L. Ceatră, G. Iavorschi*, Characteristics of Corn Grains Pyrolysis in a Fixed Bed Reactor, Rev. Chim. (Bucharest), 2011, 62 (1), 89-94;
[297] *D. R. Cioroiu, O. C. Parvulescu, T. Dobre, C. R.C. I. Koncsag, A. Mocanu, Duteanu*, Slow Pyrolysis of Cystoseira Barbata Brown Macroalgae, Rev.Chim.(Bucharest), 69, 3, 2018
[298] *T., Dobre, O.C. Pârvulescu, G. Iavorschi, A. Stoica, M. Stroescu*, Catalytic Effects at Pyrolysis of Wheat Grains Impregnated with Nickel Salts, International Journal of Chemical Reactor Engineering, 8, 1968-1992, 2010, ISSN:1542-6580, WOS:000280497700003 (FI=1,059).
[301]*T. Dobre, O.C. Pârvulescu, A. Jacquemet, V. A. Ion*, Adsorption and Thermal Desorption of Volatile Organic Compounds in a Fixed Bed – Experimental and Modelling, Chem. Eng. Commun., 203 (12), 1554-1561, 2016, ISSN:0098-6445 (Print), ISSN:1563-5201 (Online), WOS:000387245100004 (FI=1,431).
[303] *O. J. Rojas*, Cellulose Chemistry and Properties: Fibers,Nanocelluloses andAdvanced Materials Advances in Polymer Science, Adv Polym Sci (2016) 271 ISBN 978-3-319-26013-6,
[304] *T. Dobre, A Stoica, O. C. Pârvulescu, M. Stroescu, G. Iavorschi*, Factors Influence on Bacterial Cellulose Growth in Static Reactors, Rev. Chim. (Bucharest), 59 (5), 191-195, 2008, ISSN: 0034-7752, WOS:000257684800023 (FI=1,605).
[305] *R. Jonas, L. F. Farah*, Production and application of microbial cellulose Polymer degradation and Srabiliry 59 (1998) 101-106
[306] *E. J. Vandamme, S. De Baets, A. Vanbaelen, K. Jori, P. De Wulf*, Improved production of bacterial cellulose and its application potential polymer Degrnddon and Sfabihfy 59 (1998) 93-99
[311] https://www.algaebase.org/search/species/detail/?species
[312] *David L. Nelson, Michael M. Cox*, Lehninger Principles of Biochemistry, Fourth Edition, Ed.W.H.Freeman, 2004, 978-0-716-74339-2
[313] *C. Boscornea*, Curs Biochimie anul I master BBTC, CASM, Universitatea Politehnica din Bucuresti, 2013-2014;
[314] *A. Stoica Guzun, M. Stroescu, S.I. Jinga, G. Voicu, A.M Grumezescu, A.M. Holban*, Plackett–Burman experimental design for bacterial cellulose–silica composites synthesis, Materials Science and Engineering: C, 42, (2014), 280-288;

[315] *A. Stoica-Guzun, L. Jecu, A. Gheorghe, I. Raut, M. Stroescu, M. Ghiurea, M. Danila, I. Jipa, V. Fruth*, Biodegradation of Poly(vinyl alcohol) and Bacterial Cellulose Composites by Aspergillus niger, J. Polym. Environ. 19 (2011), 69–79;
[316] *O. C. Parvulescu, G. Isopencu, C. Busuioc, C. Raducanu, A. Mocanu, I. Deleanu, A. Stoica-Guzun*, Antimicrobial bacterial cellulose composites as textile materials
[317] *T. Dobre, A. Stoica, O.C Pârvulescu, M. Stroescu, G. Iavorschi*, Factors Influence on Bacterial Cellulose Growth in Static Reactors, Rev. Chim., 59, 5, (2008), 191-195, ISSN: 0034-7752;
[318] *T. Ishikawa*, Superbases for Organic Synthesis:Guanidines, Amidines, Phosphazenes and Related Organocatalysts, John Wiley & Sons, 2009, ISBN 978-0-470-51800-7;
[323] *G. Haflinger, F.K.H Kuske,* The Chemistry of Amidines and Imidates, Vol. 2 (eds S. Patai and Z. Rapport), John Wiley & Sons, Chichester, 1991, pp. 1–100.
[322] *Caubere, P*. Unimetal super bases. Chemical Reviews, 93, 1993, 2317–2334.
[319] *R.W Alder, P.S Bowman., W.R.S. Steele, D.R. Winterman,* (1968) The remarkable basicity of 1,8-bi(dimethylamino)naphthalene. Chemical Communications, 723–724;
[320] *Schwesinger, R*. Extremely strong, non-ionic bases: syntheses and applications. Chimia, 39, 2, 1985, 69–272
[321] *J.G. Verkade, P.B. Kisanga*, Proazaphosphatranes: a synthesis methodology trip from their discovery to vitamin A. Tetrahedron, 59, 2003, 7819–7858;
[324] *M. Avram*, Chimie Organica, Editura Academica R.S.R., 1983,
[325] *E Roberts, J. Griffiths*, The Synthesis of Guanidin from Urea, MS London, R (41) 1949;
[331] *H, Zhang, X., Luo, X., Li Chen, G.Z, He F. T, Wu,* Preparation and Characterization of a Sulfonated Carbon-based Solid Acid Microspheric Material (SCSAM) and its use for the Esterification of Oleic Acid with Methanol, Austin Chem. Eng., 1, (2016), 1024.
]332] *C. E. Răducanu, T. Dobre, C. Gogoaşă*, BIODIESEL PRODUCTION USING A SULPHONATED ACTIVATED CARBON-BASED CATALYST, Bulletin of Romanian Chemical Engineering Society, Vol. 3, No. 1, 2016 ISSN 2360-4697
[333] *M. A. Atieh, O.Y. Bakather, B. A. Tawbini, A. A. Bukhari, F.A. Abuilaiwi, M. B. Fettouhi*, Effect of Carboxylic Functional Group Functionalized on Carbon Nanotubes Surface on the Removal of Lead fromWater. Hindawi Publishing Corporation Volume 2010, Article ID 603978, 9 pages
[334] *C.E. RĂDUCANU, O.C. PÂRVULESCU, T. DOBRE*, TRANSESTERIFICATION OF VEGETABLE OILS TO BIODIESEL IN A FIXED BED CATALYST REACTOR: EXPERIMENTAL AND MODELLING, Bulletin of Romanian Chemical Engineering Society, Vol. 4, No. 2, 2017 ISSN 2360-4697
[335] *A., Gorsek, P Glavic.*, Design of batch versus continuous processes. I. Single-purpose equipment. Trans IChemE, 75, 1997, 709–717.
[336] *A., Gorsek, P Glavic*., Design of batch versus continuous processes. II. Multi-purpose equipment. Trans IChemE, 75, 1997, 718–723.
[337] *Zhang M., Wu H.*, Phase behaviour and fuel properties of bio-oil/glycerol/methanol blends, Energy Fuels, 28, 2014, 4650-4656
[338] *D.Y. Leung, X. Wu, M. Leung*, A review on biodiesel production using catalyzed transesterification, Appl. Energy 87, 4, 2010, 1083–1095.
[339] *H.J. Berchmans, K. Morishita, T. Takarada*, Kinetic study of methanolysis of Jatropha curcas-waste food oil mixture, J. Chem. Eng. Jpn. 43, 8, 2010, 661–670.
[340] *Ana S.R. Brásio, Romanenko A., Leal J., Santos O. L., Natércia C.P. Fernandesa*, Nonlinear model predictive control of biodiesel production via transesterification of used vegetable oils, Journal of Process Control 23 (2013) 1471– 1479
[341] *D., Darnoko M., Cheryan*, Kinetics of palm oil transesterification in a batch reactor, JAOCS, Journal of the American Oil Chemists' Society, 77, 12, 2000, 1263-1267
[342] Noureddini H., Zhu D., *Kinetics of Transesterification of Soybean Oil*, J. Am. Oil Chem. Soc. 74, 1997,1457-1462
[343] *A., Tuluc, P. Iancu, V. Plesu, J. Bonet-Ruiz., G. Bozga., G. Bumbac*., Biodiesel plant optimization study using Aspen-HYSIS Process Simulator, REV.CHIM (Bucharest), 66,4,2015, 565-569
[344] *M., Agarwal, Singh., P. S Chaurasia*, Simulation and sensitivity analysis for biodiesel production in a reactive distillation column, Polish Journal of Chemical Technology, 14, 2012, 59–65